FN-593

Fermilab Program through 1997 and Beyond

1992 HEPAP SUBPANEL on RESEARCH PRIORITIES
Site Visit to Fermilab

February 27-28, 1992

(Updated - June '92)

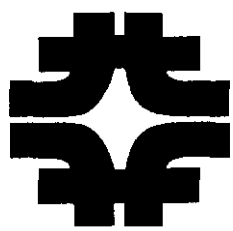

Fermi National Accelerator Laboratory
Batavia, Illinois

Operated by Universities Research Association Inc.
Under Contract with the United States Department of Energy

TABLE OF CONTENTS

1 INTRODUCTION

1 INTRODUCTION

The collection of materials here supplements the oral presentations made to the HEPAP Subpanel. Section 2 presents the upgrades to the accelerator complex. The outcome of these upgrades will be:

- a collider which can produce 500 pb^{-1} per calendar year at a center of mass energy of 2 TeV;
- an antiproton source capable of producing and accumulating almost 20 milliamps of antiprotons per hour,
- the ability to run very high intensity extracted beams *while* the collider is running,
- the doubling of the the intensity available to the Tevatron Fixed-Target program.

Sections 3 - 7 present a sample of the physics reach made possible by these upgrades. Topics discussed for the collider include,

- under the general title of 'High P_t', the search for the top-quark, the measurement of the top mass, m_t, and the study of top decays, the precision measurement of the W mass, M_W, and the implications for Electroweak theory, and the search for new physics such as supersymmetric particles and compositeness.
- the study of B's, building on the signal seen by CDF, to present the prospects for measuring CP violation in the decays of B mesons.

We have organized the presentation of the Fixed-Target Physics program into three sections.

- The Neutrino program exploiting the Tevatron and the Main Injector.
- The Kaon program exploiting the Tevatron and the Main Injector.
- Other Fixed-Target physics. This section gives a sense of the variety possible in the Fixed-Target program discussing high statistics charm experiments, an experiment to measure the spin-structure of the proton in muon-scattering, high luminosity experiments to measure rare B decays, experiments using a polarized-proton beam possible with the Main Injector and the use of The Fermilab antiproton source as the basis for a measurement of CP violation in decays of the $\Lambda\bar{\Lambda}$ system.

The experiments discussed here do not exhaust the list of what can or will be accomplished at Fermilab. They do, however, demonstrate the richness and breadth of the

experiment program. In conventional terms, the program presents a multi-pronged attack on the so-called Standard Model, topics beyond the Standard Model such as the search for neutrino generation mixing whose discovery would have tremendous implications for particle physics and cosmology, and experiments to measure the dynamics of the interactions between quarks.

The breadth of this program comes from the variety of beams and energies available at Fermilab. The Tevatron is the highest energy collider in the world and will remain so till the end of the century; this gives the CDF and D0 detectors a unique opportunity to make dramatic discoveries. Fermilab also will have the highest energy photon, kaon, muon, neutrino and electron beams and the most intense source of antiprotons - an arsenal of different probes to investigate the mysteries of particle physics. While the intensity provided by the accelerator system is essential, so are the advances in detector technology, data-acquisition and data-processing and analysis which allow the increased luminosity to be exploited fully. The Fermilab community has shown its ability to make advances in all these areas. The planned accelerator upgrades and the evolving experiment program present unequalled opportunities for discovery from now till the year 2000. The final section, 8, gives the schedule and describes the funding required to match this challenge.

2 THE ACCELERATOR

2 THE FERMILAB ACCELERATOR COMPLEX IN THE 1990's

The Fermilab Tevatron is the highest energy particle collider in the world today. It will retain this position until the initial operation of either the Superconducting Super Collider (SSC) in the U.S. or the Large Hadron Collider (LHC) in Europe around the year 2000. Fermilab has embarked upon a program, entitled Fermilab III, to raise the luminosity in the Tevatron proton-antiproton collider to in excess of 5×10^{31} cm^{-2}sec^{-1}. Components of the program include implementation of electrostatic separators, Antiproton Source improvements, installation of cold compressors, doubling the existing linac output energy, and the construction of a new accelerator—the Fermilab Main Injector.

In the Tevatron countercirculating proton and antiproton beams are brought into collision at 1800 GeV in the center-of-mass, with a typical initial luminosity achieved in the 1988-89 collider run of 1.6×10^{30} cm^{-2}sec^{-1}. Averaged over a multi-month running period typical initial luminosity is found to translate into integrated luminosity with about a 33% duty factor.

The luminosity in a proton-antiproton collider is given by the expression,

$$L = \frac{3\gamma f B N_p N_{\bar{p}}}{\beta^* \left(\varepsilon_p + \varepsilon_{\bar{p}}\right)} F\left(\sigma_z/\beta^*\right)$$

where γ is the relativistic factor of the proton (1066 at 1000 GeV), f is the revolution frequency (47.7 kHz), B is the number of bunches, N_p and $N_{\bar{p}}$ are respectively the number of protons and antiprotons per bunch, β^* is the beta function at the interaction point (assumed equal for horizontal and vertical), ε_p and $\varepsilon_{\bar{p}}$ are the proton and antiproton 95% normalized emittances respectively, and F is a form factor associated with the ratio of the bunch length to beta function at the interaction point.

The operating conditions which led to a luminosity of 1.6×10^{30} cm^{-2}sec^{-1} during the 1988-89 collider run are given in the leftmost column of Table 2.1. The luminosity was limited by two quite different effects: 1) The beam-beam tune shift experienced by the antiprotons, which limits the useable phase space density, N_p/ε_p, of the proton beam; and 2) The availability of antiprotons, which is reflected in the product $BN_{\bar{p}}$. One can note from the luminosity expression that as long as the proton and antiproton emittances are of comparable magnitude the luminosity achievable is proportional to the product of N_p/ε_p and $BN_{\bar{p}}$.

2.1 BEAM-BEAM TUNE SHIFT

The beam-beam tune shift experienced by the antiprotons is given by,

$$\Delta\nu = .00733\left(N_p/\varepsilon_p\right)N_c$$

where N_p is in units of 10^{10}, ε_p is in units of π mm-mr, and N_C is the number of bunch crossings per turn (=2B in the absence of orbit separation). As shown in Table 2.1 the achieved $\Delta\nu$ is .025. The achievable tune shift is believed to be limited by the available working space in the tune diagram as delineated by the absence of resonances of $\leq$10th order. (The collider is operated with Q_X=Q_Y=19.42, in a region bounded by the 5th order resonance 19.40, and the 7th order resonance, 19.428.)

	88-89	**Ia**	**Ib**	**II**	**Main Injector**	
Energy (Center of Mass)	1800	1800	1800	2000	2000	GeV
Protons/bunch	7.0×10^{10}	7.0×10^{10}	1.2×10^{11}	1.2×10^{11}	3.0×10^{11}	
Antiprotons/bunch	2.9×10^{10}	7.2×10^{10}	7.2×10^{10}	1.2×10^{10}	3.7×10^{10}	
Number of Bunches	6	6	6	36	36	
Total Antiprotons	1.7×10^{11}	4.3×10^{11}	4.3×10^{11}	4.3×10^{11}	1.3×10^{12}	
$\bar{p}$ Stacking Rate	2.0×10^{10}	4.0×10^{10}	6.0×10^{10}	6.0×10^{10}	1.7×10^{11}	$hour^{-1}$
ε_p	25π	15π	15π	15π	30π	mm-mr
$\varepsilon_{\bar{p}}$	18π	18π	18π	18π	22π	mm-mr
β^*	55	50	50	50	50	cm
Luminosity	$\mathbf{1.6\times10^{30}}$	$\mathbf{5.7\times10^{30}}$	$\mathbf{1.0\times10^{31}}$	$\mathbf{1.1\times10^{31}}$	$\mathbf{5.7\times10^{31}}$	$\mathbf{cm^{-2}sec^{-1}}$
$\Delta\nu$/crossing ($\bar{p}$)	.002	.003	.006	.006	.008	
Number of Crossings	12	2	2	2	2	
$\Delta\nu$ Total ($\bar{p}$)	.025	.007	.012	.012	.017	
Bunch Separation	3000	3000	3000	395	395	nsec
Interactions/crossing (@45 mb)	0.3	0.9	1.5	0.3	1.5	
What's New?	—	Separators, $\bar{p}$ Source Improv.	Linac Upgrade	Cold Compr. Fast Kicker	Main Inject.	

TABLE 2.1: Tevatron Luminosity Evolution through the 1990's.

The Fermilab complex is actually capable of producing a proton phase space density approximately 60% larger than that reflected in the table. However, the use of such intense proton bunches has been found to have a deleterious effect on the antiproton bunches which makes the achievement of higher luminosities, accompanied by good lifetimes, impossible.

2.2 SPACE-CHARGE AT BOOSTER INJECTION

Even if the proton phase space density were not limited by the tune shift experienced by the antiproton bunches, it would still be impossible to create a density more than about 60% above that listed in Table 2.1. This is because the fundamental limit on proton density in the Fermilab complex arises from space-charge forces at injection into the Fermilab Booster. With the present 200 MeV injection energy the smallest proton emittance which can be produced for injection into the Tevatron collider is about 15π mm-mr. Any planned improvements which reduce the antiproton beam-beam tune shift can only affect the luminosity in a significant manner if it allows the creation of higher phase-space densities at the upstream end of the accelerator complex.

2.3 ANTIPROTON AVAILABILITY

Antiproton availability is limited by two effects, one obvious and the other more subtle. The obvious constraint is the antiproton production rate. During 1988-89 a rate of 2×10^{10} $\bar{p}$/hour was achieved. The transfer efficiency of antiprotons from the Antiproton Accumulator to 900 GeV in the Tevatron was in the range 60-70%. Since the average store lasted 13 hours, a total of 1.7×10^{11} antiprotons were typically available in the Tevatron Collider. The antiproton production rate is limited by the proton beam intensity delivered from the Main Ring onto the $\bar{p}$ production target, by the Main Ring cycle rate, and by the admittance of the Antiproton Source rings. The Main Ring beam intensity itself is limited by the Main Ring admittance.

Antiproton availability is also limited by a more subtle effect having to do with the correlation between the antiproton transverse beam emittance and stack size in the Accumulator. The beam emittance arises as a result of the attainment of equilibrium between intrabeam scattering and stochastic cooling. As the stack size increases, the heating due to intrabeam scattering increases, while the effectiveness of the cooling system decreases. The resultant antiproton beam emittance rises as the stack size increases.

Unfortunately, the Main Ring admittance is less than the emittance emanating from the Accumulator at a stack size in excess of 6×10^{11}. In general this guarantees that accumulated antiprotons in excess of 6×10^{11} will not be transmitted through the Main Ring on their journey to the Tevatron. Since we are currently capable of delivering about 40% of the antiproton stack from the Accumulator, with 60-70% transmission to the collider this also limits antiproton availability in the collider to 1.7×10^{11}.

2.4 LUMINOSITY EVOLUTION THROUGH THE 1990S

Fermilab has initiated a series of improvements to the existing accelerator complex to provide a luminosity capability in excess of 5×10^{31} $cm^{-2}sec^{-1}$ by 1996. These improvements are aimed at attacking the above-described limitations associated with the beam-beam tune shift, space-charge in the Booster, and antiproton availability. Specifically included are:

1) implementation of electrostatic separators in the Tevatron;

2) a series of Antiproton Source improvements;

3) upgrading the Linac energy from 200 MeV to 400 Mev; and

4) construction of a new accelerator, the Fermilab Main Injector, to replace the existing Main Ring.

The expected progression of luminosity throughout the decade is summarized in Table 2.1. Note that in addition to the items listed above the table reflects the implementation of cold compressors which will lower the operating temperature of the Tevatron magnets by about 0.5°K and provide an energy of 1000 GeV per beam.

2.5 ELECTROSTATIC SEPARATORS

Electrostatic separators will create helically separated orbits in the Tevatron which will keep up to 36 proton and antiproton bunches separated everywhere but at the B0 and D0 collision points. This will reduce the total beam-beam tune shift by providing N_C=2 with B up to 36.

Each separator is 3 meters in length and is capable of generating 250 kV over a 5 cm aperture. Twenty units are required to create the desired orbits. The peak field, 50 kV/cm, is required only during injection—during a proton-antiproton store no unit will be required to operate above 40 Kv/cm.

Several units have been tested in the Tevatron with protons and antiprotons stored at 150 GeV. These studies have shown no anomalous behavior, i.e. unexpected tune shifts, emittance growth, or lifetimes, for separations as low as 1s.

Thirteen of the required twenty units are installed at this time. The remaining units, which are located in the region currently occupied by slow extraction equipment, will be installed following the completion of the current fixed-target run. All separators will be in place and operational for the collider run scheduled to start in late 1991.

It should be noted that separators themselves do not create higher luminosity in the collider. They only create the potential for raising the luminosity if one has the capability of raising the proton phase space density and/or the number of antiprotons in the Tevatron.

2.6 ANTIPROTON SOURCE IMPROVEMENTS

Improvements implemented in the Antiproton Source since 1989 have been aimed at increasing the accumulation rate and reducing the emittance characteristic of a given stack size. An enlargement of antiproton collection line and Debuncher ring apertures, and implementation of Debuncher momentum cooling are expected to increase the antiproton stacking rate by a factor of 2-3 beyond that achieved in 1988-89. A 4-8 GHz core cooling system has replaced the original 2-4 GHz system in the Accumulator Ring. The new system will reduce the emittance at a given stack size relative to that currently achieved. Future improvements to the targeting system and a new Accumulator stack-tail system will be required for Main Injector operations, leading to an ultimate capability of of stacks containing 2×10^{12} antiprotons and stacking rates of 1.7×10^{11}/hour.

2.7 THE LINAC UPGRADE

The existing 200 MeV linac is in the process of being upgraded to 400 MeV by replacement of the second half of the existing drift tube linac with a side coupled structure generating 300 MeV in the same length. The result of the higher energy will be a reduction in the space-charge forces which lead to emittance dilution at injection into the 8 GeV Booster. It is anticipated that achievable proton transverse beam densities delivered from the Booster will increase by 75% following implementation of 400 MeV injection. This will benefit antiproton production by increasing the proton flux through the Main Ring, and will simultaneously allow for the creation of higher proton phase space densities in the Tevatron collider.

The Linac Upgrade was initiated in Fiscal Year (FY) 1990, and is scheduled for completion in FY1992. Commissioning is expected to start in the winter of 1992-93.

2.8 THE MAIN INJECTOR

The Fermilab Main Injector is a new 150 GeV accelerator which will replace the existing Main Ring. The purpose of the FMI is to remove forever the bottleneck that the Main Ring presents in the delivery of high intensity proton and antiproton beams to the Tevatron, and to increase the antiproton production rate sufficiently to be able to utilize this new capability.

The Fermilab Main Injector will be constructed tangent to the Tevatron in a separate tunnel on the southwest corner of the Fermilab site. The FMI will be roughly half the size of the existing Main Ring yet will boast greatly improved performance. The FMI will allow the production of about seven times as many antiprotons per hour (1.7×10^{11}/hour) as are currently possible using the Main Ring and will have a capability for the delivery of four times as many protons to the Tevatron (at least 3×10^{11} protons/bunch for collider operations). Additionally the FMI will support the delivery of very intense proton beams (3×10^{13} protons every 2.9 seconds with a 34% duty factor) for use in state-of-the-art studies of CP violation and rare Kaon decays, and for experiments designed to search for transmutation between different neutrino generations. Low intensity proton beams emanating from the FMI will support test and calibration beams required for the development of new experimental detection devices which will be required both at Fermilab and at the SSC. In contrast to the present situation at Fermilab, simultaneous antiproton production and FMI slow spill operation will be possible under normal circumstances, as will simultaneous FMI and Tevatron fixed target operations.

The Fermilab Main Injector parameter list is given in Table 2.2. The FMI will perform at a significantly higher level than the existing Main Ring as measured either in terms of protons delivered per cycle, protons delivered per second, or transmission efficiency. For the most part expected improvements in performance are directly related to optics of the ring. The MI ring lies in a plane with stronger focussing per unit length than the Main Ring. This means that the maximum betas are half as big and the maximum (horizontal) dispersion a third as big as in the Main Ring, while vertical dispersion is nonexistent. As a result physical beam sizes associated with given transverse and longitudinal emittances are significantly reduced compared to the Main Ring. The elimination of dispersion in the RF regions, raising the level of the injection field,

elimination of sagitta, and improved field quality in the dipoles will all have a beneficial impact on beam dynamics. The construction of new, mechanically simpler magnets is expected to yield a highly reliable machine.

Circumference	3319.419 meters
Injection Momentum	8.9 GeV/c
Peak Momentum	150 GeV/c
Minimum Cycle Time (@120 GeV)	1.5 sec
Number of Protons	3×10^{13}
Harmonic Number (@53 MHz)	588
Horizontal Tune	26.4
Vertical Tune	25.4
Transition Gamma	20.4
Natural Chromaticity (H)	-33.6
Natural Chromaticity (V)	-32.9
Number of Bunches	498
Protons/bunch	6×10^{10}
Transverse Emittance (Normalized)	20π mm-mr
Longitudinal Emittance	0.4 eV-sec
Transverse Admittance (at 8.9 GeV)	40π mm-mr
Longitudinal Admittance	0.5 eV-sec
β_{max}	57 meters
Maximum Dispersion	2.2 meters
Number of Straight Sections	8
Length of Standard Cell	34.3 meters
Phase Advance per Cell	90 degrees
RF Frequency (Injection)	52.8 MHz
RF Frequency (Extraction)	53.1 MHz
RF Voltage	4 MV
Number of Dipoles	216/128
Dipole Lengths	6.1/4.1 meters
Dipole Field (@150 GeV)	17.2 kGauss
Dipole Field (@8.9 GeV)	1.0 kGauss
Number of Quadrupoles	128/32/48
Quadrupole Lengths	2.1/2.5/2.9 meters
Quadrupole Gradient	196 kG/m
Number of Quadrupole Busses	2

TABLE 2.2: Fermilab Main Injector Parameter List.

The FMI is seven times the circumference of the Booster and slightly more than half the circumference of the Tevatron. Six Booster cycles will be required to fill the FMI and two FMI cycles to fill the Tevatron. The FMI is designed to have a transverse aperture of 40π mm-mr (both planes, normalized at 8.9 GeV/c). This is 30% larger than the expected Booster aperture following the 400 MeV Linac upgrade, and a factor of three to four larger than that of the existing Main Ring. A single Booster batch will be accelerated for antiproton production while six such batches are required to fill the FMI. Yields out of the FMI for a full ring are expected to lie in the range $3\text{-}4 \times 10^{13}$ protons ($6\text{-}8 \times 10^{13}$ delivered to the Tevatron.) By way of contrast the existing Main Ring is capable of accelerating 1.8×10^{13} protons in twelve batches for delivery to the Tevatron.

The power supply and magnet systems are designed to allow a significant increase in the number of 120 GeV acceleration cycles which can be run each hour for antiproton production, as well as to allow a 120 GeV slow spill with a 34% duty factor. The cycle time at 120 GeV can be as low as 1.5 seconds. This is believed to represent the maximum rate at which the Antiproton Source might ultimately stack antiprotons and is to be compared to the current Main Ring capability of 2.6 seconds.

2.9 STATUS

The design of the Fermilab Main Injector has been developed over the past several years and is now well advanced. Several independent reviews have verified the soundness of the design. The Total Estimated Cost of the Fermilab Main Injector is $177.8M. Congress has appropriated $15M for FMI construction in FY1992. This money has not yet been made available to Fermilab by the Department of Energy.

Magnet R&D was initiated on this project in 1990. Two full-scale prototypes have been built and have undergone extensive measurement at the Fermilab Magnet Test Facility. Measurements show that these magnets are very well described by the computer models and satisfy the magnet field quality specification. The focus of the FY1992 magnet R&D is the development of outside vendor manufacturing capability.

Environmental permitting is well advanced on this project. A Clean Air and Water, Section 404, permit for construction was received in June of 1991 from the U.S. Army Corps of Engineers. Permits have also been received from the Illinois Environmental Protection Agency, the Illinois Department of Transportation, the Illinois State Historic Preservation Office, and the U.S. EPA. *All permits required for initiation of construction*

of the project have been secured. In addition an Environmental Assessment has been prepared and is currently under review by the Department of Energy. A Finding of No Significant Impact (FONSI) is expected soon.

2.10 ACCELERATOR PHYSICS RESEARCH IN THE 1990'S

The accelerator physics projects anticipated for the remainder of the decade fall into two broad categories. First, meeting the aggressive upgrade schedule designed to dramatically increase the fixed target beam intensity and collider luminosity will require studies of phenomenon such as instabilities, space charge induce emittance growth, intrabeam scattering, ion trapping, and stochastic cooling for both antiproton production and luminosity lifetime optimization. In support of this research instrumentation design and engineering development activities like room temperature and superconducting magnets, kickers, conventional RF, and power supply upgrades will be required. Second, research and development efforts aimed at future accelerators, such as proton therapy rings and linear colliders, are necessary in the 1990's in order to bring them into reality beyond the year 2000.

In both categories, graduate students from the Fermilab accelerator graduate program are expected to play a strong role. The Fermilab accelerator physics graduate program was founded because university physics departments were not generating enough accelerator physicists to meet the country's demand. With a total of approximately 9 students and an average graduation rate of 2-3 students per year, Fermilab produces more accelerator physicists than any other institution. Students who have finished their course work come to Fermilab to work with an advisor on an accelerator physics experiment. The energy of the students and the focus generated by the need to do thesis quality work make the students an invaluable source of innovation. The improvements to accelerator performance due to direct student participation are a testament to the quality of the program.

2.10.1 Programmatic Research

In order to meet both the fixed target intensity and collider luminosity goals set for the 1990's, the dominant accelerator physics research topic is expected to be beam instabilities. From the Linac to the Tevatron, as a result of concentrated searches, instabilities have been recently observed in every Fermilab accelerator with symptoms and operational implications which vary significantly between machines. Examples are transverse head-tail in a coupled lattice, transverse resistive wall, and ion trapping induced instabilities. By far

the most common phenomenon observed to date and expected in the future is the longitudinal coupled bunch instability caused by higher order resonant modes in RF cavities. Given recent successes at identifying and eliminating the offending impedances causing coupled bunch and other instabilities, it is clear that the foundation has been established for interesting and innovative instability and impedance research in the future. In addition, research into new beam feedback and damper designs made possible by technological advances in electronics and fiber optics will lead to complementary solutions for future instabilities.

In the past the dominant limitation to peak luminosity in the Tevatron Collider was the beam-beam tune shift of the antiprotons due to collisions with the intense proton bunches. With the introduction of electrostatic separators to create helical proton and antiproton closed orbits the maximum beam-beam tune shift was reduced by a factor of six. After the Linac and Main Injector upgrades are completed the proton brightness will again be high enough to warrant beam-beam studies. A related subject expected to be a source of concern throughout the 1990's is that of detector backgrounds. First, the mechanisms for the generation of large amplitude particles destined to be lost near the high energy physics detectors CDF and D0 are not well understood. Second, the placement and depth of collimators around the ring to scrape these particles depend on the particle loss mechanism, the linearity of the Tevatron lattice, and the machine operating conditions. The instrumentation being developed for an experiment (presently called P853) aimed at proving the principle of crystal extraction of particles from a collider beam should produce additional important data for detector background research.

Once the beams are brought into collision, a goal during Tevatron Collider operations is to maximize the luminosity lifetime. In the future two methods presently under development will be employed. It has been established through work over the last few years that the dominant mechanism causing short luminosity lifetime is transverse emittance dilution due to external noise introduced by power supplies for magnets, kickers, etc. Techniques and calculations developed to search out and eliminate these noise sources will continue in the future. In order to further improve the luminosity lifetime transverse bunched beam stochastic cooling systems for both protons and antiprotons already in the testing stage will evolve in the 1990's to keep up with increasing intensities. Some anticipated developments are 8-16 GHz bandwidth, increased usage of optical signal processing and transmission, and the design of beam pickups and kickers capable of

compensating for bad mixing. By increasing the optimum store length, these systems will force the Antiproton Source to maintain much larger stack sizes.

To meet this demand for larger stacks while maintaining optimum stacking rates, significant upgrades in the Antiproton Source are planned. To implement the same upgrades anticipated for bunched beam stochastic cooling, modifications to the Accumulator lattice are necessary to modify the bad mixing between the pickups and kickers. Along with these higher stack intensities comes the problem of ion trapping induced emittance growth and coherent instabilities. A coordinated set of accelerator physics experiments have been initiated to characterize and eliminate ion induced phenomenon which degrade Accumulator performance. In both the Tevatron and Accumulator intrabeam scattering is anticipated to become the dominant source of (presumably) uncorrectable performance degradation. Calculations and experiments testing the immutability of this phenomenon will be important in the future, especially after the commissioning of the Main Injector. For example, calculations have been done which show that the particle dynamics of intrabeam scattering is dramatically altered for beams with energies below the transition energy of the accelerator lattice.

Another implication of high intensity beam is the phenomenon of space charge induced transverse emittance growth. The major motivation for the Linac energy upgrade from 200 to 400 MeV, as the demand for higher beam intensity increases the need to understand the effects of space charge at injection into the Booster ring will again become important. With the installation of a number of powerful tune and emittance diagnostics, and the recent completion of a number or relevant space charge computer simulation programs written by graduate students, the study of space charge will become an important and interesting project.

Transverse emittance growth is unacceptable for collider beams because of the dependence of luminosity on beam emittance. On the other hand, fixed target performance or antiproton stacking efficiency do not depend strongly on transverse emittance. The limit to transverse beam size during these operations is accelerator aperture due to both vacuum chamber size and magnetic fields irregularities. The study of dynamic aperture caused by field irregularities or remnant fields is very important to accelerator physicists. With beams accelerated to higher and higher momenta, the ability to provide uniform fields over sufficient apertures becomes increasingly more expensive and difficult. Therefore, to confidently calculate the performance of future accelerators the beam dynamics implications of these irregularities must be quantitatively understood. Because of the present and future

implications of dynamic aperture in Fermilab accelerators, and the advanced state of their beam instrumentation, Fermilab is a perfect setting for accelerator physics experiments designed to test theories and calculations.

2.10.2 Development of Future Accelerators and Technologies

A few years ago an important collaboration of medicine, industry, and Fermilab accelerator physicists and engineers was formed to produce the Loma Linda proton therapy facility. Composed of a source, linac, RFQ, fast cycling synchrotron, and complicated beam distribution network, this facility provided an excellent example of the applicability of national laboratory accelerator technology to other scientific fields and industry. Building upon this experience, a group of accelerator and medical physicists are designing the next generation of fast cycling proton therapy accelerators. It is expected that such design work, with the possibility of attempting the construction of another machine, will continue for the remainder of the decade.

In an attempt to investigate possible programmatic futures for Fermilab, the idea of building a colliding e^+e^- linac top-quark factory based on superconducting RF technology has emerged. Since a collaboration of laboratories and universities around the world (called TESLA) has been designing a 1×1 TeV colliding e^+e^- linac also based on superconducting RF, Fermilab joined that collaboration to begin the process of learning the relevant technologies and drawing upon the design work already completed to date. Using the various strengths of the Fermilab staff, development work is presently underway to design high power, superconducting power feeds for the RF cavities. It is expected that as participation within this collaboration continues and expands, and as accelerating fields in superconducting RF cavities attain a reproducible gradient of approximately 25 MeV/m, Fermilab will be in a position to make a strong proposal for a dedicated e^+e^- top-quark factory.

In the category of development of future accelerator technologies, an exciting experiment has been proposed to test the concept of crystal extraction of particles from a collider beam. Presently called P853, the purpose of this experiment is to prove the principle of crystal extraction for a proposed fixed target B-meson experiment at the SSC. The idea is to extract a small number of halo particles (up to 10^{-6}/sec of the circulating beam) without significantly affecting luminosity lifetime or backgrounds in the primary high energy physics detectors. The manipulation central to this scheme is to diffuse beam particles out to the aperture defined by the crystal. Since the silicon crystal is bent, particles

entering its lattice structure within a specific angular tolerance will be bent by the strong fields generated by the lattice atoms. But because of irregularities on the leading edge of the crystal, the particles must jump over an effective septum width of approximately 1 μm. The production of this step size while simultaneously preserving the integrity of the circulating beam requires an excitation of the beam with a special frequency spectrum. This Tevatron experiment will monitor detector backgrounds and the efficiency of crystal channelling for a number of proposed types of particle diffusion excitations. Once the concept of crystal extraction has been successfully demonstrated, potential applications for other types of fixed target research will be opened.

Another accelerator technology potentially useful in the 1990's and beyond presently being investigated at Fermilab is the production and acceleration of polarized beams for medium and high transverse momentum spin experiments. Presently proposed for Main Injector fixed target operations, a 150 μA H^- source is envisioned which may produce a 10^{12} protons/pulse polarized proton beam with a cycle time of 2.8 sec. This plan requires the installations of RFQs, polarimeters, and partial Siberian snakes in the Booster and Main Injector to preserve the polarization produced by the H^- source. The scale of this proposal and the required expertise necessary for designing various components requires the collaboration of a number of universities and national laboratories from the United States and around the world.

3 HIGH P_t AT THE COLLIDER

3 HIGH Pt AT THE COLLIDER

3.1 THE STANDARD MODEL UNDER SIEGE

The standard model is a fundamental theory of electroweak interactions having no known discrepancy with current experiments. When its calculable quantum corrections are included, it can be subjected to precise laboratory tests and subtle effects of new physics may emerge. The Fermilab Main Injector program will achieve a high level of precision in unique measurements of standard model parameters. It will determine the W boson mass, M_W, to a precision of ±50 MeV. If the top quark lies in the expected range, the Fermilab program will also discover it and measure its mass, m_t. In so doing, it will test one of the most dramatic predictions of the standard model, the relationship between M_W and m_t. The program will also study the decay modes and couplings of the top quark.

In the conventional three-generation standard model, the masses M_W and m_t are related. This relationship strikes at the heart of the mechanism of mass generation. If a Higgs boson exists, this test also depends on its mass, M_H~ in a subtle fashion. With the Main Injector a precision of ±3 GeV on m_t is attainable. Combined with the measurement of M_W this will allow discrimination between a heavy (~ 1 TeV), and a light (~ 100 GeV) Higgs boson. Moreover, if there is a new dynamics beyond the standard model, e.g., a fourth generation, technicolor, or supersymmetry, then the relationship between M_w and m_t can fail dramatically.

Why is the top quark so heavy? Is it special? What is the origin of electroweak symmetry breaking? Both the precision tests, as well as the top quark decay studies, will address these tantalizing questions. The top quark is of paramount importance because it is so much heavier than the other known fermions. It is likely to be the fermion most strongly coupled to the symmetry breaking dynamics of the standard model. The top quark decay modes may be non-standard, possibly involving a charged scalar technipion or SUSY partner. New physics can emerge in angular correlations of leptons and b-jets; top production through the W-gluon fusion mechanism may be observable and allow study of polarized top decay.

It is expected that the Main Injector will provide integrated luminosities of 1 fb^{-1} experiment in a two year running period. Without it, we can expect only 200 pb^{-1} in the same period. The main injector will allow the discovery of a top quark of mass up to 240

GeV. The current CDF lower limit on m_t is 91 GeV. This is indicative of the range of new energy scales that can be probed with the main injector. No accelerator has ever opened such a grand window on high energy scales before. The opportunity for tests of electroweak and QCD processes, as well as the discovery potential for new physics at the Fermilab Main Injector is substantial. The Fermilab Main Injector program will place considerable new pressure on the standard model at the highest energy ever probed in elementary particle physics.

3.2 THE TOP QUARK

3.2.1 Current constraints on m_t

The lower limit on the mass of the standard model top quark from the Tevatron is 91 GeV. In the standard model further constraints on the top quark mass can be inferred from measurements of the electroweak parameters. The mass splitting of the W and the Z depends quadratically on the mass of the top quark because of fermion loop contributions to vacuum polarization. The mass splitting of the W and the Z also depends logarithmically on M_H because of Higgs contributions to vacuum polarization. Thus the known parameters of the standard model imply a direct relationship between M_W and m_t, which is weakly sensitive to M_H. Figure 3.1 shows the current situation. The limits on mt from direct searches at the Tevatron, and on M_W from combined Tevatron and S$\bar{p}p$S measurements are shown. Also shown are the standard model predictions for the effect of electroweak radiative corrections. If we assume a minimal Higgs of 100 GeV, the predicted value of the top quark mass is $m_t = 130^{+45}_{-45}$ GeV. Using M_H = 1000 GeV and the 95% c.l. upper limit on M_W, an upper limit on m_t of 225 GeV is obtained in the minimal standard model.

If we assume the standard model, recent global fits of electroweak data can be combined to yield a 95% c.l. upper limit on m_t:

(1) For the high precision LEP data, assuming m_H = 300 GeV one obtains $m_t \leq 193$ GeV.[1)]

(2) Including all world data (LEP plus neutrino scattering and M_W from CDF and UA-2), and assuming a value of M_H = 250 GeV we have $m_t \leq 183$ GeV. Allowing for an arbitrarily heavy $M_H \rightarrow 1000$ GeV one obtains $m_t \leq 198$ GeV.[2)]

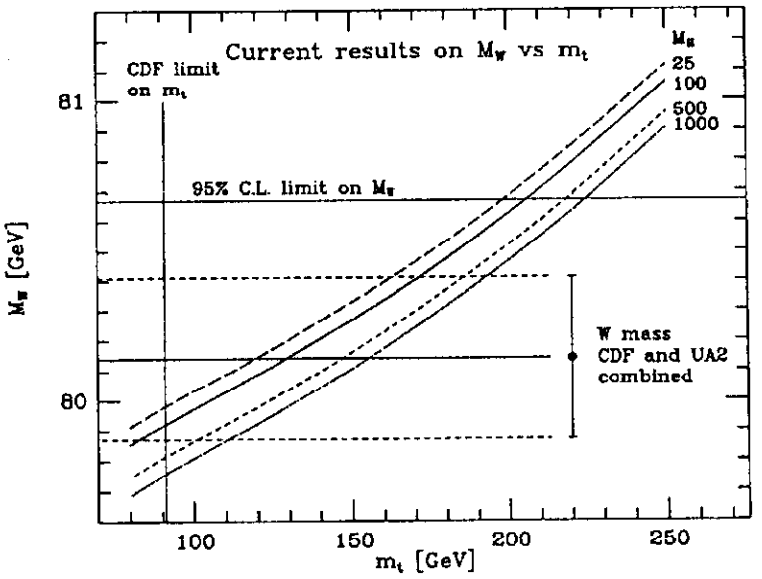

FIGURE 3.1: Current limits on m_t and measurements of M_W plotted with standard model predictions.

3.2.2 Discovery potential at the main injector

In the standard model, heavy top quarks are produced as $t\bar{t}$ pairs mainly by annihilation of a quark antiquark pair. For the $m_t > 85$ GeV the standard decay mode is into a real W and a b quark. There are two dominant signatures. The first involves only single lepton tag, where one W decays to ev *or* $\mu\nu$ and the other decays to a $q\bar{q}$ pair:

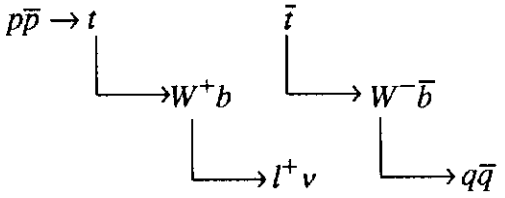

The other signature is two leptons and requires that both W's decay into lepton+neutrino:

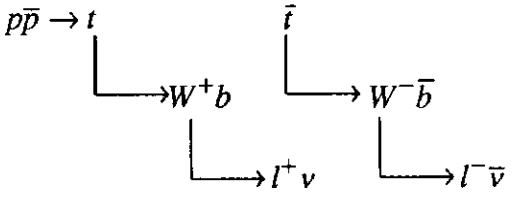

Table 3.1 shows the expected number of observable top events as a function of the top mass. The estimate of lepton plus jets events includes the efficiencies associated with a b vertex tag. Below we shall present estimates of the signal to background ratio.

3.2.2.1 Lepton plus multijet signatures

The signature for the first decay mode is an event with a lepton, four jets, and missing p_t. Figure 3.2 shows the expected observable cross sections for a lepton plus 3 or 4 jets from top production. Also shown is the background from high-p_t W produced in association with 3 or 4 jets.[3] A lepton with $p_t \geq 15$ GeV and 3 or 4 jets, each with $E_t \geq 20$ GeV were required. In Fig. 3.2, it is assumed that a b tag has been made to reduce the QCD background substantially. The b tag is based on a displaced vertex seen in a vertex detector (or μ near a jet). For this figure and Table 3.1 a 50% efficiency was assumed. The background from high-p_t W's is reduced by at least a factor of 10.

mt [GeV]	*e* or λ + 4 jets	*e*–μ
120	1380	240
140	850	98
180	260	24
210	140	12
240	60	5

TABLE 3.1: Number of observable top events in 1 fb^{-1} in the e or μ plus four jets mode and the e-μ mode.

The results shown in Fig. 3.2 include a cut on the transverse energy of jets, ($E_T > 20$ GeV). For a high mass top, the background from high-p_t W's can be further reduced without appreciable reduction in the signal by increasing the cut on jet E_t. By raising this cut judiciously, a signal to noise ratio of at least 4 is possible over the entire accessible mass range. The W plus jets backgrounds were estimated using the exact tree level parton matrix elements for a W produced in association with n partons. These calculations are expected to be more reliable for high-p_t, well separated jets than estimates using Monte Carlo showers.

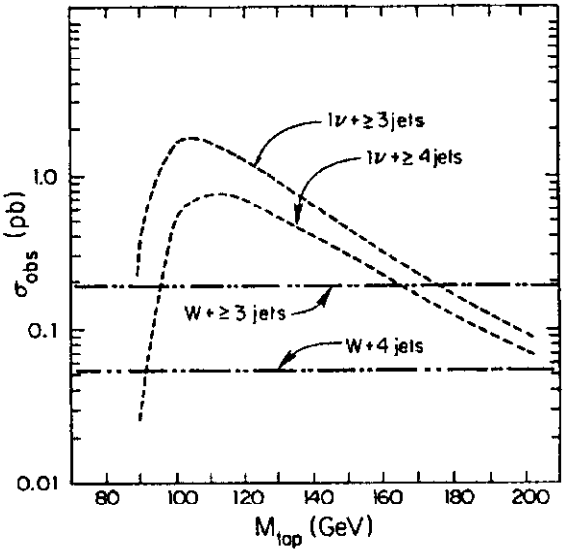

FIGURE 3.2: Observable production cross sections for $t\bar{t}$ into $e\nu$ and 4 jets as a function of m_t. Also shown are the backgrounds from QCD production of W's accompanied by 3 or 4 jets. These assume the use of a b vertex tag to reduce the QCD background. For heavy top ($m_t > 150$ GeV), the background can be further reduced by imposing a more severe cut on the minimum jet transverse energy.

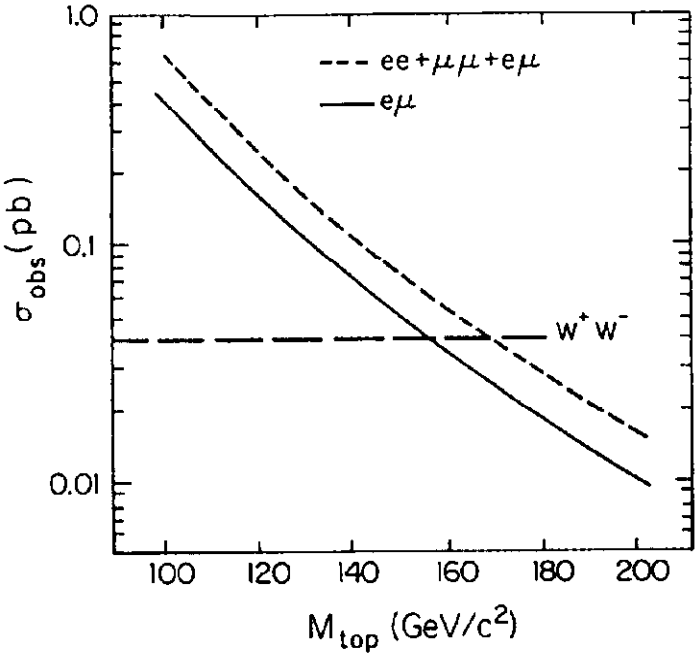

FIGURE 3.3: Dilepton cross sections for $t\bar{t}$ production with detector efficiencies included. The background from W pair production can be reduced for a heavy top by requiring a b quark tag in the events.

3.2.2.2 Two lepton signatures

Figure 3.3 shows the expected observable cross section for $t\bar{t}$ to go into two leptons plus missing energy. This is considered the primary discovery channel because of its freedom from backgrounds. For a high mass top, W pair production becomes a background. The use of a b vertex tag will reduce this source to a level such that a signal to noise of at least 10:1 is achievable. Because the dilepton mode is the cleanest, it can be used as a reference for the top discovery potential. If one defines a discovery as a minimum of 4 events in the e–μ channel, then the discovery reach is approximately 185 GeV with 200 pb^{-1} and 245 GeV with 1 fb^{-1}.

3.2.3 Top mass measurement

The measurement of m_t has achieved a certain primacy because its relation to the other electroweak parameters (e.g. the Higgs sector). The mass measurement in the dilepton mode is more difficult because of the two neutrinos in the event with unmeasured momenta. The lepton+jets+missing p_t is considered the best mode for a mass measurement since there is only one neutrino in the final state and backgrounds are manageable. For each event, there are two top mass measurements: one from the three jet invariant mass combination, the other from the neutrino, lepton and b jet combination. Figure 3.4 shows a peak from the three jet invariant mass combination. Because the resolution for both modes is rather broad, a significant number of events are required to measure m_t with any precision. For m_t = 210 GeV, the width of the three jet invariant mass combination is approximately 30 GeV. For the reach of the Main Injector, a yield of 80 events gives a statistical accuracy of about 3 GeV. On the side opposite the purely hadronic decay, one can reconstruct the top mass using the lepton + neutrino + b jet invariant mass. The longitudinal motion of the neutrino is unknown, but can be inferred correctly 85% of the time by imposing the W mass constraint and choosing the more central solution. The lepton + neutrino + b jet invariant mass then gives a distribution which is roughly comparable in width to that obtained from the three jet invariant mass distribution.

The main systematic uncertainty associated with m_t comes from the determination of the jet energy scale. Current estimates give a 5% overall uncertainty. This result is obtained using test beam data and models for jet fragmentation to estimate the detector response. This would give a 6 GeV uncertainty for m_t = 130 GeV. Techniques for better determining the jet energy scale using collider data can be used. For example, requiring p_t balance between "photon" and hadron jets allows transfer of the well understood EM

calibration to the hadronic calorimeter. Studies have shown that this technique allows $\leq 2\%$ jet energy scale calibration. Finally, the reconstructed W mass values in top events provide an excellent calibration. The statistical precision of determining the central value of M_W from a large sample of top events is roughly $25\ \text{GeV}/\sqrt{N}$.

Incorrect association of underlying event particles with the correct top quark decay products gives additional systematic error. Studies have shown this effect to be about 2 GeV for $m_t = 150$ GeV; we expect that the error associated this combinatorial effect should be about one-half of this, or 1 GeV. It is expected that the additional factor of 5 in integrated luminosity from the Main Injector will not only shrink the statistical uncertainty, but must also help improve the systematic uncertainties on m_t. For $m_t \leq 200$ GeV, where systematics will dominate, a reasonable prediction is that the overall uncertainty can be reduced from 5 GeV to 2-3 GeV. Given the precision of fitting M_W, it is not out of the question that one may approach a 1 GeV systematic uncertainty.

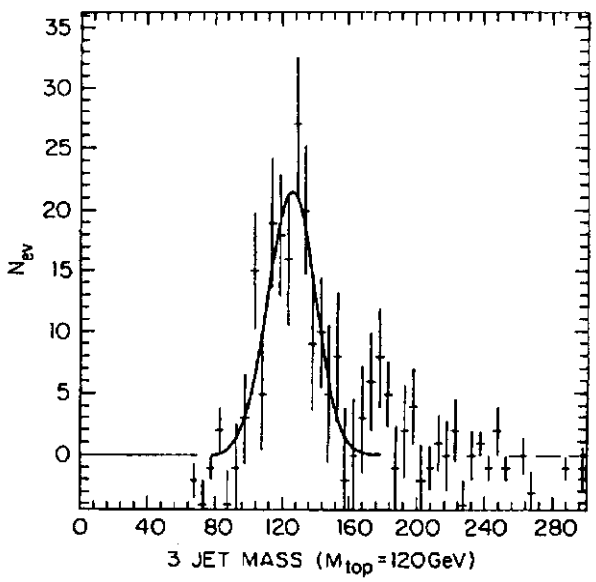

FIGURE 3.4: Reconstructed 3-jet invariant mass distribution for top with a mass of 120 GeV in events with leptons, 4 jets and missing transverse energy. This is representative of the statistics from 1 fb^{-1} of integrated luminosity. A b jet is tagged via a soft lepton. The combinatoric background has been suppressed via a sideband subtraction.

3.2.4 Top quark properties

In addition to a discovery and mass measurement for top, a significant yield of top events (of order 1000) can provide important information on its couplings and on the possible presence of new physics. In some cases with dynamical symmetry breaking there will be departures from the left-handed couplings of top. A yield of 1250 top events (assuming 130 GeV for m_t) in observable channels dilepton or lepton + jets will allow significant tests of the couplings of the top quark to W –b. In the rest frame of the W, one can construct the decay angle $\tilde{\theta}$ as the angle between the direction of the outgoing lepton and the boost direction of the W. In the limit of very heavy top, longitudinal W's dominate and the decay distribution goes like $sin^2\tilde{\theta}$. In this limit left and right handed decays are not distinguishable. For m_t = 120 (240) GeV, the asymmetry is 15% (11%). For the lighter values of m_t (≈ 130 GeV) giving a significant event yield, it should be possible to be sensitive to a 25% admixture of right handed coupling.

In models with charged Higgs or technipions, the top can decay into H^+b. Decay modes for H include $c\bar{s}$ and $\tau\nu$. The existence of these decay modes will change the ratio of branching fractions into dileptons versus lepton and jets significantly. This can be detected with the large sample of events that would be available with the Main Injector if the mass is near the canonical value. A contribution of 10% charged Higgs to the total branching fraction should be observable for m_t near the central value (140 GeV).

3.3 THE MEASUREMENT OF M_W

The precision of M_W is still limited by statistics. With the Main Injector, the Tevatron Collider will become a W factory with one million W's expected. There are three dominant sources of uncertainty in the determination of M_W:

a) Statistics (≈ 350 MeV at present).

b) Systematic uncertainty in the determination of the transverse momentum of the neutrino and energy scale (≈ 190 MeV at present).

c) Structure function uncertainties which lead to uncertainties in the longitudinal motion of the W (≈ 50 MeV).

The statistical uncertainty will decrease with increasing luminosity. The systematic uncertainty on the determination of the missing transverse momentum will also shrink with an increase in luminosity. The detector response can be calibrated with a large (100,000)

sample of Z's, where one electron or muon leg is excluded, and the recoil motion is determined from hadronic energy in the rest of the detector. With a) and b) becoming smaller as the luminosity increases, the error associated with parton distribution functions becomes the limiting uncertainty. This uncertainty is related to the longitudinal motion of the W and its effect on the shape of the transverse mass distribution. One major element in this uncertainty is the u/d quark ratio. Since this effect has not been the dominant uncertainty in any of the analyses to date, the true limit has not been fully explored. We assume that knowledge of the parton distribution functions will improve, and that this contribution to the uncertainty will shrink.

With 1 fb^{-1} the statistical uncertainty (including calibration of the detector response to missing transverse momentum and event pileup) is less than 40 MeV. Combined with the uncertainties from parton distribution functions, an overall uncertainty of 50 MeV is attainable. This error is smaller the estimated precision from LEP 200 ($\approx$ 100 MeV). With 200 pb^{-1} at the Tevatron an uncertainty of 100 MeV is achievable. As shown below the difference between a 100 MeV and 50 MeV error is significant in attempts to place constraints on the Higgs mass. Table 3.2 summarizes the estimated contribution to the M_W uncertainty from all known sources. Also given are the uncertainties from the present CDF measurement.[4)]

Source	Projected Uncertainty [MeV]	Present CDF [MeV]
W Statistics	20	350
Energy Scale	20	190
Resolution, p_t^W	10	145
Lepton Subtraction	10	170
Background	20	50
Fitting	20	50
Parton Distribution Functions	25	50
Overall	50	470

TABLE 3.2: Estimated uncertainties on M_W with 1 fb^{-1} of integrated luminosity and the uncertainties from the current CDF measurement using 4.2 pb^{-1}.

3.4 CONSTRAINING ELECTROWEAK PHYSICS

For the purposes of precision studies of the electroweak standard model one must specify essentially four observables. To date we have precise determinations of three of these, α, G_F and M_Z. Given a fourth quantity, such as M_W, the underlying gauge parameters of the standard model (the two couplings g_1 and g_2, and the two masses M_W and M_Z) are fixed, and one can then use the calculus of the standard model to compute other quantities for comparison to experiment, e.g., m_t (with weak dependence upon m_H), or $sin^2\bar{\theta}$, etc.

The reduced uncertainties of the Main Injector, $\sigma(M_W) = 50$ MeV and $\sigma(m_t) = 2$ to 5 GeV, give a tight constraint in the M_W - m_t plane. If the minimal standard model is correct the data point must lie on one of the lines in Figs. 3.5 and 3.6. Figure 3.5 shows the discovery potential of the Tevatron Collider without the Main Injector (assuming 200 pb^{-1}). A measurement of M_W with a precision of 100 MeV and a discovery reach on m_t up to 185 GeV are obtainable. Figure 3.8 shows the expected reach and precision resulting from 1 fb^{-1} of data collected with the Main Injector.

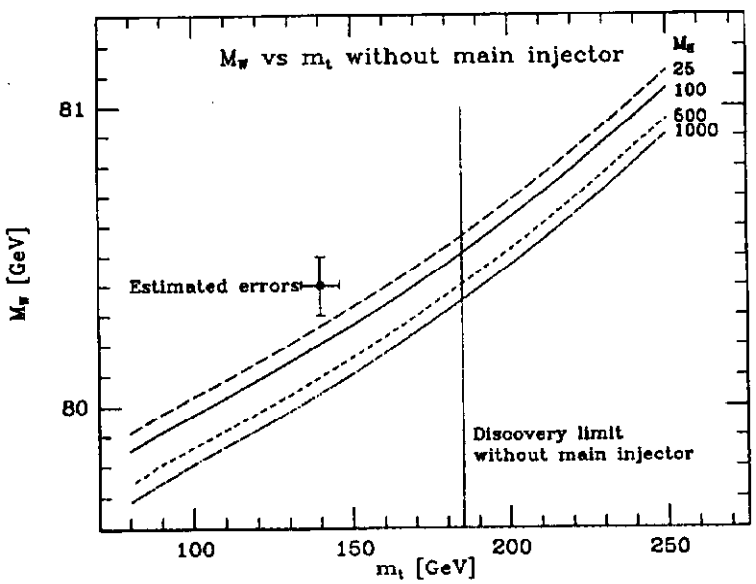

FIGURE 3.5: Expected precision on M_W and m_t with 200 pb-1 of data collected at the Tevatron Collider. Also shown is the discovery reach on m_t.

This is the most crucial test to which the standard model will be subjected in the coming years. The failure of the measured point in the M_W - m_t plane to lie on one of the standard model curves is a direct harbinger of new physics, e.g., a new heavy $M_{Z'}$, or a fourth sequential generation, etc. Moreover, with the main injector we can hope to discriminate between mass scales for the Higgs boson if the point does lie on the one of the lines. Discrimination between 100, 300 and 1000 GeV Higgs boson mass scales will be possible only with the main injector, and unlikely without it. We should mention that when the top mass is measured precisely, together with M_W, one can recalibrate the S and T and U parameters, which allow the search for new physics in other precision measurements, such as $sin^2\overline{\theta}$.

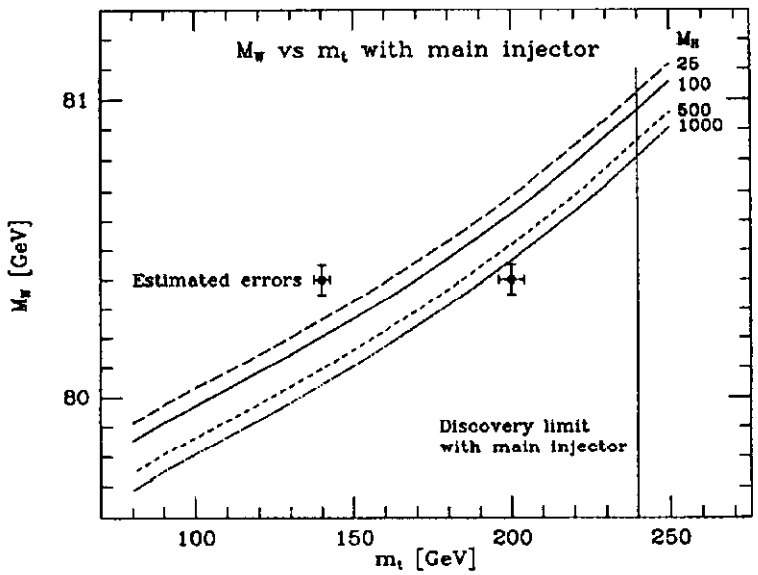

FIGURE 3.6: Expected precision on M_W and m_t with 1 pb-1 of data collected at the Tevatron Collider. Also shown is the discovery reach on m_t.

The Tevatron and main injector allow study of the interference between a virtual photon and a Z in the process $q\bar{q} \rightarrow l^+l^-$ which gives rise to the forward-backward asymmetry in the angular distribution of lepton pairs. The measured asymmetry A_{fb} can be used to derive $sin^2\overline{\theta}_W$. Using $\alpha(M_w)$, and G_F one can translate this into an effective M_w determination within the standard model by the approximate formula, $M_W^2 = \pi\alpha(M_W)/G_F\sqrt{2}\sin^2\overline{\theta}$ which is fairly insensitive to m_t and M_H. One thus finds $\delta M_W/M_W = \delta\sin^2\overline{\theta}/2\sin^2\overline{\theta}$.

With a sample of 100,000 events, the statistical uncertainty in $sin^2\overline{\theta}_W$ will be 0.0009 from the asymmetry on the resonance. This measurement is relatively insensitive to detector acceptances. The dominant systematic uncertainty should come from the proton structure functions. With the large sample of jet, direct gamma, W and Z events in a 1 fb^{-1} exposure, this systematic uncertainty should become insignificant. Thus an error on $sin^2\theta_W$ of 0.0009 should be obtainable. This uncertainty is comparable to the ultimate value from LEP in the mode $e^+e^- \rightarrow \mu^+\mu^-$ (≈ 0.001).

Using the relationship with M_w one finds an implied precision of $\delta M_w \sim 160$ MeV. The implied M_w can be compared to the on-shell measurement, and can be used to extract the S parameter, which is a measure of new physics. Moreover, the combined analysis of $sin^2\overline{\theta}$, M_w and m_t in the Tevatron collider experiments can be expected to lead to a partial cancellation of some of the residual systematic uncertainties such as those coming from energy scale or structure functions.

3.5 NEW PHYSICS

The Tevatron Collider with the Main Injector offers the possibility of discovery of new phenomena outside of the Standard Model. The possibilities are diverse, and we mention here a small handful. Most speculations about new physics revolve around the issue of electroweak symmetry breaking and fall roughly into two categories: (1) Supersymmetry, in which a plethora of new states, the SUSY partners of known and additional new particles, must materialize near the weak scale; (2) Dynamical symmetry breaking as in Technicolor, ETC, and Top Quark Condensate models in which new strong forces in analogy to QCD are expected near the weak scale or above.

3.5.1 Supersymmetric particles

Supersymmetry is an attractive candidate mechanism for generating and protecting the delicate electroweak hierarchy. It is expected in the effective low energy theory of superstrings, which is the best known candidate for accommodating unification of all the known forces, including gravity. Moreover, there are recent arguments[5] that the unification of the strong, electromagnetic and weak interactions requires the existence of supersymmetry at scales not far above the weak scale. This in turn implies the existence of SUSY particles of masses as low as 200 GeV.

Gluinos are likely to be most copiously produced in colliders. For searches above the presently excluded region ($m_{\tilde{g}} \leq m_{\tilde{q}} \leq 130$ GeV) the most likely scenario provides for cascade decays of $\tilde{g}$, $\tilde{q}$ into intermediate chargino states ($\tilde{W}$ etc.) before final decays to the lightest supersymmetric particle. This cascade decay chain reduces the missing E_T somewhat, but opens some possibility for detection of leptons from the charginos. We expect that gluino searches assuming cascade decays and based upon multijet and missing E_T signatures can be extended out to $m_{\tilde{g}} \leq 300$ GeV in the Main Injector era. The primary background is expected to be (Z+jets production, with $Z \rightarrow \nu\bar{\nu}$). The presence of charginos in $\tilde{g}$ decays gives the added possibility for confirmation of $\tilde{g}$ production up to 250 GeV/c^2 through observation of energetic leptons, multijets and missing E_T.

3.5.2 Dynamical symmetry breaking

In dynamical symmetry breaking schemes a new QCD-like interaction between techniquarks, or conventional quarks and leptons, must exist at scales above the weak scale. Powerful constraints on the fermion content of such models already exists from the S parameter which arises from measurements of $sin^2\overline{\theta}$, in particular in Cesium atomic parity violation.

In most of these models one expects a large number of pseudo-Nambu-Goldstone bosons which mimic charged Higgs bosons. These are expected to most strongly coupled to the heaviest fermions, and point to non-standard top quark decay modes as a possible signature.

Charged scalar bosons occur in several extensions to the SM. LEP will search for these up to about m_Z The prospect for heavy top opens a window for Tevatron searches for $m_Z \leq m_{H\pm} \leq m_t$, where $t \rightarrow H^+ + b$ can occur and compete with $t \rightarrow W + b$. The relative branching ratios are controlled by the unknown ratio of vacuum expectation values of the Higgs doublet, but are typically between 0.01 and 100. Decay of the H^+ occurs dominantly into $c\bar{s}$ or $\tau\nu$ in a ratio that is also controlled by the Higgs v.e.v.'s. The existence of the $H^{\pm} \rightarrow \tau\nu$ permits sensing the Higgs by the excess of τ's over μ's or e's.

3.5.3 Compositeness

Although at present there is no model for quark or lepton substructure, the 3 generations of Fermions provides some motivation to search for signs of compositeness. On general grounds, one can parameterize the effects of substructure by adding a four-fermi term to the QCD Lagrangian with a characteristic energy scale Λ_c.[6] Quark/lepton

substructure would be indicated by a statistically significant excess of jets and/or Drell-Yan pairs at very high transverse energies. Currently limits on substructure from the process $q\bar{q} \sim q\bar{q}$ gives $\Lambda_c^{qq} \leq 1.4$ TeV (95% C.L.), and $\Lambda_c^{qe} \leq 1.7$ TeV (95% C.L.) from $qq \sim l+l-$ (CDF results). In the future, the collider experiments should be sensitive to values of Λ_c^{qq} of 2 TeV and 3 TeV for Λ_c^{qe}. Sensitivity to strongly interacting guage bosons, like axigluons, should extend to masses of approximately 1 TeV.

3.6 REFERENCES

1. J. Carter, Lepton Photon Symposium Rapporteur Talk, Geneva, July 1991.
2. P. Langacker, Univ. of Penn. preprint, UPR-0492T, Jan. 6 1992.
3. F. A. Berends, *et al* ., FERMILAB-PUB-90/213-T (1990).
4. F. Abe, *et al* ., (CDF collaboration), *Phys. Rev.* D48: 2070 (1991).
5. U. Amaldi, W. de Boer, H. Fürstenau, CERN-PPE/91-44 (March 8, 1991).
6. E. J. Eichten, *et al* ., *Phys. Rev. Lett.* 50: 811 (1983).

4 COLLIDER BEAUTY PHYSICS

4 COLLIDER BEAUTY PHYSICS

4.1 INTRODUCTION

A systematic and high statistics study of the decays of B mesons will provide a number of basic tests of the Standard Model. For this reason many groups have considered the feasibility of experiments at both e^+e^- and hadron colliders which would permit the production and measurement of sufficiently large samples of B mesons. Due to the large production cross section of B's at the Main Injector many people believe that a particularly good opportunity exists for addressing many of the interesting and fundamental questions in B physics there. The basic challenge which faces this approach is certainly technological. Detector systems must be developed and commissioned which are generally more sophisticated than previously used in order to isolate the necessary sample in a well measured and unbiased way.

In recent years a number of studies have been made and proposals submitted to Fermilab concerned with the study of B decays at the collider.[1-9] These have represented both evolutionary upgrades of the existing collider detectors (CDF and D0) as well as completely new initiatives (BCD and P845). In this section we will discuss the prospects for making basic Standard Model tests and more general studies of B production and decay as outlined in these contributions. It is significant to point out that hadron collider B physics has been rapidly maturing since the early inclusive studies of UA1 at CERN. From its last run, CDF has fully reconstructed a number of exclusive decays. Furthermore, many of the important technological issues are already being addressed at Fermilab and within the user community.

To pursue this program considerable technical development is necessary in triggering, data acquisition, and particle identification. Many of the assumptions in these studies need to be verified with either careful simulation, or preferably, data from CDF and D0.

4.1.1 B Physics at the Collider

Assuming the standard model, the structure of the CKM matrix forces states which exhibit CP violation to have small branching ratios, typically a few $\times 10^{-5}$. As a consequence experiments which measure CP violation will need to collect huge samples of tagged b decays. At Tevatron energies the cross section for b pair production is about

60μb. [10, 11] At the Main Injector peak luminosity of 5.7×10^{31}, 3400 b pairs are produced per second. In a three year run 9×10^{10} b pairs will be produced. The signal to minimum bias background ratio is approximately 0.1%, similar to the signal/background successfully addressed in fixed target charm studies. The issue at the Main Injector is how to trigger on, collect, and reconstruct these events.

Figure 4.1 shows a scatterplot of the relativistic boost, γ, vs the pseudorapidity of B mesons simulated using ISAJET. The plot exhibits several essential features which drive experimental design.

1) The production cross section is a broad distribution in pseudorapidity, this translates into a forward peaked distribution in the laboratory.

2) B's produced in the central rapidity region tend to be soft, with γ typically less than 2. Secondary vertices in this region will be compromised due to multiple scattering and short decay lengths.

3) In the forward region (η~3) γ is typically less than 10, implying approximately 50 GeV/c Bs and rather low P_T decay products.

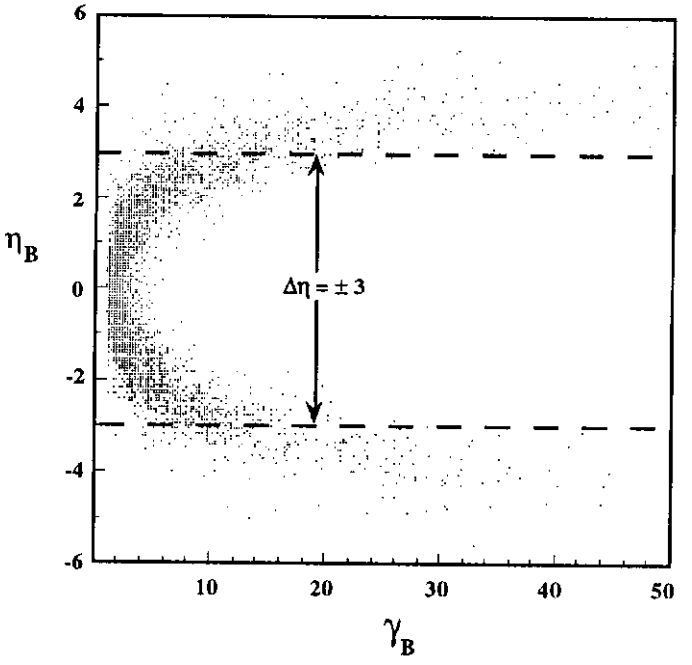

FIGURE 4.1: Plot of η_B vs γ_B for B's produced at the collider.

In addition the B pairs are expected to be correlated in rapidity with $\Delta\eta$ less than 2. From these considerations we can list the capabilities of an "optimized" B physics detector. This description serve as a reference point to the explicit discussion of rates and signals

given in the following sections. In what follows we will assume a detector with the following properties unless otherwise noted.

- Charged particle tracking and momentum analysis to $\eta = 3$
- 3D vertexing to $\eta = 3$
- Secondary vertex or impact parameter trigger for $B \rightarrow \pi\pi$
- Particle ID for pions and kaons
- Finely segmented electromagnetic calorimetry over the full tracking coverage
- High speed readout and DAQ
- Online processing farm

In Section 4.6 various technological developments required or under way will be discussed. We list here however areas of work in which people in the Fermilab community are already active.

- CDF has installed a silicon vertex detector and is studying upgrades to it.
- The Pisa/CDF group are developing a secondary vertex trigger.
- D0 has proposed a sophisticated silicon tracker for its upgrade and is undertaking mechanical and cooling design studies.
- R&D on particle ID for hadron colliders is being pursued at Fermilab.
- BCD has carried out mechanical studies of a 3D vertex detector.
- A secondary vertex trigger will be tested at CERN in conjunction with the new P-845 proposal.
- Fermilab is in the process of constructing a dedicated facility for silicon detector work.
- A number of groups have developed and tested radiation hard electronics for silicon readout.
- Fixed target experiments at Fermilab have developed a number of high rate triggering and DAQ systems.
- A number of SSC related developments such as the pixel work at LBL could find application in B physics at the Main Injector.

In addition, Fermilab has held a number of workshops on the physics and technology of B decay at the collider.[12, 13] Most important, data from the existing collider detectors and their near-term upgrades will guide experimental design of an optimized detector.

We assume the Main Injector running at a luminosity of 5×10^{31}. The total cross section for b quark production is taken to be 60 μb. Current CDF data indicates that this is conservative. The production above some minimum P_T is shown in Fig. 4.2.

4.1.2 CDF B Physics Results and Near Term Prospects

The CDF experiment has made two measurements of the b-quark cross section using 5 pb^{-1} of data acquired in 1988-1989. The first uses the inclusive electron sample. Evidence that these electrons are from semileptonic b decay comes from associated charm and strange particles. CDF observes the decay chain $D^0 \rightarrow K\pi$ when taking pair-mass combinations of all tracks within an $\eta - \phi$ cone of 0.6 around the electron candidate. This is presumably from the decay chain $B \rightarrow e\nu D^0 X$. If the electron-D^0 rate were from $c\bar{c}$ pairs, one would expect roughly equal rates of K^{0*} and $\bar{K}^{*0}$ to be found in the region of the electron. Instead the K - π mass spectra in the $K^*(890)$ region for 'right-sign' combinations to come from b decay ($e^- \bar{K}^{*0}$) and for 'wrong sign' ($e^- K^{*0}$) combinations are quite different. There is a significant excess of right-sign events in the K^{*0} peak, consistent with the expected $b \rightarrow e^- \nu c$ transition and little evidence for wrong-sign events. The observed D^0 rate agrees with ISAJET predictions and verifies that roughly 75% of the inclusive electron sample is from semileptonic b decay. The b cross section derived as a function of b quark P_T from the electron rate is shown in Fig. 4.2.

Another measure of the b-quark cross section can be derived from the sample of events containing at least two muons. This sample contains a clean ψ peak of about 2900 events. CDF has succeeded in the first B meson reconstruction outside of e^+e^- experiments.[14] Two final states are observed, $B^+ \rightarrow \psi K^+$ and $B \rightarrow \psi K^*$. Figure 4.3a shows a signal of 35 ± 9 events. A typical ψK^+ event is shown in Fig. 4.3b. Using the rate of $B^{\pm} \rightarrow \psi K^{\pm}$, the cross section for b quarks with $P_T > 9$ GeV is measured, and also shown in Fig. 4.2.

CDF also measured χ, the combined mixing parameter for B_d and B_s mesons, to be 0.176 ±0.031 (stat+sys) ±0.032(model) using e-μ and e-e dilepton events.[15] When combined with CLEO and ARGUS measurements of χ_d, assuming a reasonable production fraction of B_s mesons, the CDF result implies χ_s is near the saturation point of 0.5, as

expected. Finally, CDF has placed a preliminary upper limit on the branching fraction for $B^0 \rightarrow \mu\mu$ of 3.2×10^{-6}. [16] This result is the world's best limit.

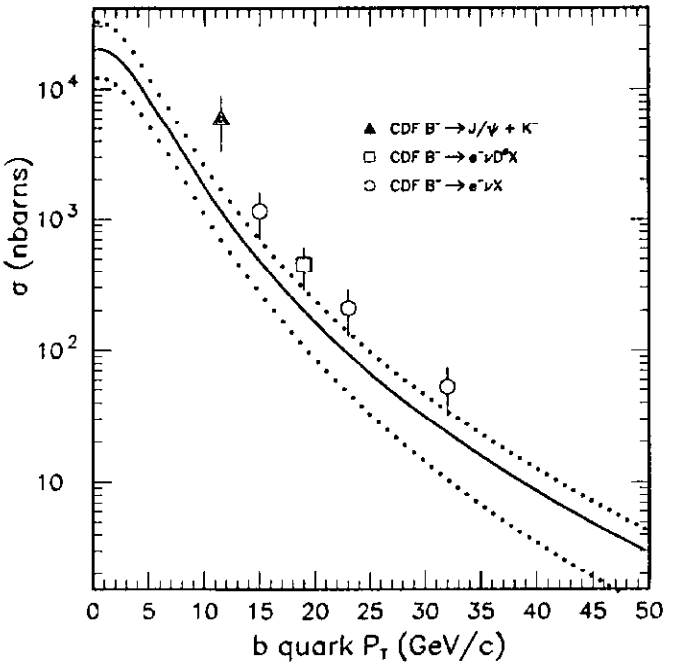

FIGURE 4.2: b quark cross section as a function of $P_{T,min}$ (GeV/c) for $|\eta_b|<1$.

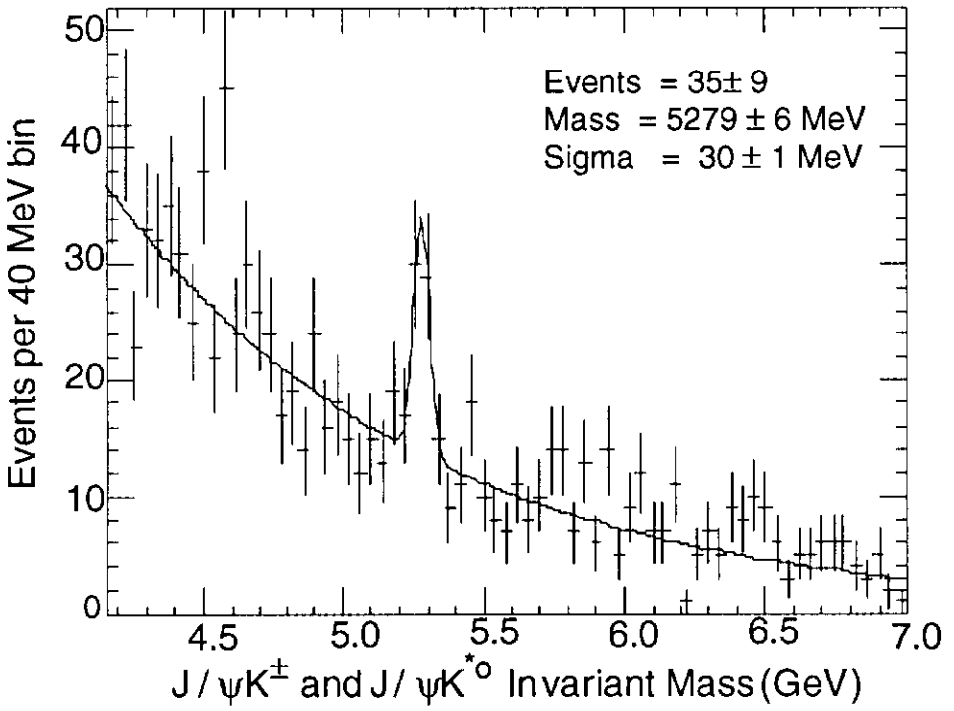

FIGURE 4.3a: The two B decay modes, $B^0 \rightarrow \psi K^{*0}$ and $B^{\pm} \rightarrow \psi K^{\pm}$ observed in CDF.

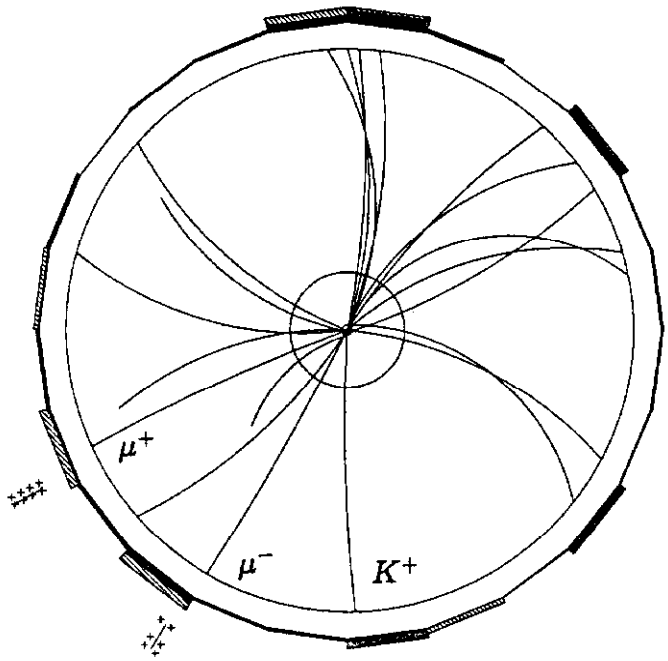

FIGURE 4.3b: CDF event display showing the Central Tracking Chamber and muon hits for a candidate $B^+ \rightarrow \psi K^+$, $\psi \rightarrow \mu\mu$ event.

These results allow us to predict, with a few assumptions, the rates of fully reconstructed B_u, B_d and B_s, as well as Λ_b decays expected in future runs. In the 1992-1993 run D0 and CDF hope to collect roughly 100 pb^{-1}. CDF will have improved muon coverage, a more efficient dimuon trigger, and the recently installed Silicon Vertex Detector. This should yield thousands of fully reconstructed B mesons and on order 10^6 semileptonic b decays. Exclusive lifetimes for the B^0, and $B^{\pm}$ should be made with a few percent error. The B_s and Λ_b should be observed, and possibly the B_c as well. In addition, the next CDF dataset will be quite informative about the prospects for future high rate b measurements at the Tevatron. B tagging studies and the experience gained using the SVX, for example, will certainly clarify the b-physics potential of future runs.

4.2 CKM PARAMETERS

Within the Standard Model quark mixing is described by the Cabibbo-Kobayashi-Maskawa unitary 3×3 matrix:

$$VQq = \begin{pmatrix} Vud & Vus & Vub \\ Vcd & Vcs & Vcb \\ Vtd & Vts & Vtb \end{pmatrix}$$

CP violating effects are accommodated naturally in this formulation since the matrix elements may include a complex phase. CP violation may arise in both the Kaon system, where it has been extensively studied, and in the B system, where it is yet to be observed There is currently no evidence confirming the hypothesis that a single phase in the CKM matrix can accommodate CP violation in both the K and B systems. The matrix itself arises from the quark mass matrix in the electroweak model and thus has a deep connection to fundamental physics.

Because this matrix is unitary various constraints must exist between its elements. A useful representation of the matrix was written by Wolfenstein:[17)]

$$V_{Qq}=\begin{pmatrix} 1-\lambda^2/2 & \lambda & A\lambda^3(\rho-i\eta) \\ -\lambda & 1-\lambda^2/2 & A\lambda^2 \\ A\lambda^3(1-\rho-i\eta) & -A\lambda^2 & 1 \end{pmatrix}$$

A and λ are related to well measured quantities, the Cabibbo angle and the B lifetime. Parameters ρ and η remain to be measured to define the CKM matrix. Measurements are often displayed as angles of the "unitarity triangle", shown in Fig. 4.4. The parameters are in turn related to a number of experimental measurements in the B and K systems detailed in Table 4.1.

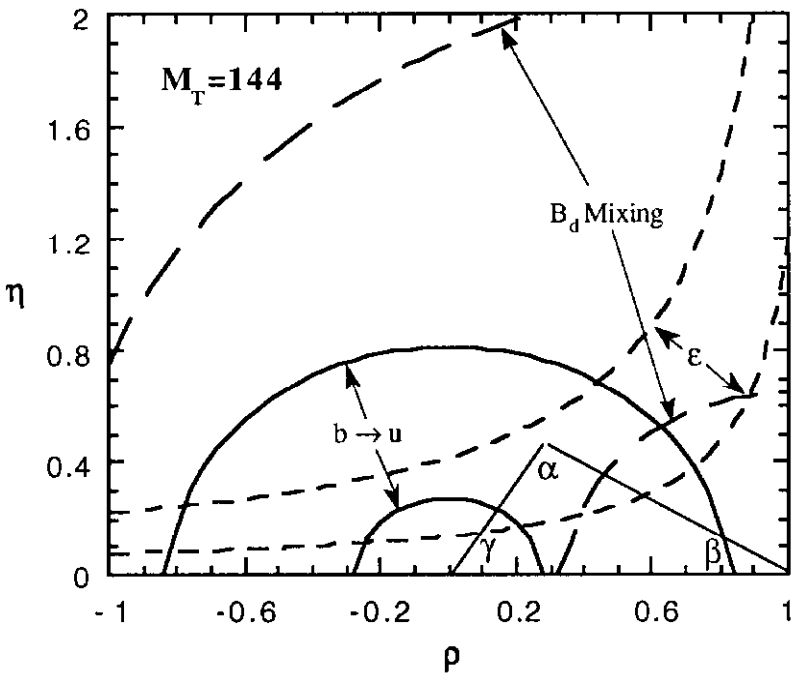

FIGURE 4.4: Present knowledge on ρ and η.

Measurement	Constraint
1) b→u	$\frac{\lvert V_{ub}\rvert^2}{\lvert V_{cb}\rvert} \approx \lambda(\rho^2+\eta^2)$
2) B_s, B_d mixing	$\approx ((1-\rho)^2+\eta^2)$
3) CP violation in $B_d \rightarrow \psi K_s$	lines in ρ vs η plot (sin 2β)
4) CP violation in $B_d \rightarrow \pi\pi$	circles in ρ vs η plot (sin 2α)
5) CP violation in $B_d \rightarrow D^0 K$	lines in ρ vs η plot (sin 2γ)
6) $\frac{\varepsilon'}{\varepsilon}$ from K decay	lines of constant η
7) ε from K decay	curves in ρ vs η plot

TABLE 4.1: Constraints on ρ and η.

Our current knowledge of ρ and η (with 1 σ errors) assuming a 144 GeV/c^2 top mass is shown in Fig. 4.4. The relation of measurements in the K system to the ρ vs η plot are currently subject to considerable theoretical uncertainty.[18-20] The top quark mass is a crucial parameter in interpreting the measurements from K decays and mixing. Much of the theoretical uncertainty in the B mixing measurement cancels if both B_s and B_d mixing are measured.

An important goal for High Energy Physics in the next decade is to overconstrain the unitarity triangle, thus testing the CKM model. In addition precise measurements of the CKM parameters may provide insight into the physics underlying quark mixing and mass. We expect that the Main Injector will contribute substantially to this work by:

- Measuring the top quark mass to 5 GeV/c^2
- Measuring $\frac{\varepsilon'}{\varepsilon}$
- Measuring sin (2β) to $\pm$ 0.07
- Measuring x_s directly if $x_s < 20$

We have studied the possibility of measuring sin(2α) using a tagged sample of B→$\pi\pi$. We are hopeful that the technical obstacles can be overcome. If so, a measure of sin(2α) to $\pm$0.1 is possible. In addition there is the possibility that rare decays can give information on V_{td}/V_{ts} if x_s is greater than 20. We also expect CLEO to improve the accuracy of V_{ub} to 10% in the next 5 years. The combined result of these measurements is shown in Fig. 4.5.

It is worthwhile to note that errors in ρ and η from measurements other than sin(2β) and sin(2α) will probably be dominated by uncertainties in theoretical calculations.

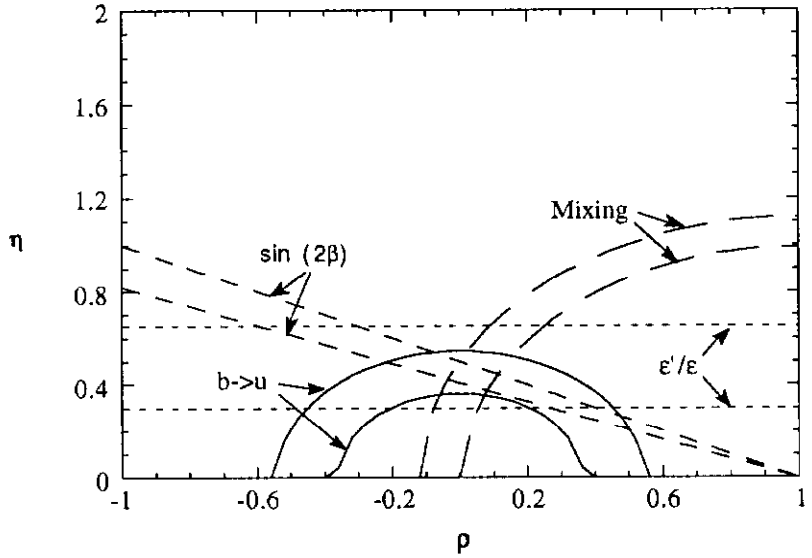

FIGURE 4.5: Predicted knowledge on ρ and η Main Injector and e^+e^- (b→u) experiments.

4.2.1 CP Violation

Accuracy of the CP violation measurement depends on the yield of tagged events, the dilution factor caused by mixing of the tagging B, and mistagging due to charm decays or background. At the Tevatron an explicit measurement of the time evolution of the decay is not required. The accuracy in sin(2β) for such a time integrated measurement is:

$$\delta(\sin 2\beta) = \frac{1+b}{D(1-2w)\sqrt{N(1+b)}}.$$

The dilution factor, D, is defined as $D = \frac{x_d}{(1+x_d^2)}$, and accounts for mixing on the signal side, N is the number of tagged events, *w* is the fraction of wrong sign tags including wrong tags due to mixing and b is the background to signal ratio. The resolution in sin 2β depends on the mix of B flavors on the tagging side, their mixing rates, and the fraction of wrong sign tags due to backgrounds or mistagging. D0, BCD and P845 have discussed dilution in their Tevatron proposals.

Most CP violation studies require a tag on the meson flavor at birth. Flavor tagging can be done by using either a lepton or kaon from the b→c→s chain. The efficiency of lepton tags suffer from the ~22% B semileptonic branching ratio. Kaon tags are, in

principle, a factor of four more efficient in tagging b flavor, but require particle identification. Kaon identification is discussed in more detail in the technology section.

The overall yield depends on the triggering and tagging strategy chosen. A decay such as $B^0 \rightarrow \psi K_S$, $\psi \rightarrow \mu\mu$, is straightforward to trigger on with an efficiency of 15-20%. Decays which do not involve leptons, such as $B^0 \rightarrow \pi\pi$, or B_s decays, can be collected using a secondary vertex trigger. Single lepton triggers on the partner B are also viable for less rare decays and spectroscopy and lifetime studies. Efficiencies for these triggers are more difficult to calculate and depend on the lepton P_T cut in the case of the lepton trigger and the detailed implementation of a secondary vertex trigger. A possible secondary vertex trigger is discussed in the section on $B \rightarrow \pi\pi$. Table 4.2 summarizes the triggering and tagging efficiencies and dilution factors expected at the Main Injector for dimuon and vertex triggers based on the D0, BCD, and P845 studies.[2-9]

	$B_d \rightarrow \psi K_s$ dimuon trigger	$B_d \rightarrow \pi\pi$ vertex trigger
Branching ratio	1.9×10^{-5}	2×10^{-5}
trigger efficiency	0.15	0.06
tag efficiency(e,μ)	0.03	0.03
tag efficiency(K)	.15	.15
Wrong sign fraction(e,μ)	.2	.2
Wrong sign fraction(K)	.3	.3

TABLE 4.2: Efficiencies for measurement of CKM angles.

4.2.2 CP Violation in $B \rightarrow \psi K_s$

The decay of the B_d into the CP eigenstate, ψK_S, with the dilepton decay of the ψ, provides the cleanest signature for CP violation. The trigger efficiency depends primarily on the angular coverage of the lepton identification system and the P_T threshold of the trigger. CDF has shown that the ψK mode can be reconstructed with adequate signal/background without the benefit of vertex detection and accompanying kinematic constraints (P_T balance...), only modest angular coverage, and an inefficient trigger. Sophisticated vertex triggering is not necessary for ψK_S.

The error in $\sin(2\beta)$ is 0.07. This is based on $1 fb^{-1}$ of data, the decay $B \rightarrow \psi K_S \rightarrow \mu^+\mu^-\pi\pi$, and the values in Table 4.2. The error can be reduced if a combination of multilepton (electron and muon) triggers are used. A D0 study, which assumes only muon

tagging, finds an error of 0.15 in $1fb^{-1}$. In the experiment tagging efficiencies and mistagging rates can be measured accurately using reconstructed charged B decays. We expect that the optimal tagging scheme will emerge from these studies and may well include a combination of lepton and kaon tagging as well as the use of partial reconstruction.

4.2.3 CP Violation in $B \rightarrow \pi\ \pi$

The second angle in the unitarity triangle can be measured from the $B \rightarrow \pi^+\pi^-$ decay asymmetry. At hadron colliders triggering on such all-hadronic modes is difficult. In addition rejecting the large combinatoric background is a challenge. However with technologies that are now available, it appears the trigger problem can be solved. There have been studies by BCD which indicate vertex cuts can achieve the necessary background rejection. In the following section we discuss a possible trigger implementation based on CDF experience. P845 has discussed similar techniques.

The detector assumed for this study is a solenoid design with high resolution tracking out to pseudorapidity of 2 for detecting the $B \rightarrow \pi^+\pi^-$ decay, and muon detectors, moderate resolution tracking for electrons, and kaon identification out to a rapidity of 3 for tagging the other B in the event. A 3-D silicon vertex detector will cover this entire rapidity region. The trigger is a three level system similar to that in CDF. In fact the trigger described below is modelled on CDF hardware currently in use or being designed for the 1995 Collider run as well as designs which have been prototyped for the SDC.

The Level 1 trigger uses fast trigger signals from the calorimeters. It requires two calorimeter cells each with $E > 1$ GeV and $|\eta| < 2$. The sum of the two cell energies must be > 4 GeV, and at least one of the cells is required to have $E_T > 1.5$ GeV. The resulting trigger rate, based on existing CDF minimum bias data, is 280 KHz at $L = 5 \times 10^{31}$ cm^{-2} sec^{-1}. The trigger decision can be made in 1.3μ sec. Since the bunch crossing time will be 132 nsec, a switched capacitor array with 10 capacitors per channel could serve as the Level 1 pipeline. When a Level 1 trigger occurs, the data is transferred into the Level 2 pipeline. The Level 2 trigger described below takes 10μsec; thus a pipeline 6 events deep will keep the Level 2 deadtime below 5%.

The Level 2 trigger decision is based on tracking information. To avoid trigger bias that could produce a B- $\bar{B}$ asymmetry, events are selected using the $B \rightarrow \pi^+\pi^-$ decay, not the B that flavor tags the event. Two tracks with $P_T > 2$ GeV/c and $|\eta| < 2$ are required. At least one of the tracks must have a 2-D impact parameter $> 200\mu$. The two track invariant mass is required to be within 500 MeV/c^2 of the B mass. The mass is determined using a

2-D hardware track finder and coarse z information from a tracking layer at the outermost radius of the tracking system. The impact parameter requirement is based on a hardware track finder being designed for the CDF silicon vertex detector. The resulting Level 2 trigger rate is 70 Hz. This rate easily allows full event readout into a farm of high speed processors.

The Level 3 trigger is a software decision based on partial or complete reconstruction of the event in the farm of high speed general purpose processors. Events with a $\pi^+\pi^-$ invariant mass close to the B mass and a flavor tag for the second B will be recorded on tape. In addition, samples of events needed for efficiency and background measurement will also be retained.

The b quark production cross section at 1.8 TeV is 60μb. The probability that the b quark forms a B^0 meson is 35%, and the $B^0\rightarrow\pi^+\pi^-$ branching ratio is assumed to be 2×10^{-5}. The efficiency for the trigger criteria described above is 6%. Thus in a 1 fb^{-1} data run, 54,000 $B^0\rightarrow\pi^+\pi^-$ events should be collected. The expected two-body mass resolution is 25 MeV.

BCD has studied the signal to background ratio using a ISAJET/GEANT simulation. Decays of B baryons and higher mass B mesons were included. With limited statistics and a P_T cut on the pions of 1 GeV the signal/background was about 1:1. More recent preliminary high statistics studies are showing slightly worse signal/background. The signal/background will improve for the assumed P_T cut of 2 GeV/c. The decay $B\rightarrow K\pi$, expected to have a similar branching ratio to $B^0\rightarrow\pi^+\pi^-$, was not included in the BCD study. With the expected mass resolution and modest kaon ID, this background should not be a problem. With over 10^6 semileptonic B decays and vertex identification, CDF should be able to measure the background rejection in the next run.

B tagging will be done with leptons (e and μ) and kaons not pointing to the primary vertex. The lepton tagging efficiency should be 2.7%, while the K tagging efficiency should be 15%. Taking into account dilution from mixing, reconstruction efficiency, the presence of 100% background , and the fraction of incorrect tagging (20% for leptons, 30% for kaons), the uncertainty in $\sin(2\alpha)$ should be 0.12 for K tags and 0.19 for lepton tags. The net uncertainty thus should be 0.1.

In summary, with a trigger strategy based on currently available technology, the CP asymmetry in $B^0\rightarrow\pi^+\pi^-$ decay could be very competitively measured at the Fermilab Collider after the Main Injector is commissioned.

4.2.4 B_S Mixing

Both the B_d and B_s are expected to mix with their antiparticles. This mixing is related to the V_{td} and V_{ts} CKM elements:

$$x_d \sim |V_{td}|^2 \; m_t^2 \, F(m_t^2, m_W^2) \; m_B \; f_{Bd}^2 \, B_{Bd} \, \eta_{Bd} \, \tau_{Bd}$$

$$x_s \sim |V_{ts}|^2 \; m_t^2 \, F(m_t^2, m_W^2) \; m_B \; f_{Bs}^2 \, B_{Bs} \, \eta_{Bs} \, \tau_{Bs}$$

where x is the ratio of the mass difference to the width, $\frac{\Delta m}{\Gamma}$, m_t is the top quark mass, $F(m_t^2, m_W^2)$ is a function of the top and W masses, m_B is the B mass, f_B is the decay constant and B_B is the bag parameter. Both x_d and x_s contain substantial theoretical uncertainties in f_B^2 and B_B. However many of these uncertainties cancel out in the ratio since B_s and B_d parameters are correlated:

$$\frac{x_s}{x_d} = \frac{f_{Bs}^2 \, B_{Bs} \, \eta_{Bs}}{f_{Bd}^2 \, B_{Bd} \, \eta_{Bd}} \frac{1}{\lambda^2((1-\rho)^2+\eta^2)}$$

Given the measurement of $x_d = 0.69 \pm 0.17$, current theoretical expectation is that x_s will be greater than 8 and may indeed be quite large if f_{Bs} is substantially larger than f_{Bd}.

The prospects for measuring B_s mixing were studied using resolution and acceptance from the D0 upgrade Monte Carlo. Similar studies have been performed for BCD and P845. A large sample of events was generated using a GEANT Monte Carlo and the resulting tracks were fit. The track resolution was parameterized as a function of vertex position, slope and momentum. The Monte Carlo assumes 50μ pitch SSDs with coverage of ±3 in η and a 2.4 cm beam pipe radius. Vertices were fit using a vertex fitting package from the fixed target experiment E653.

In this study B_s were identified by reconstructing the φ from the $B_s \rightarrow D_s$ chain. Two scenarios were considered:

1) Full reconstruction of both B_s and D_s. Using a simple single lepton trigger with $P_T > 4$ GeV we expect ~5400 tagged fully reconstructed events in the $B_s \rightarrow D_s \pi\pi\pi$, $D_s \rightarrow \phi\pi$ chain in 1 fb^{-1}. These events are tagged using the trigger lepton.

2) Partial reconstruction assuming 1 or more missing neutrals. We expect 10-30 times more partially reconstructed events with $D_s \rightarrow \phi X$.

Full reconstruction has the advantage that the B momentum is well measured, thus reducing the lifetime error. On the other hand the estimated branching ratio for $B_S \rightarrow D_S\pi\pi\pi$ is only about 1%. The oscillation itself has the form:

$$N(B_S \rightarrow \bar{B}_S) = \frac{N_0}{2} e^{-t/\tau}(1 - \cos(x_S t)/\tau)$$

Where N_0 is the number of B_S at t=0 and τ is the B_S lifetime. The $\cos((x_S t)/\tau)$ term is extracted by taking the difference of mixed and non-mixed events.

Figure 4.6 shows the result of the simulation for 2000 tagged, reconstructed $B_S \rightarrow D_S\pi\pi\pi$, $D_S \rightarrow \phi\pi$ events with x_S=12. A five sigma cut was imposed on the significance of the vertex (decay length/δ(decay length)). Background is expected to be small in the fully reconstructed sample. A simple fit to the term $\cos((x_S t)/\tau)$ yields x_S=12.01±.05.

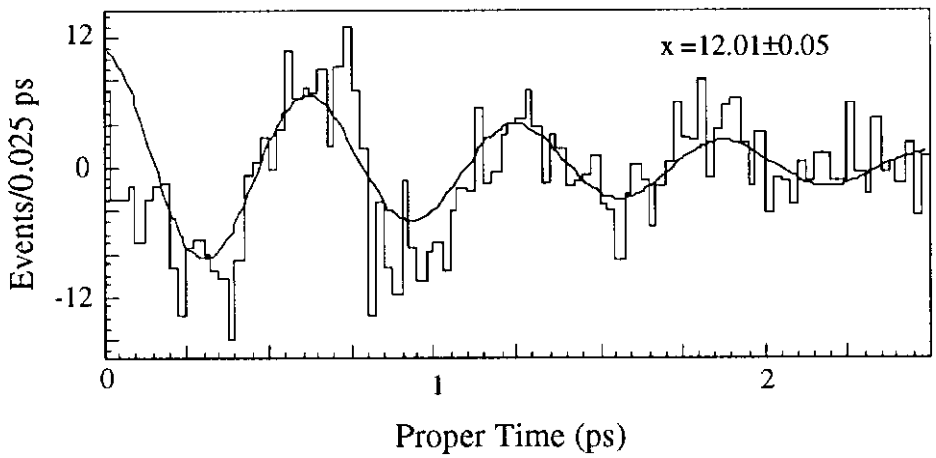

FIGURE 4.6: Proper time distribution for reconstructed B_S^0 decays. Events tagged as mixed are subtracted from events tagged as unmixed. A 5σ cut is placed on the significance of the decay length. The fit is to an exponential lifetime term times $\cos(x_S t/\tau)$.

BCD has estimated the number of tagged events needed for a 5σ measurement as a function of x_S, including effects of mistagging fraction, and lifetime resolution. Their result is:

$$N = \frac{50}{\pi(1-2w)} x \; e^{4\pi/x} \; e^{(x^2-1)\sigma_t^2/2}$$

where w is the mistagging fraction and σ_t is the fractional lifetime resolution. For fully reconstructed events the error in the lifetime is dominated by the decay length measurement. The reach in x_S depends directly on the lifetime resolution which in turn depends on the decay length cuts. Figure 4.7 shows the lifetime error in the simulation with 5σ and 10σ cuts on the calculated decay length significance. The lifetime error can be reduced from

7.5% to less than 4% with a 38% loss in efficiency. Resolution for partially reconstructed states is limited to ~15% by the momentum errors. The expected mistagging fraction is 0.2. Figure 4.8 shows the number of events needed for a 5σ measurement of x_S for σ_t=0.04, 0.075 and 0.15.

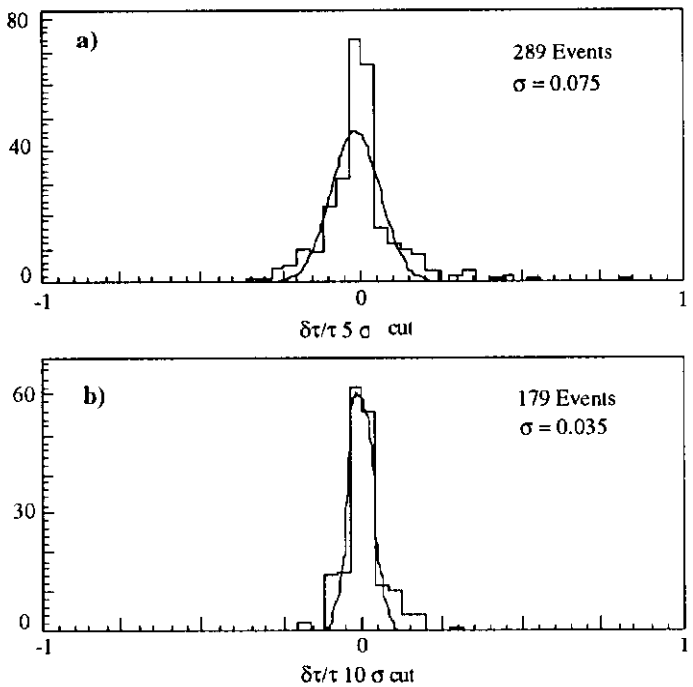

FIGURE 4.7: Lifetime resolution for (a) 5 and (b) 10 σ cuts on the significance of the fitted decay length.

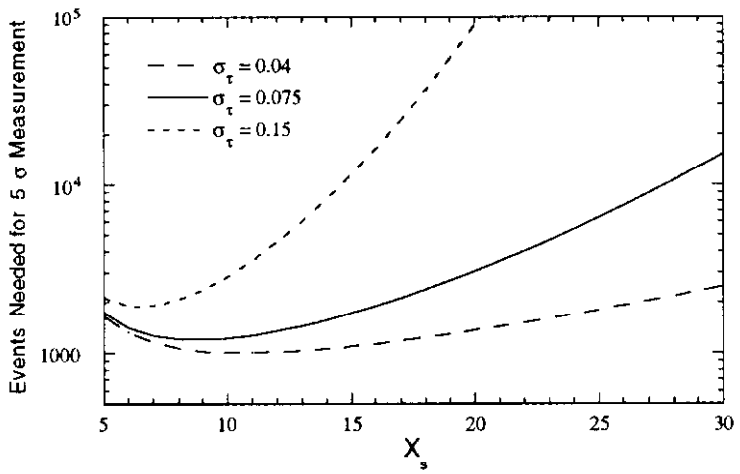

FIGURE 4.8: Events needed for a 5 σ determination of x_S as a function of x_S and lifetime resolution, σ_t.

4.3 B_C PHYSICS

With an integrated luminosity of 1 fb^{-1}, the Tevatron Collider will produce approximately 5×10^{10} b quarks. This opens for study the rich spectroscopy of mesons and baryons beyond $B_u^{\pm}$ and B_d^0. In addition to B_s and Λ_b, a particularly interesting example is the spectrum of $b\bar{c}$ states[21] shown in Fig. 4.9. The $b\bar{c}$ states that lie below the $B\bar{D}$ threshold cannot decay by annihilation into gluons, so their total widths are less than a few hundred keV. All decay by E1 or M1 transitions or their strong-interaction analogs, ultimately reaching the $^1S_0$ ground state, which decays weakly. It may be possible to map out the excitation spectrum by observing photons in coincidence with a prominent B_c decay, in much the same way as CDF has reconstructed the χ_c states by observing photons in coincidence with leptonic decays of ψ.

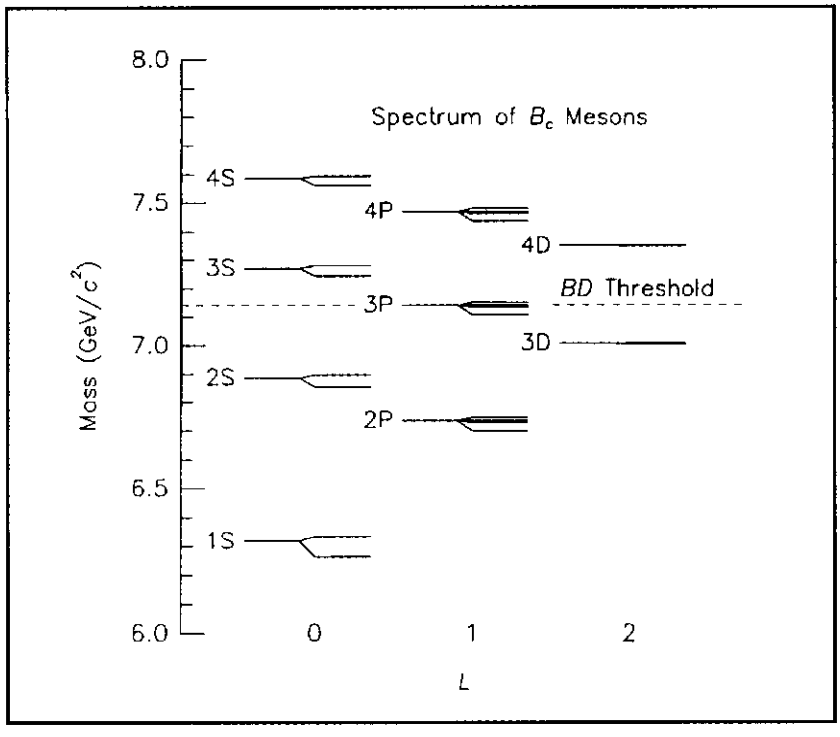

FIGURE 4.9: Spectrum of B_c mesons.

The weak decays of the $b\bar{c}$ ground state are of particular interest because the effects of QCD can be estimated reliably. The deep binding of the charm quark within the B_c leads to a rather long expected lifetime, $\tau(B_c) \approx (1.35 \pm 0.15)$ ps, that implies easily observable secondary vertices. The deep binding also influences the B_c branching ratios. The inclusive branching ratios are predicted[21] to be:

Inclusive Decay Mode	Branching Fraction (%)
$b \rightarrow c$	53 ± 3
$\overline{c} \rightarrow \overline{s}$	15 ± 4
$b\overline{c} \rightarrow W_{virtual}$	33 ± 3

B_c production at the Tevatron Collider has been estimated[22] to be $(1.2 \pm 0.3) \times 10^{-3}$ times the b-quark cross section. This suggests that in a two-year run approximately 7×10^7 B_c mesons will be produced in the CDF and D0 detectors. At LEP, approximately 500 B_c mesons are produced in 10^6 Z^0 decays, so details of the spectrum will not be studied there.

Signatures that will serve to identify and reconstruct Bc mesons include the modes $B_c \rightarrow \psi\, \pi^+$, $B_c \rightarrow \psi\, l^+\, \nu$, $B_c \rightarrow \psi\, \rho^+$, and $B_c \rightarrow \psi\, D_s$. The branching ratio for the discovery channel $B_c \rightarrow \psi(\rightarrow \mu^+\mu^-)\, \pi^+$ is expected to be approximately 10^{-4}, so several thousand events should be produced.

4.4 RARE DECAYS

The study of rare B decays offers very interesting and fundamental physics possibilities. They offer a way to observe new high energy phenomena through low energy processes. Also in principle they offer a way to constrain V_{ts}/V_{td}.

The decays $b \rightarrow l^+l^-$ and $b \rightarrow l^+l^-\, s$ are rather sensitive to the top quark mass(See Fig. 4.10).[23] By the same reasoning they are also sensitive to other heavy particles that couple like the top quark, such as 4th generation quarks,[24] or objects associated with physics beyond the minimal Standard Model.[25-26]

The branching ratios for the exclusive decays $B_d \rightarrow \mu^+\mu^- K(K^*)$ and $B_s \rightarrow \mu^+\mu^-\, \phi$ should be between 10^{-6} and 10^{-7} and should be observable at Fermilab with the main injector upgrade. Current CDF data for the $B \rightarrow \psi\, K^*$ show that the resonant (ψ) and nonresonant dimuon backgrounds, without the aid of kaon identification or vertex information, are comparable. The signal for $B \rightarrow \mu^+\mu^-\, K^*$ is expected to be roughly a factor of 100 lower than that for $\psi\, K^*$. This implies that added background rejection of roughly 100 is needed from vertexing and kaon identification to observe these states. In 1 fb^{-1}, with a dimuon trigger and assuming an efficiency comparable to that for $\psi\, K^*$, one expects 2500 events in the $\mu^+\mu^-\, K^*$ mode for a 5×10^{-7} branching ratio. A measure of the top mass to 5 GeV predicts the branching ratios for $B \rightarrow K^*(K)\mu\mu$ to about 28%. There are

models, such as the two Higgs doublet model of Grinstein et al.,[26] which predict a deviation from this of up to an order of magnitude. Not all models predict an increase in these branching ratios, which places an added emphasis on higher luminosity.

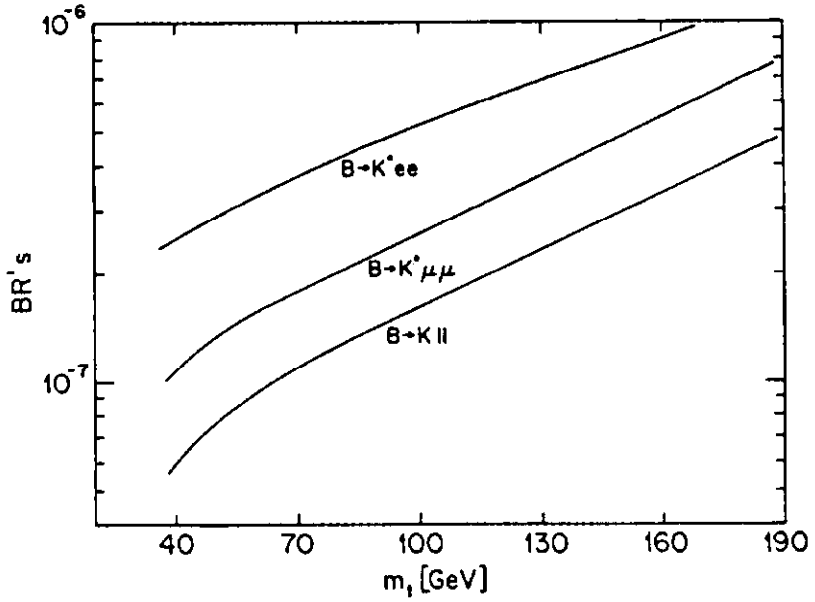

FIGURE 4.10: Branching ratios of the rare processes $B \to Kl\bar{l}$, $B \to K^* e\bar{e}$, and $BB \to K^* \mu\mu$ as a function of m_t.

CDF data indicates background rejection of 1000 is needed from vertexing to observe $B_s \to \mu\mu$. If background problems can be resolved, the sensitivity for $B_s \to \mu\mu$ should be $\sim 10^{-9}$, close to the theoretical prediction for this branching ratio.

The second possible physics measurement gleaned from rare b decays is a measure of V_{ts}/V_{td}. There are several ways of extracting V_{ts}/V_{td} from rare decay modes at the Tevatron. If the minimal Standard Model holds, radiative penguins and box-diagram rare decays will couple dominantly through the top quark. By measuring the ratio of final states such as $b \to s\mu\mu / b \to d\mu\mu$, one would effectively be measuring $(V_{ts}/V_{td})^2$, with cancellation of most theoretical uncertainties.

To obtain V_{ts}/V_{td} we can measure the ratio of branching ratios such as $B \to \mu\ \mu\ K^*$/ $B \to \mu\ \mu\ \rho$. Here the limiting factor is statistics and background rejection on $B \to \mu\ \mu\ \rho$, which will be produced about a factor of 10 less than $\mu\ \mu\ K^*$. Assuming similar trigger and reconstruction efficiencies as ψK_S we can expect 300 reconstructed $B_d \to \mu\ \mu\ \rho$ events in each 1 fb^{-1}. We could add statistics by looking for other modes such as $B \to \mu\ \mu\ \pi$.

The larger rate expected for $B \rightarrow K^* \gamma$ and $B \rightarrow \rho \gamma$, which are thought to be about 5×10^{-5} and 5×10^{-6}, respectively, make this an attractive pair in which to attempt to measure V_{ts}/V_{td}. At CDF the mass resolution for B into modes like this is about 150 MeV. As has been suggested, a dedicated B experiment could possibly benefit from a high resolution electromagnetic calorimeter.[27] Also, a particle identification system with π/K discrimination would help cleanly separate the signals for $B \rightarrow \rho \gamma$ and $B \rightarrow K^* \gamma$. With the existing CDF data, the signal/background for $B \rightarrow K^*$ gamma is about 1/10 before the advantage of vertex information. Background rejection via vertex tagging can be tested in the upcoming CDF run. With a gamma trigger with threshold of $P_T > 5$ GeV would yield over 7,000 reconstructable $B \rightarrow \rho \gamma$ events in a 1 fb^{-1} run.

In conclusion, the study of rare B decays at the main injector offers the possibility for unique and fundamental measurements by placing constraints on extensions to the SM, constraints on the CKM matrix elements V_{ts} and V_{td}.

4.5 COMPARISON TO e^+e^-

The b-quark was discovered at Fermilab. Most of our knowledge of the properties of the B-mesons have been derived from experiments at e^+e^- storage rings at Cornell and DESY. However, to attack the exciting topic of CP violation in the B sector, one needs higher luminosity than can be achieved at these facilities. Several studies have been undertaken to design e^+e^- storage rings which have enough luminosity to begin the exploration of CP violation. All these design efforts have reached the same conclusion: that the best way to proceed is with an asymmetric collider running on the prominent low lying resonances such as the $\Upsilon(4S)$ and the $\Upsilon(5S)$. The asymmetric configuration gives the center of mass of the system a boost characterized by $\beta\gamma$ of approximately 0.42, which permits the measurement of the time evolution of the B-decay. We compare the capabilities of experiments at such facilities with those of the Fermilab Main Injector(MI).

A word of caution: both approaches to B-physics have difficulties which must be overcome. For the e^+e^- colliders, the problems are mainly related to the machine design. In order to achieve the sensitivity required for CP violation studies, much higher luminosities need to be achieved and the detectors must be made to work in potentially severe synchrotron radiation fields. For the Fermilab Main Injector, the most serious problems are related to the capabilities of the experiments. Experiments must achieve

higher levels of triggering and reconstruction efficiency than have been obtained in the past, when experiment design was driven mainly by high P_T physics.

Table 4.3 shows the luminosity assumptions on which the rate estimates are based. For the existing facilities, the numbers are based on projections obtained from members of the experiments.[28] For the future facilities, the numbers are extracted from the appropriate design reports.[29] Also included in the table are the relevant production cross sections. It can be seen from the Table that the very high B-production cross section at the Main Injector overcomes the projected higher luminosity of the e^+e^- storage rings leading to potentially much larger samples of B-meson pairs.

Facility	Luminosity	$B\text{-}\bar{B}$ cross section	Luminosity per year	B pairs per year
CESR/CLEO Υ(4S)	3×10^{32}	1.15 nb	3.3 fb^{-1}	4×10^6
LEP	2×10^{31}	6.3 nb	0.2 fb^{-1}	1.3×10^6
FNAL(Pre MI)	1×10^{31}	60 μb	0.1 fb^{-1}	6×10^9
e^+e^- B-FACTORY Υ(4S)	3×10^{33}	1.15 nb	30 fb^{-1}	3.5×10^7
$\Upsilon(5S) \rightarrow B_S \bar{B}_S$	3×10^{33}	0.1 nb	30 fb^{-1}	3×10^6
FNAL MI	5×10^{31}	60 μb	0.5 fb^{-1}	3×10^{10}

TABLE 4.3: Luminosity assumptions, cross sections, rates of produced B's

Table 4.4 gives the details used in going from raw rate of produced events to the accuracy of the final measured number for B factories and the Main Injector. It includes triggering efficiency, tagging efficiency, reconstruction efficiency, the effect of mistagging, the effect of backgrounds, etc.

The B-factory is limited by the choice of running conditions (e.g. Y(4S) vs Y(5S)) to a few physics topics at a time. On the other hand, the B-factory constrains the final state in ways which simplify the problem of tagging events and reduces backgrounds. This must be compensated, in the hadron collider experiments, by excellent triggering and reconstruction efficiency, good secondary vertex resolution, and particle identification. If these objectives can be achieved,experiments at the Main Injector are fully competitive in measuring $\sin(2\alpha)$ and $\sin(2\beta)$. Measurement of $\sin(2\gamma)$ via charged B decays may also be feasible at the Main Injector. V_{ub} probably can not be measured very well at a hadron collider and probably could be measured at a B-factory or possibly even CLEO II. B_s

mixing is probably out of reach of B-factories given what is believed about the size of f_b but is probably within the capabilities of the Main Injector. Moreover, experiments at the Main Injector will have better sensitivity to rare decays and new physics than the B-factory. Finally, the Main Injector experiments allow one to study a wide range of topics simultaneously. This includes studies of the baryon sector, which may also bear on CP violation and studies of the B_c system, which are interesting from the standpoint of QCD.

Determination of sin 2β	**LEP** ψ K_s **only**	**B Factory** Σ **6 modes**	**FNAL MI** ψ K_s **only**
Integrated Luminosity	4×10^{38}	6×10^{40}	1×10^{39}
B pairs	2.5×10^6	6.9×10^7	6.0×10^{10}
B→final states	74	5796	8.5×10^5
Trigger efficiency	1	1	0.15 (μμ)
Reconstruction efficiency	0.46	0.61	0.2
Tag efficiency	0.61	0.48	0.15+0.027
Tagged, reconstructed	21	849	4500
Wrong sign fraction	0.125	0.08	0.3
Dilution	0.61	0.61	0.47
δ(sin 2β)	0.48	0.05	0.07

TABLE 4.4: Determination of sin(2β) in two years of running for LEP, a B Factory and a dedicated experiment at the Main Injector.

4.6 HARDWARE R&D

The hardware necessary to accomplish the b-physics program outlined above is either being developed for the upgrade of CDF and DO or is well within the technical envelope of the hardware that is being developed for the SSC. Many of the ideas we are investigating have been inspired by SSC electronics R&D. In addition the next run will give the first solid data about the behavior of a Silicon Vertex detector in a hadron collider and will furnish the base for the program being envisaged here.

At present, the CDF SVX is a two-dimensional device, and it is generally recognized that for adequate event reconstruction, a 3D device is necessary. Next in line is the development of faster readout electronics since the data is needed in the trigger. The electronics to process this data must be implemented to the point where a secondary vertex can be used in the level 2 triggers. Finally particle ID must be designed.

Both CDF and D0 have considered how to solve the foregoing problems. In addition there has been a proposal from BCD as well as P845 from a U.S.-European Collaboration. All of these groups have concluded that the hardware problem is well within our technical ability. We now discuss the needed developments.

4.6.1 SVX Geometry

The SVX must provide 3D vertex reconstruction in an extended angular range of 3 units of rapidity. This is an extension of the present CDF device. The obvious solution is to use a double sided detector. The accurate mechanical alignment of the plates and discs and the removal of the additional heat from the electronics must be worked out. There is a big premium on extending the tracking in the forward direction, and it is possible that a shorter bunch length would be beneficial. Whether or not this is cost effective must be determined. Finally we note the vulnerability of the electronics to radiation. Rad hard electronics have already been developed for the CDF SVX, and we do not believe that radiation will limit the detector.

4.6.2 SVX Readout

The present CDF SVX is far from optimum in its readout. A natural development would be to read out optically each detector of 128 strips. We envisage two fibers and two power leads per readout chip. The GEM Collaboration has an active program to investigate a system using Mach Zehnder electro-optical modulators to read out the data. These devices operate by splitting the incoming light into two channels. One channel is a wave guide a few microns on a side that is filled with $LiNbO_3$. The two beams are then recombined. An electric field applied to the $LiNbO_3$ arm causes a phase shift of that light relative to the other arm. The devices are such that a 5 volt signal will modulate the combined signal from on to off. The field is applied to the $LiNbO_3$ by means of a 50Ω transmission line that is 15 mm long, and the device has a band width of 4 GHz. Most important here is that the readout uses fiber optics with a low volume, mass, and Z. In addition the power on the chip is limited to the modulator. If we assume that we readout by using edge transition (as is done for magnetic tape) then an 0.2 V signal would be sufficient. The power is then limited on the 50Ω line to $(0.2)^2 / 50 = 0.8$ mW dc which is much smaller than the chip power.

The chip itself must have a pipeline on it for level 1 and 2. The first is necessary because the Tevatron upgrade will have bunch spacings of 130 nsec. A trigger system that

can operate from the calorimeter in 1.3 μsec is already being developed for the CDF and D0 upgrades. Thus a switched capacitor or some other storage device 10 deep will suffice to make level 1 free from deadtime. A secondary storage will then be necessary to hold the event in a buffer for level 2. Such a device is already well along in its development for the SSC including an ADC to digitize the pulse height from the strips.

Studies have shown that an individual detector will have perhaps a 2% occupancy. Thus with 7 bits for an address, and 5 bits from the ADC, there are only $0.02 \times 128 \times (7 + 5)$ bits, 30 bits/chip/event that need reading out. A readout time of 1 μsec is then reasonable. If the ADC takes 1 μsec, then the event is available after 3.3 μsec for use in level II.

4.6.3 Event Processing

Several approaches have been taken to the event processing. P845 has the silicon in a field free region and use the Nevis-University of Massachusetts processing technology to detect a track not coming from the primary vertex. A group at Pisa has been working on a device that will work with the present two-dimensional CDF geometry. Since the particles are in a magnetic field, the impact parameters must be calculated using the track momentum as well as the SVX information. CDF already has developed two such fast tracking devices that give the track momentum and are used in the Level II trigger. A design for the computer and memory that combines the fast tracker with the SVX data exists but has not yet been implemented. This is an area where the power of fast processors is rapidly increasing and again is in the mainstream of the type of hardware that must be developed for the SSC.

4.6.4 Particle ID

Finally we come to particle ID. The most effective tag as to particle/antiparticle character of a neutral B is via the sign of the kaon from $b \rightarrow c \rightarrow s$ cascade decay of the second B in the event. The majority of all-charged decays of B and D mesons include one or more Kaons. In studies performed by the BCD collaboration it was demonstrated that a Kaon tag would be about four times as effective as combined electron and muon tags. Considering the extended momentum range which must be covered by the particle identification device and the limited geometry available the most efficient solution involves a combination of Time-Of-Flight(TOF), $\frac{dc}{dx}$, and Ring-Imaging Čerenkov (RICH) techniques.

Figure 4.11 shows the momentum spectra of K's from B→DK for three pseudorapidities regions between 0 and two. Figure 4.12 shows the momentum spectra of K's from B→D, D→KK for pseudorapidities between 0 and 2. It is worth noting that these are rather soft. The time of flight difference between a 3 Gev/c pion and kaon is about 80ps for a flight path of two meters. It is clear that a system with an off line resolution of better than 100 psec would be very useful. Additional work on low pressure parallel plate counters with TMAE-CsF_2 cathodes may help solve this problem. Alternatively we note that CLEO has a system with a σ of 120 psec in use now. dE/dx is a well developed technique and can be implemented on the wires of the tracking chamber. The disadvantage is a hole in the πK separation at about 800 MeV/c. However, a TOF system fills this hole and complements the dE/dx system.

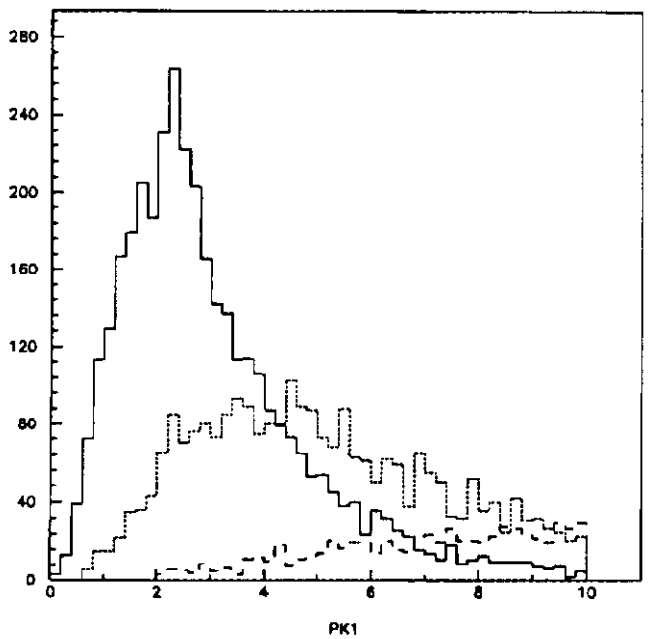

Figure 4.11. Momentum spectra for kaons from B→Dk for pseudorapidity ranges 0-1 (solid line), 1-2 (dotted line), and 2-3 (dashed line).

The viability of the RICH technique, which was proposed by Ypsilantis and Sequinot,[30] has been established by a number of groups who have successfully built and tested devices for use in high-energy physics experiments. The central problem to be faced in designing a RICH counter for use at TEV I (or the SSC) is obtaining stable operation in the anticipated high-rate high-multiplicity environment. The RICH detector must be sensitive to the single-photoelectron pulses from Čerenkov light, but insensitive to the ionization trails of through-going charged particles. Furthermore, it must be possible to extract signals using a narrow timing gate to minimize confusion from out-of-time events.

In most devices built thus far, an intrinsic jitter in the photoelectron detection time arises because the absorption length of the photosensitive gas is long enough that the photoelectrons are produced at varying distances in the amplification region and arrive at varying times. A very promising solution to this problem has been under study since the summer of 1990 in a research effort at Fermilab conducted by D.F. Anderson, B. Hoeneisen, S. Kwan and V. Peskov.[31] The objective has been to develop a fast-imaging UV detector based on a solid CsI-TMAE photocathode with low pressure parallel plate avalanche multiplication and a pad readout. When coupling this detector to a C_6F_{14} or solid NaF Čerenkov radiator, the majority of limitations mentioned above can be eliminated. The quantum efficiency of this device at 185 nm is around 35% and gains of between 10^5 and 10^7 with a signal-to-noise ratio for single photo-electrons of 10,000:1 have been routinely obtained.

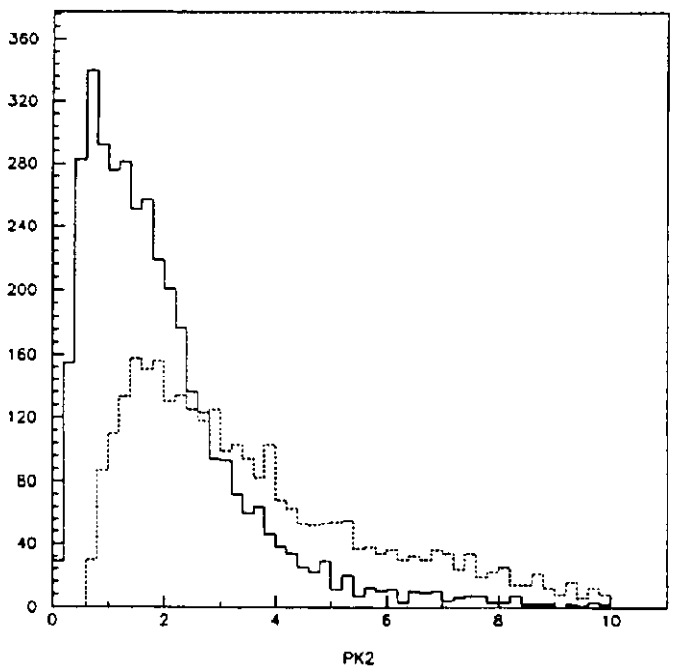

FIGURE 4.12: Momentum spectra for kaons from B→D,D→KK for pseudorapidity ranges 0-1 (solid line), 1-2 (dotted line).

The next step is to continue the R&D program with increased emphasis on understanding the aging process and solving the construction problems with small test chambers. The near-term goal is to begin construction of a prototype central RICH section which would be installed in a data-taking experiment for the 1994 fixed target run.

4.8 REFERENCES

1. B Physics at CDF, CDF/DOC/HEAVY FLAVOR/PUBLIC/1482.
2. Fermilab Proposal 845, *A Dedicated Beauty Experiment for the Tevatron Collider*, January 7, 1991.
3. BCD SCC Letter of Intent.
4. Fermilab Proposal 827, The μBCD, October 8, 1990.
5. Fermilab Proposal 823, The D0 Upgrade.
6. N. Roe, *Measuring CP violation at the Upgraded TeV II*, D0 note #1122, May 1, 1991.
7. D0 Response to the Fermilab PAC, June 18, 1991.
8. D. Hedin, *B Physics Possibilities at D0*, D0 Note 742, August 7, 1988.
9. D. Hedin, *Muon Rates and Distributions and $B \rightarrow \psi K_S$ Study*, D0 Note 666, Febuary 9, 1988.
10. E.L. Berger, *Benchmark Cross Sections for Bottom Quark Production, Proceedings of the Workshop on High Sensitivity Beauty Physics*, p185, Nov. 1987.
11. P. Nason, S. Dawson, R.K. Ellis, *The total cross section for the production of heavy quarks in hadronic collisions*, Fermilab 87-222-T.
12. Workshop on High Sensitivity B Physics at Fermilab, Nov 1987.
13. Symposium on Particle Identification at High Luminosity Hadron Colliders, April, 1989.
14. F. Abe, *et al.* (CDF Collaboration), *A Measurement of the B Meson and the b-quark Cross Sections at $\sqrt{s}$ = 1:8 TeV Using the Exclusive Decay $B \rightarrow \psi K^+$* , FERMILAB-PUB-92-21-E, Submitted to *Phys. Rev. Lett.*, January, 1992.
15. F. Abe, *et al.* (CDF Collaboration), M*easurement of $B^0\overline{B}^0$ mixing at the Fermilab Tevatron Collider, Phys. Rev. Lett.* 67, 3351 (1991).
16. L. Pondrom, Proceedings of the 25th International Conference on High Energy Physics, Kent Ridge, Singapore, August 2-8 1990, also available as Fermilab-Conf-90/256-E.
17. L. Wolfenstein, *Phys. Rev. Lett.*, 51(1983) 1945.
18. J. Rosner, *CKM and B Physics*, EFI-92-02.

19. M. Witherell, *Heavy Quark Physics and the CKM Matrix*, UCSB-HEP-91-06.

20. J. Rosner, *The CKM Matrix*, EFI-91-49.

21. Estia J. Eichten and Chris Quigg, *Mesons with Beauty and Charm*, FERMILAB–PUB–92/42–T (in preparation).

22. M. Lusignoli, M. Masetti, and S. Petrarca, *Phys. Lett.* B **266**, 142 (1991).

23. G. Eilam and A. Soni, *Phys. Lett.* 215B, 171 (1988).W.S. Hou, R.S. Willey and A. Soni, *Phys. Rev. Lett.* 58, 1608 (1987).

24. N.G. Deshpande and J. Tampetic, *Phys. Rev. Lett* 60, 2583 (1988).

25. D. Cocolicchio, G. Costa, G.L. Fogli, J.H. Kim and A. Masiero, *PRD* 40, 1477 (1989).

    S. Bertolini, F. Borzumati, A. Masiero and G. Ridolfi, *NPB* 353, 591 (1991).

    I. Bigi and F. Gabbiani, *NPB* 352, 309 (1991).

26. B. Grinstein, M.J. Savage and M.B. Wise, *NPB* 319, 271 (1989).

    B. Grinstein, R. Springer and M.B. Wise, *NPB* 339, 269 (1990).

27. M. Artuso, *et al.*, *Letter of Intent to Measure CP Violation in B Meson Decay at the Fermilab Collider*, Sept. 26, 1990.

28. J.M. Soares, *et al.*, *Nuc Phys B* 367 (1991) 575-590.

29. SLAC 353, *Physics Program of a High Luminosity Asymmetric B Factory at SLAC* , Oct. 1989.

30. J. Sequinot and T. Ypsilantis, *Nucl. Instrum Meth.* 142, 377 (1977).

31. *Nucl. Instrum Meth* A302 447 (1991).

5 NEUTRINO PHYSICS

5 NEUTRINO PHYSICS

5.1 NEUTRINO OSCILLATIONS

5.1.1 Introduction

Neutrino oscillations are transitions among neutrino species. Mixing in the neutrino sector, although mathematically similar to mixing in the $K^0\overline{K}^0$ system, differs in a fundamental way: neutrino oscillations mix lepton generations. The discovery of neutrino oscillations would reinforce the symmetry between the quark and lepton sectors and profoundly advance our understanding of the nature of quark and lepton generations.

The probability of transitions is given by:

$$P = \sin^2 2\theta \sin^2 1.27\Delta m^2 \frac{L}{E} \tag{1}$$

where θ is a mixing angle between neutrino generations, analogous to the Cabibbo mixing angles among quarks; Δm^2 is the difference in the squares of the neutrino masses in eV^2. L is the distance over which the neutrino has traveled (in km) and E is its energy (in GeV). The masses of the neutrino species can be linked in the "See Saw" mechanism, which predicts the hierarchy of neutrino masses determined by the masses of their associated leptons. However, the See-Saw Mechanism does little more than arrange the neutrino masses in a hierarchy; there is little or no content about the underlying physics. That physics comes from mass scales of 10^{13}–10^{15} GeV, at least ten billion times greater than SSC energies.

The discovery of neutrino oscillations would be at least as important as the discovery of a new quark species or the discovery of the W and Z bosons, proving the existence of physics completely outside the Standard Model and providing the first data about what lies beyond it. Such a discovery would immediately establish the existence of a non-zero neutrino mass. It would show that there exists a mixing matrix among the neutrinos analogous to the Cabibbo-Kobayashi-Maskawa matrix among the quark sectors, and the size of the mass splitting would provide an estimate of the Grand Unification Scale. Neutrinos may solve a cosmological puzzle as well: according to Big-Bang cosmology there are almost as many neutrinos per unit volume as photons; massive neutrinos could provide the gravitational attraction to close our Universe.

Three sets of experiments have been proposed to test for neutrino oscillations at the Main Injector.[1)]

The first is based on the attractive hypothesis that dark matter could close the Universe and stop the initial expansion of the "Big Bang". A ν_τ with a mass of approximately 10–100 eV would suffice; such a measurement will probably never be achieved by conventional kinematic techniques. In addition to determining whether "hot dark matter" closes the Universe, the experiment could settle the question of the 17 keV neutrino; if the 17 keV neutrino is the ν_τ, the experiment would see a large, statistically significant effect. The experimental technique is based on a hybrid emulsion spectrometer, which could see the decays of the τ from ν_τ interactions; this is now a "third-generation" experiment, proposed by the same group that pioneered the method in E–531.

The second is motivated by the Atmospheric Neutrino Deficit seen in the deep underground detectors at IMB and Kamioka. A statistically significant deficit is seen in the ν_μ/ν_e ratio of neutrinos produced in the Atmosphere; this effect seems impossible to explain with known physics. The experimental technique is entirely new: a beam of neutrinos will be sent through the Earth and its properties measured hundreds of kilometers away; hence the name "long-baseline."

The two experiments have a wonderful synergy as well: by placing the first experiment at the end of a conventional beamline, but along the flight path of the long-baseline experiment, we can perform a measurement of the beam in two locations. The ν_τ experiment requires a densely instrumented, well-understood spectrometer and can provide a variety of useful measurements of the beam composition and spectrum. These will provide the cross-checks necessary to yield a believable signal from measurement hundreds of kilometers downstream of the source.

A third experiment proposes to use the Fermilab Debuncher to search for $\nu_e \rightarrow \nu_\tau$ oscillations, which have never been carefully studied.[2)] It would shed light on the 17 keV neutrino, but in any case, would provide the first high-energy ν_e beam. Such experiments have been carefully studied in the past and showed considerable promise.[3)] Eventually, a unique program of ν_e physics could be established.

All these experiments require intense, high-energy neutrino beams, and no machine other than the Main Injector fulfills their requirements. Without it, we will be throwing away a unique opportunity to study physics at energies far beyond that of even the SSC, and to answer questions that the collider experiments at the SSC or elsewhere are incapable

of even addressing. The community has enthusiastically determined that the experiment could and should be performed; the missing ingredient is the Main Injector.

5.2 EXPERIMENTAL PLAN FOR THE OSCILLATION PROGRAM

Main Injector protons must be targeted at dip angles from 30–70 milliradians toward a long-baseline detector separated by hundreds of kilometers from the Fermilab site. A double-horn focusing system will bend secondary particles into a 300 meter-long tapered vacuum decay pipe, followed by 300 meters of earth in order to range out muons. A short-baseline hall located just downstream will house the short-baseline detector plus a small copy of the long-baseline detector. Since both the short and long-baseline detectors will be located in the same place, the two can cross-calibrate each other and the performance of the long-baseline detector can be accurately measured with high statistics. Flux comparisons between the two locations will also search for oscillations into sterile neutrinos. The layout from the Fermilab Conceptual Design Report is shown in Fig. 5.1.[1)]

5.2.1 Long-Baseline Experiments and the Atmospheric Neutrino Deficit

Underground detectors, originally designed to detect proton decay, have unearthed one of the most tantalizing questions in physics. A simple calculation tells us that there should be approximately twice as many ν_μ as ν_e created by the decays of cosmic rays in the atmosphere. The observed ratio, in these deep underground detectors shielded from background, is roughly 1.2. The result implies a deficit of ν_μ and the effect has been named the Atmospheric Neutrino Deficit. The experiments were not designed to study such effects, making the analysis lengthy and difficult. Nonetheless, a strong case now exists that the Atmospheric Neutrino Deficit is real, seen in two detectors (IMB at $\approx 2.5\sigma$ and Kamiokande at nearly 5σ) and is the same size within errors. Combining all experiments with their errors yields a 6σ effect: the effect is unquestionably real, but the interpretation is far from settled.[4)]

The most natural interpretation of the Deficit is that the muon neutrinos have oscillated into another neutrino species. Interpreting the Atmospheric Neutrino Deficit as neutrino oscillations puts a central value at $\Delta m^2 \approx 10^{-2}\,\mathrm{eV}^2$ and $\sin^2 2\theta \approx 0.75$, assuming $\nu_\mu \rightarrow \nu_\tau$ oscillations. This region in parameter space could be definitively studied in a Main Injector experiment. The necessary value of L, the neutrino flight path, would be at least 600 km; hence the name "long-baseline". The neutrino beam, pointed down into the Earth at an

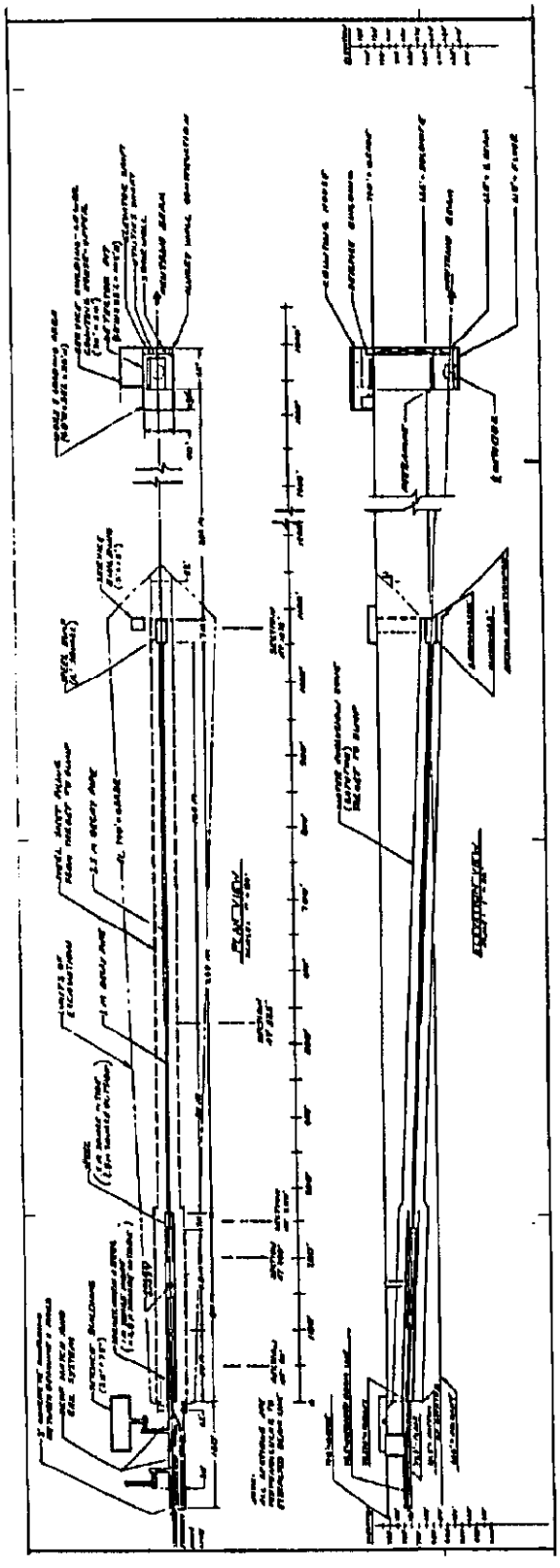

FIGURE 5.1: Layout of the Long/Short Baseline Experiment from the Conceptual Design Report. The distances given are correct, although the Figure is not to scale.

angle of a few degrees, would pass through the Earth in a straight line. The neutrinos would then exit at a location depending on the initial direction and the Earth's curvature, as discussed earlier.

Two long-baseline detectors submitted proposals and were encouraged to make further studies by the Fermilab PAC. The IMB detector is a 7 kiloton water detector; Soudan 2 is a 0.7 kiloton effective-fiducial volume highly segmented iron calorimeter. We concentrate on Soudan 2 both because it is well-designed for the measurement discussed below and because its present site has room for up to 5 kilotons of expansion without additional civil construction. Shown in Fig. 5.2 are the per-run 90% CL oscillation limits for the present Soudan 2 (600 contained interactions per 2.4 x10^{20} protons on target), and an ultimate curve based on 4 kilotons of fiducial volume and four running periods (14,000 contained interactions). Ultimate measurement sensitivities of 2% and Δm^2 as low as 0.002 eV^2 are within reach.

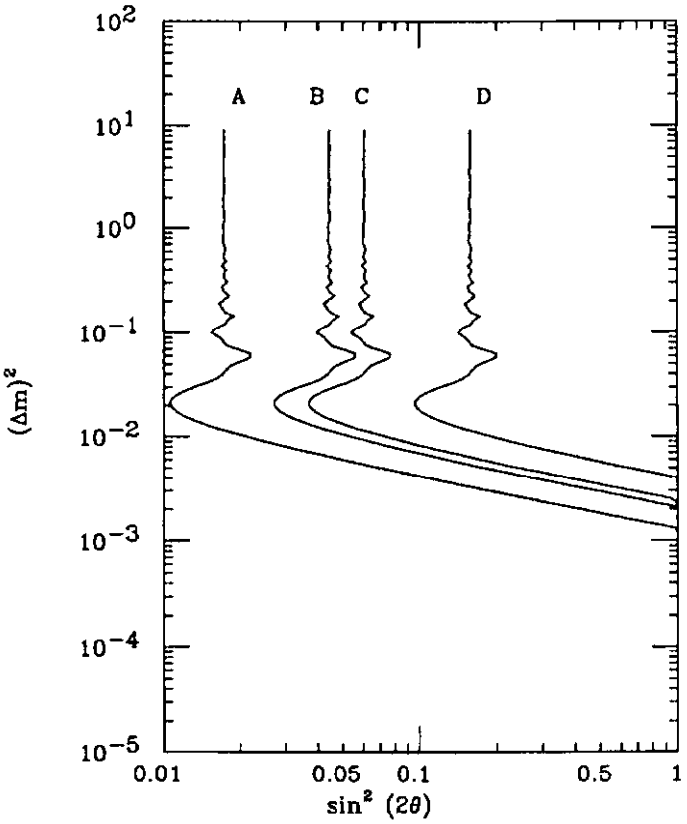

FIGURE 5.2: The A,B and C,D curves are 90% CL limits for $\nu_\mu \rightarrow \nu_e, \nu_\tau$ using the NC/CC method described in the text. The ν_τ limits are weaker because at these intermediate energies the tau-neutrino interaction cross-section is smaller. The A and B curves assume 4 runs in a 4.0 kton fiducial volume detector. C and D are for one run in the existing 0.7 kton fiducial detector.

5.2.2 Experimental Method

The preferred technique is to measure the ratio of neutral to charged currents in two locations with nearly identical detectors. The techniques are quite similar to those used in the extraction of $\sin^2\theta_W$ in deep-inelastic scattering at the Tevatron and are well understood.

Since the beam will be 98% pure ν_μ, charged-current interactions (CC) can be defined as those containing primary muons, while neutral-current interactions (NC) by analogy can be defined those events lacking primary muons. Only 18% of taus decay into muons, and these have a rather different kinematical dependence than standard CC interactions. Electron neutrino interactions do not generate primary muons. Thus, an increase in the ratio of NC/CC interactions ($\equiv R_\nu$, as in the Weinberg angle measurements) at long distances can be taken as positive evidence for oscillations. Although the measured R_ν is a function of the detector, isotopic content of the target, and energy distribution of the beam, these effects cancel when R_ν is measured in two locations with identical detectors. A further reduction in systematic errors is achieved by studying R_ν as a function of hadronic energy, which cancels spectral differences at the two locations up to effects from resolution smearing. A potential error from ν_e contamination will be small; if the ν_e content changes between the two detectors, this could fake a signal or obscure an existing one. However, the ν_e/ν_μ content is only about 1% and the change in the content will be small. Initial studies indicate systematic errors of 1% are achievable. Oscillations into sterile neutrinos will be studied by the conventional means of comparing fluxes at near and far detectors. On-going meetings are sharpening the detector issues and systematic questions, but a year of debate has developed a consensus on the technique and technology. Neither pose any special difficulty.

5.2.3 Short-baseline Experiment: $\nu_\mu \rightarrow \nu_\tau$ and the Missing Mass

A plan view of the short-baseline detector discussed in Fermilab proposal P–803 is shown in Fig. 5.3. It is designed to precisely measure oscillations of electron and muon neutrinos into tau neutrinos. The apparatus consists of a 0.8 ton emulsion target viewed by a high-acceptance electronic-magnetic spectrometer. By using emulsion, short-lifetime tau decays coming from charged-current interactions of ν_τ may be easily located and accurately measured.

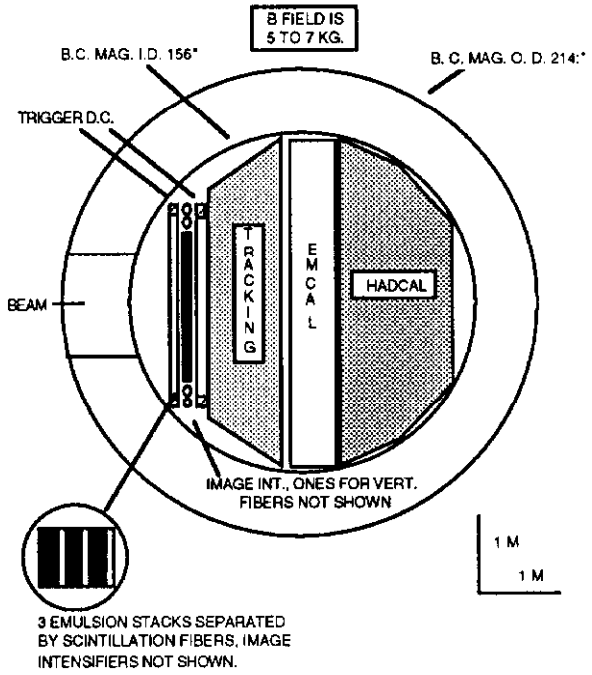

FIGURE 5.3: Plan View of the P–803 Experiment. Note the use of the existing 15 ft. BC magnet.

In order to reduce backgrounds, the experiment will concentrate on the 83% of decays which are single-prong ($\tau \rightarrow \mu\nu\nu$, $e\nu\nu$, $\pi\nu$, $K\nu$, $\rho\nu$, $\pi\nu\gamma$) About half of found single-prong decays will be two-body and hence have a minimum reconstructed mass near that of the parent tau. Single-run 90% CL limits are shown in Fig. 5.4 together with limits coming from E–531 at Fermilab, the first experiment to use the technique.[5] However, emphasis also has been placed on giving strong evidence for a positive signal should one exist. A positive signal five times the 90% CL limits would yield an excess of decays with masses and lifetimes determined to within errors of ±20% . A second run will improve sensitivity by a factor of two and the Δm^2 reach by 40% as compared to single-run values. This open-geometry spectrometer also will measure the overall short-baseline neutrino interaction spectrum down to energies below 4 GeV, and the NC/CC ratio as a function of various kinematic cuts. The P–803 detector, together with a small subset of the long-baseline detector will operate simultaneously during all long-baseline operation for calibration purposes (and to search for sterile neutrinos) either with emulsion targets or ones better matched to the isotopic concentration of the long-baseline apparatus. The ability to precisely measure masses and lifetimes, unique to the Fermilab experiment, distinguishes it from its CERN competition. Establishing that the observed lepton is a τ is essential; we must produce an unambiguous signal and this is the only proposed experiment that can do it.

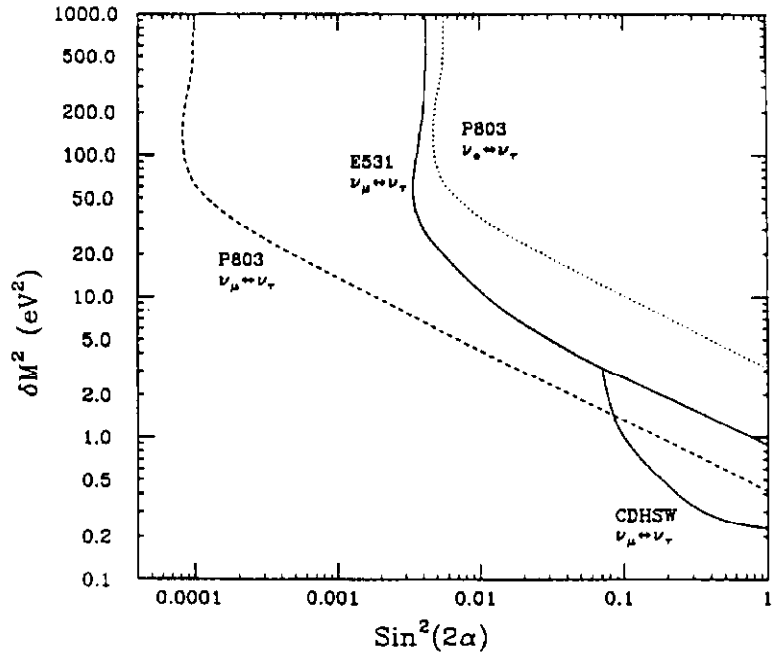

FIGURE 5.4: Δm^2 vs. $\sin^2 2\theta$ plane showing the previous limits for $\nu_\mu \rightarrow \nu_\tau$ oscillations (solid curves) and the improved limits on $\nu_e \rightarrow \nu_\tau$, relevant to the 17 keV neutrino (dotted curves).

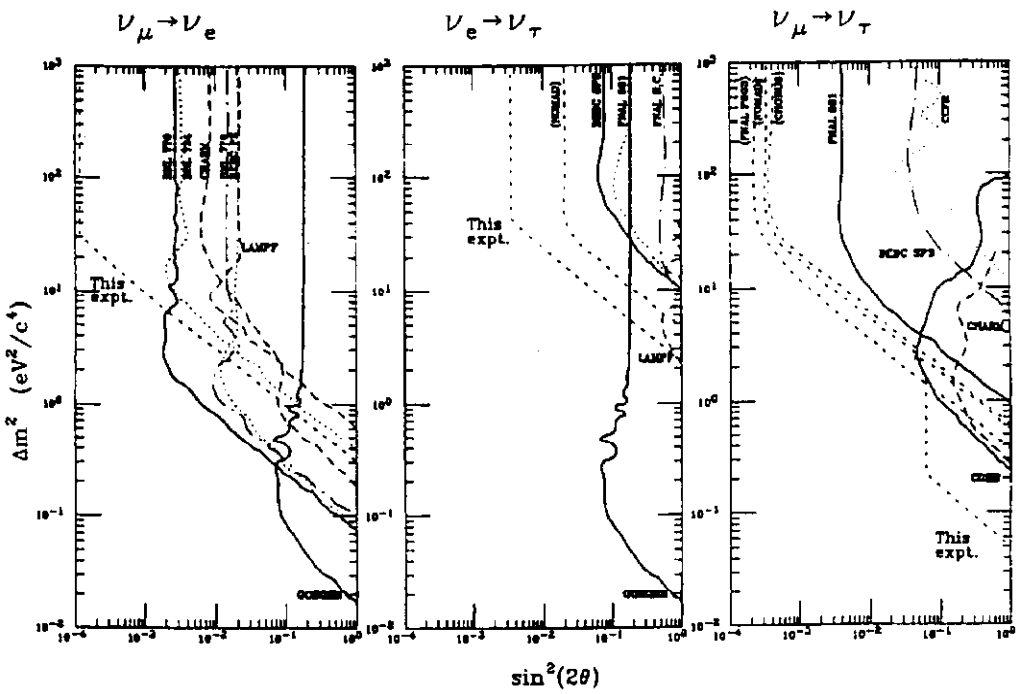

FIGURE 5.5: Expected limits for $\nu_e \rightarrow \nu_\tau$ oscillations from P–860.

5.2.4 $\nu_e \rightarrow \nu_\tau$ in the Debuncher

During conventional collider operation, π^-, μ^-, and e^- are trapped along with the $\bar{p}$'s in the Debuncher ring. After a few turns, the π^-'s decay to yield μ^-'s and $\bar{\nu}_\mu$'s. The subsequent decays of the μ^-'s into electrons produce a time-separated $\bar{\nu}_e$ beam. The energy distribution is in the 3–9 GeV range, adequate to permit τ production. Hence the experiment would permit a clean, definitive search for the 17 keV neutrino (identified with $\nu\tau$). The choice of concentration has been more one of convenience than of logic; searches for $\nu_e \rightarrow \nu_\tau$ oscillations have never been carefully made because accelerator beams at sufficient energy to produce ν_τ are predominantly ν_μ. This experiment will create the first high-energy ν_e beam, permitting tests of universality and $(\sigma_{\nu_e}/\sigma_{\nu_\mu})$ and electroweak measurements, in addition to searches for oscillations. The expected limits from such an experiment (P–860) are shown in Fig. 5.5.

5.3 TEVATRON PROGRAM

5.3.1 Electroweak Physics

Precision measurements of $\sin^2\theta_W$ and ρ are among the top physics priorities of the 1990's. A program of measurements in deep-inelastic scattering, combined with the collider measurements of the boson masses and decay asymmetries, are essential tools in searching for physics beyond the Standard Model. The range of tests is impressive; we summarize them in Table 5.1. The Main Injector's improvements to the Tevatron program will allow the neutrino experiments to reach a 1% error on both these quantities in a timely way.

Tree-Level Physics:	extra Z: χ, ψ, η, Z_{LR} non-standard Higgs representations leptoquarks extra fermions: $u'_{L,R}$, $d'_{L,R}$, $e'_{L,R}$, $\nu'_{L,R}$ compositeness
Loop-Level Physics:	m_t, M_H extra fermions S–T parameters: gauge boson self-energies two Higgs doublets supersymmetry

TABLE 5.1: Some of the new physics accessible with a set of high-precision electroweak experiments. Some of these, such as non-standard Higgs representations or extra fermions, are best tested through neutrino scattering. Taken from Langacker, Luo, and Mann, UPR-0458T.

These measurements will test the radiative corrections to the Standard Model as well as any planned measurement at the colliders, but are not merely duplicates of the collider experiments. New physics will change the radiative corrections to different processes in different ways; hence an ensemble of measurements is necessary to isolate and understand phenomena beyond the Standard Model. Deep-inelastic neutrino scattering is a critical ingredient in this enterprise, providing two powerful measurements. First, the measurement of ρ is a sensitive probe of the Higgs sector which is not yet accessible in other experiments. Second, the measurement of $\sin^2\theta_W$ in deep-inelastic scattering has been the most significant upper limit on the top mass; after the top is discovered and its mass measured, the comparison of the predicted result from deep-inelastic scattering to the measured m_t will be one of our most powerful tests for physics beyond the Standard Model. The existence of this sort of synergy is perhaps the best physics argument for the Main Injector. A variety of measurements, each challenging and checking the others, is a requirement for progress in science. This process will not occur without the construction of the Main Injector and a healthy fixed-target program at Fermilab.

There is a variety of schemes for calculating $\sin^2\theta_W$ and ρ which has lead to considerable confusion; depending on the scheme ($\overline{\text{MS}}$, Sirlin, $\sin^2\theta^*$) some variables will have small errors and some large, depending on their sensitivity to different radiative corrections.[7] We stress that the only way to fairly compare measurements is to translate all variables to the same scheme and then plot the results. Plots on the ρ–$\sin^2\theta_W$ plane, or the S and T plane, can then be used to compare different variables. It is important to realize that the information contained is "scheme-invariant" and that particular claims for particular variables are meaningless unless all measurements have been compared within the same framework. Finally, we note that except for deep-inelastic scattering, precise measurements of $\sin^2\theta_W$ give no information on ρ.

We follow Rosner and write:[8]

$$\sin^2\theta_W = 1 - \frac{M_W^2}{M_Z^2} \equiv 1 - \frac{\pi\alpha}{\sqrt{2}G_F M_Z^2}\frac{1}{\bar{x}} \tag{2}$$

where $\bar{x} = \sin^2\theta_W$ is now defined in terms of coupling at the Z pole ($\overline{\text{MS}}$). With this definition,

$$\rho = \frac{M_W^2}{M_Z^2\cos^2\bar{\theta}} \tag{3}$$

and in this scheme, $\rho = 1 + \alpha T$ as defined by Peskin and Takeuchi.[9]

A useful relation indicating the power of a precise measurement of ρ is

$$\Delta\rho_{top} = \frac{3\alpha}{16\pi}\left(\frac{m_t}{M_W}\right)^2 \tag{4}$$

so if m_t = 150 GeV then $\Delta\rho$ = + 0.007. In contrast, the value of $\sin^2\theta_W$ measured in deep-inelastic scattering is almost insensitive to m_t; this is the result of fortuitous cancellations in the radiative corrections.[11)]

The Higgs sector can also be probed with ρ. Veltman's original definition of ρ was

$$\rho_0 \equiv \frac{\sum_i \left(L_i^2 - L_{3i}^2 - L_{3i}\right)\left|\langle\Phi_i\rangle\right|^2}{\sum_i 2L_{3i}^2\left|\langle\Phi_i\rangle\right|^2} \tag{5}$$

where $\left|\left\langle\Phi_i^2\right\rangle\right|^2$ is the vacuum expectation value of the i^{th} Higgs field and L_i its weak isospin. We see that for Higgs doublets, $\rho_0 \equiv 1$. For Higgs triplets, or more complicated structures, ρ_0 may differ significantly from unity.

We compare the power of deep-inelastic scattering in the Main Injector era to the collider boson-mass measurements and to the decay asymmetries at SLC below. Figure 5.6 gives the allowed region in $\sin^2\theta_W$ and ρ space (now in the Sirlin scheme). The vertical lines are the allowed region from the W mass measurements. The two sets of diagonal lines give us the allowed regions from the Z mass and from A_{LR} to be measured at SLD. We have assumed a deep-inelastic measurement of $\sin^2\theta_W$ to 1%, M_W to 50 MeV, and M_Z to 10 MeV. We have used the A_{LR} error corresponding to 100,000 Zs at 40% polarization, an optimistic goal; the width of the A_{LR} band is dominated by the statistical error. If the allowed regions do not overlap, there must be physics beyond the Standard Model; the precise values and nature of the discrepancies among the experiments would give us the underlying physics. Note that the deep-inelastic ellipse ($R_\nu/R_{\overline{\nu}}$) is nearly orthogonal to the Z-mass measurement band; this increases the power of the tests taken in combination. The A_{LR} band is nearly parallel to the Z-band; hence despite the impressive potential precision of the A_{LR} measurement, given by the width of the band, the additional knowledge gained is relatively small.[1]

Another useful parameterization of radiative corrections to the the electroweak observables highlights the separate contributions to extensions of the Standard Model and of a class of new physics. The parameter $T = \alpha\Delta\rho$ is a measure of weak-isospin breaking

---

1 Atomic Parity Violation, not shown on this graph, is the last important input. It will soon produce measurements of $\sin^2\theta_W$ to 0.003 and will further enhance our constraints on the Standard Model.

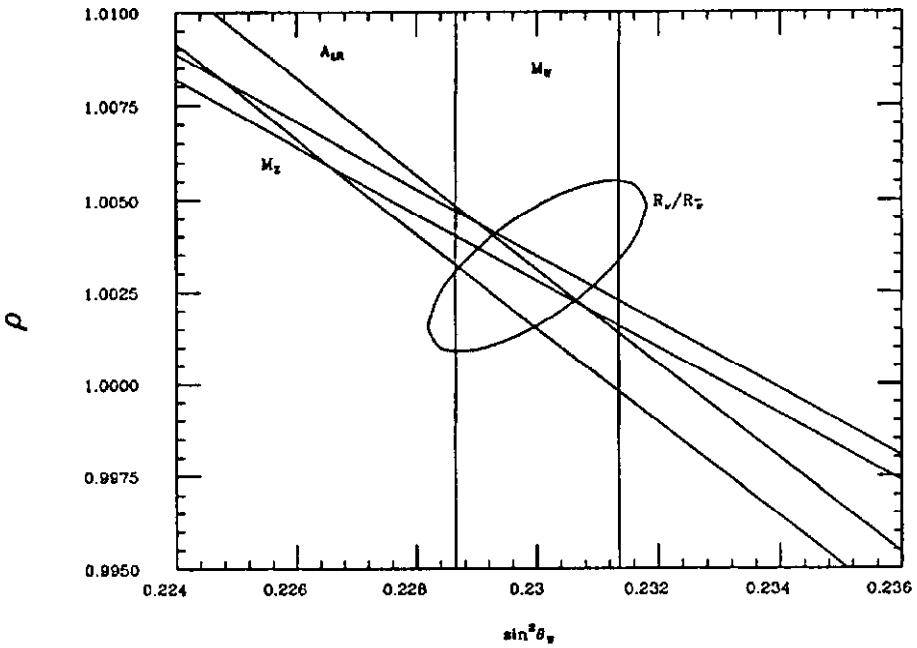

FIGURE 5.6: Sensitivity of the various experiments in the ρ–$\sin^2\theta_W$ plane assuming a common central value of ρ=1.0032 and $\sin^2\theta_W$ = 0.23. $R_\nu/R_{\bar{\nu}}$ is the neutrino deep-inelastic scattering measurement.

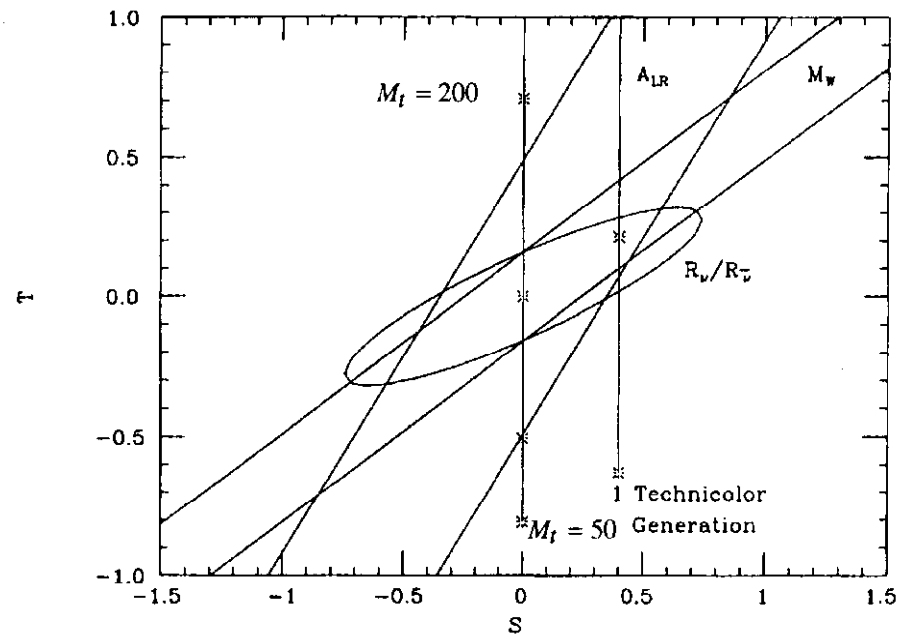

FIGURE 5.7: Sensitivity of the various experiments in the S–T plane. $R_\nu/R_{\bar{\nu}}$ is the neutrino deep-inelastic scattering measurement. The shift in S from one technicolor generation is shown.

effects such as non-standard Higgs structures, and is also sensitive to a heavy top quark in the same way as is ρ itself. S is insensitive to the top mass but reflects new physics such as technicolor. An important but often-overlooked point is that when all variables are translated into the same scheme (ρ and $\sin^2\theta_W$, or S and T, for example) the knowledge we gain only depends on the experiments we have performed and their errors; the new information is "scheme-invariant". Assuming a central value for M_Z from LEP, the S-T plot is shown in Fig. 5.7.

Within the context of the Standard Model and using the accurately measured Z mass we can express all measurements as predictions (or measurements) of the W-mass. Table 5.2 shows how the W mass has been determined by each of the electroweak measurements; this is perhaps the most succinct comparison. We quote the current results; extrapolation to the future is straightforward.

Process	Equivalent W Mass Measurement
CDF/UA2 Mass Measurement	80.14 ± 0.31 GeV
Neutrino (Neutral to Charged Current Ratio)	79.90 ± 0.30 GeV
Combined LEP Results (700K events)	80.15 ± 0.27 GeV

TABLE 5.2: Comparison within the Standard Model of the error of M_W from different electroweak measurements.

We see that the collider experiments have only recently caught up with neutrino deep-inelastic scattering as probes of the radiative corrections. The improvements in P–815, approximately a factor of three, will keep pace with the future of direct measurements, overconstraining the M_W, M_Z, and m_t determinations as a probe for new physics.

5.3.2 Experimental Method

E–770 at FNAL has recently analyzed the 1985–1987 Quadrupole Triplet data and extracted $\sin^2\theta_W$. E–594 has reported preliminary results in the same beam.[11] The Quadrupole Triplet produces ν_μ and $\bar{\nu}_\mu$ simultaneously, preventing us from measuring $\sin^2\theta_W$ and ρ separately; hence E770 and E–594 only measured a combination of the Llewellyn Smith variables R_ν and $R_{\bar{\nu}}$, the ratio of neutral-to-charged current cross-sections for neutrinos and antineutrinos.[12] E–594 reported a measured R_ν of 0.305 ± 0.005. We discuss the E–770 errors below as proof that P–815 can achieve its goals, since the experiments will share a common detector.

P–815[13] will measure ν_μ and $\overline{\nu}_\mu$ separately, providing both R_ν and $R_{\overline{\nu}}$, and with a measured $\overline{\nu}_\mu/\nu_\mu$ flux ratio the measurements can be translated into the Paschos-Wolfenstein R^+ and R^-.[14] In a two-parameter fit, the variables chosen cannot alter the measured ρ and $\sin^2\theta_W$. However, in a one-parameter fit (assuming $\rho = 1$ at tree-level) the Paschos-Wolfenstein R^- is the cleanest measurement of $\sin^2\theta_W$. P–815 will have more than 100 times the existing sample of identified $\overline{\nu}_\mu$, and will provide the first precision measurement of ρ.

There are three significant sources of error in an extraction of $\sin^2\theta_W$ and ρ from neutrino scattering. The first arises from the production of charm. Charm-production is forbidden in the neutral current numerator (no flavor-changing neutral currents) although it is a 7% contribution to the charged current denominator. The prediction is complicated because there is a kinematic penalty for production of the charmed quark; it is modeled by the replacement $x \rightarrow x\left(1 - m_c^2/Q^2\right)$ (slow-recaling). CCFR has measured $m_c = 1.34 \pm 0.25$ from opposite-sign dimuon production.[14] We expect the errors on $\sin^2\theta_W$ from this source with Main Injector intensities (better statistics) and Tevatron energies (higher Q^2) to be less than 0.001.

The second two sources, from backgrounds and crosstalk in the ratios, are well under control. The primary source of background is ν_e contamination in the beam. Since electromagnetic showers are short, they are obscured by the hadronic shower. Hence ν_e charged-current events appear as neutral currents and shift the numerator in the NC/CC ratios. The ν_e contamination comes from two sources: K^+ decays and K_L decays. The first has been accurately modeled and checked in the E–770 analysis. We measure the $K^+ \rightarrow \mu\nu_\mu$ contribution in the charged-current data and thereby obtain the flux and spectrum of K^+ decays in the beam. We then translate this into a $K^+ \rightarrow \pi^o e \nu_e$ decay and predict the ν_e flux at the detector (the normalization is to the charged-current data itself). We estimate errors from this technique at $\delta(\sin^2\theta_W) \leq \pm 5 \times 10^{-4}$. The second contribution is from $K_L \rightarrow \pi^o e \nu_e$. These cannot be easily measured from the charged-current spectrum and were modeled in E–770, providing an error of > 0.003, far too large for the new experiment.

P–815 will overcome the ν_e error with a newly constructed Sign-selected Quadrupole Triplet. This new beam has two advantages: (1) ν_μ and $\overline{\nu}_\mu$ are separated, permitting separate measurements of $\sin^2\theta_W$ and ρ; (2) the sign-selection will bend the beam away from the neutral mesons; hence the K_L will *miss* the detector. The result is an exceptionally clean beam at high statistics with nearly the same energy as the Quadrupole Triplet.

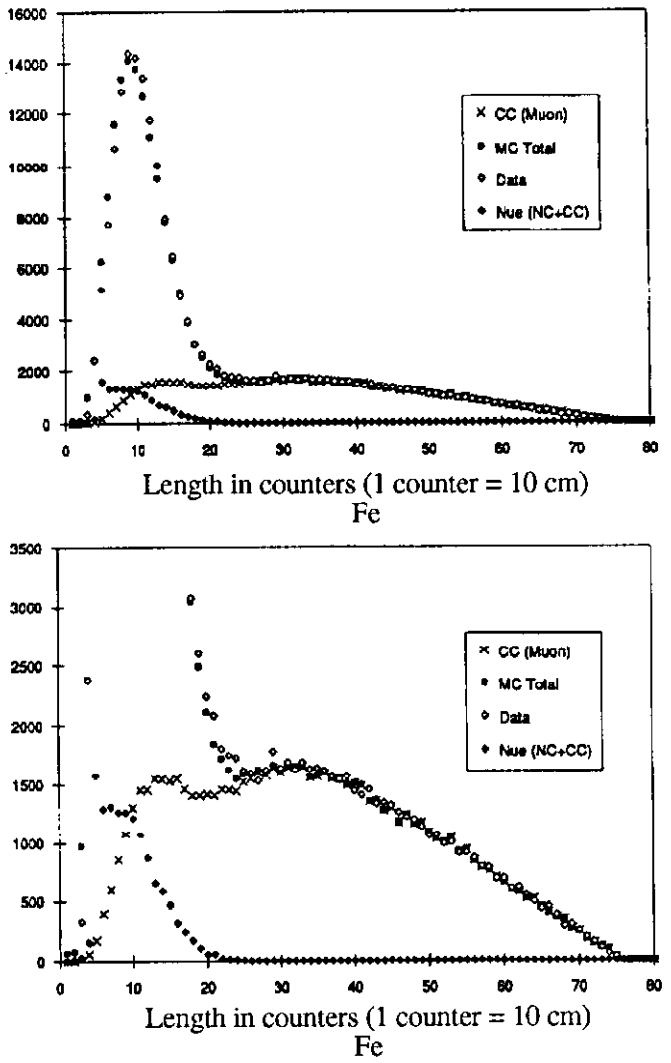

FIGURE 5.8: The length distribution and its simulation from E–770. The peak is from hadronic showers belonging to neutral currents, and the tail and extrapolation under the peak is from charged currents. The full simulation includes a determination of the shape of electromagnetic showers from ν_e and the length distribtuion of hadronic showers, both determined by test-beam measurement. The upper graph shows the entire distribution; the lower graph shows the details in the region of the backgrounds.

Crosstalk from the charged current denominator to the neutral current numerator is the final source of error. Charged-current events at high-y (small muon energy) may not produce a visible muon, resulting in a mis-classification of the event. The E–770 analysis measures the length of the event: hadronic showers are between 1–2 meters but muons, which lose energy by dE/dx, are longer. Hence a distribution of the measured length yields a neutral current peak and a charged-current tail. The experiment has successfully modeled the length distribution (the first to do so!) and the extrapolation to the P–815 measurement is straightforward. The result is shown in Fig. 5.8.

5.3.3 Structure Functions and QCD

Precise measurements of structure functions have been the most significant product of past. Precision tests of perturbative QCD, neutrino experiments are a subject of some controversy arising largely due to the incalculable contributions from "nonperturbative" effects. Nevertheless, within the framework of deep-inelastic experiments, there exist elegant and unambiguous predictions that can be directly tested against measurements. The first step in such a program would be to restore the high-flux, high-energy Quadrupole Triplet. With ten times the integrated flux of the last Quadrupole Triplet runs we would have the samples shown in Table 5.3.

Experiment	ν_μ-CC	$\bar{\nu}_\mu$-CC	NC	$\mu^-\mu^+$
E744 + E770	1.4×10^6	0.3×10^5	0.4×10^6	1×10^4
New Experiment	15×10^6	5×10^6	5×10^6	15×10^5

TABLE 5.3: The Proposed Statistical Sample in P–815 in a Quadrupole Triplet Run at the Main Injector. Number of $\nu(\bar{\nu})$-induced charged current (CC), neutral current (NC), and charm-induced opposite sign dimuon ($\mu^-\mu^+$) events in the new experiment, are presented below.

We remind the reader of the definitions of the relevant structure functions:

$$2xF_1\left(x,Q^2\right) = q\left(x,Q^2\right) + \bar{q}\left(x,Q^2\right) \tag{6}$$

$$xF_3\left(x,Q^2\right) = q\left(x,Q^2\right) - \bar{q}\left(x,Q^2\right) \tag{7}$$

$$F_2\left(x,Q^2\right) = q\left(x,Q^2\right) + \bar{q}\left(x,Q^2\right) + 2k\left(x,Q^2\right) \tag{8}$$

where a sum over quark species is understood. The variable R is defined through

$$F_2\left(x,Q^2\right) = \frac{2xF_1(x,Q^2)\left(1+R(x,Q^2)\right)}{1+4M_N^2\,x^2/Q^2} \tag{9}$$

and reflects the spin–0 content of the nucleon. This term arises from the gluon component along with "intrinsic" p_T of the quarks within the nucleon. Two compelling tests of QCD within deep inelastic experiments are the evolution of structure functions with Q^2 at fixed x and the dependence of R (σ_L/σ_T) on x and Q^2.

Neutrino-nucleon scattering is particularly important since it provides the cleanest measurement of xF_3. By determining $\partial \ln xF_3 / \partial \ln Q^2$ we measure $\alpha_S(Q^2)$ and hope to extract Λ_{QCD} with an error of ±15 MeV. The quantity $R_{QCD} = F_2/2xF_1$ has never been adequately measured; although measurements at low Q^2 at SLAC have been performed, R at Tevatron energies has never been cleanly distinguished from zero, let alone shown to be consistent with QCD.

The evolution of the parity violating structure function, $\partial \ln(xF_3)/\partial \ln(Q^2)$ is the simplest. It is free of the details of gluon densities or the knowledge of R and therefore provides the cleanest channel for testing the Q^2 evolution predicted by the theory. Specifically, the leading-order evolution equation at fixed x is:

$$\frac{\partial \ln xF_3(x,Q^2)}{\partial \ln Q^2} = \frac{\alpha_S}{2\pi}\frac{4}{3}\left[\int_z^1 dz \frac{1+z^2}{1-z}\left[\frac{x}{z}F_3\left(\frac{x}{z},Q^2\right) - xF_3(x,Q^2)\right] - xF_3(x,Q^2)\int_0^x dz \frac{1+z^2}{1-z}\right] \tag{10}$$

This complicated-looking equation breaks into two simple parts: (1) an overall factor of α_S and (2) an integral proportional to xF_3 itself. Hence the logarithmic derivative can be measured with almost no theoretical complications. The new CCFR QTB-data demonstrate, for the first time, a Q^2 evolution of xF_3 consistent with the Altarelli-Parisi equation and have determined $\Lambda_{\overline{MS}}$ to 50 MeV.[20] The statistical and systematic precision of the earlier measurements of xF_3 in the narrow band beam data of CCFR and the wide band data of CDHSW[16] did not permit conclusive tests; hence the most recent experiments at the Tevatron have provided the first such precision QCD measurements.

The F_2 measurements have unambiguously resolved the controversies among CDHS, EMC, SLAC, and BCDMS. These long-standing disagreements have prevented clear confirmation of QCD and have been lacking in systematic precision as well as x and Q^2 coverage. The data is shown in Fig. 5.9 and Fig. 5.10. The current errors have approximately equal contributions from systematic and statistical sources With an order of magnitude more statistics, the errors will drop between a factor of two and three; the experimental challenge is to improve the relative calibration between the hadronic energy and the muon momentum to take advantage of the increased statistics.

Next, since (to first-order)

$$\alpha_S = \frac{4\pi}{\left(11 - \frac{2}{3}n_f\right)\ln\frac{Q^2}{\Lambda^2}} \tag{11}$$

(where n_f is the number of quark flavors) we can use the xF_3 evolution to determine Λ_{QCD}. The primary systematic uncertainty will be the relative calibration between the hadronic energy measured by the calorimeter and muon momentum from the toroids. This will smear the events to different values of x and Q^2, thereby altering the derivatives. The next goal for QCD tests is a demonstration that $R=R_{QCD}$. Fortunately, perturbative QCD predicts the absolute magnitude and shape of $R(x,Q^2)$ which can then be confronted in an deep inelastic scattering experiment. Current data are consistent with R_{QCD}, but they are also consistent with R constant.[17] With an order-of-magnitude more data, a precise test could be made.

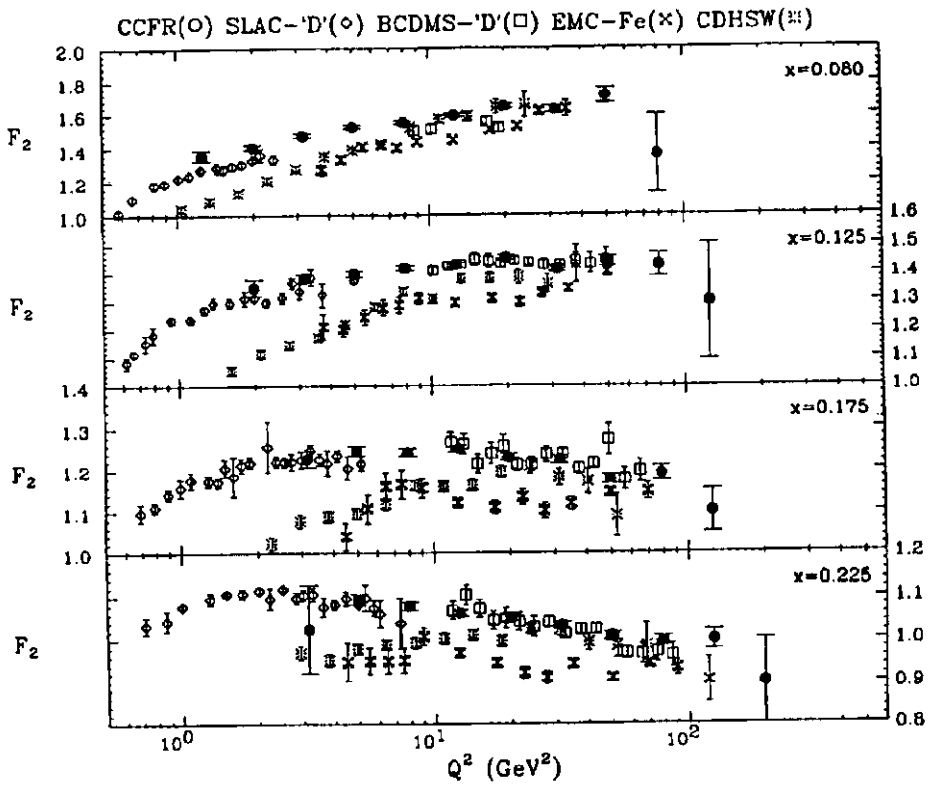

FIGURE 5.9: Comparison of F_2 from CCFR, SLAC, BCDMS, EMC, and CDHS.

We also point out the power of neutrino scattering in determining the gluon structure function. We evolve both

$$F_2^{\nu(\bar{\nu})} = 2\left[xq^{\nu(\bar{\nu})} + x\bar{q}^{\nu(\bar{\nu})} + 2xk^{\nu(\bar{\nu})} \right]$$

$$xF_3^{\nu(\bar{\nu})} = 2\left[xq^{\nu(\bar{\nu})} - x\bar{q}^{\nu(\bar{\nu})} \right] \qquad (12)$$

where the k term represents the spin–0 component from the gluon distribution $G(x,Q^2)$ (and from higher-order QCD effects). By simultaneously evolving both of these structure functions, we put constraints on the gluon distribution (since the integrals of F_2 and xF_3 are fixed).

The statistical strength of a new experiment will permit the extraction of quark and antiquark distributions separately for neutrinos and antineutrinos. Hence we may also test the assumption that the structure functions are the same for neutrinos and antineutrinos. Furthermore, the only direct measurement of the strange sea comes from a study of neutrino induced opposite sign dimuon events. The 150,000 opposite sign dimuons will give an unprecedented determination of the strange sea density, including its Q^2 evolution. The traditional quark-parton model integral tests, such as the Gross-Llewellyn Smith sum rule and the mean square charge test will be significantly improved as well.

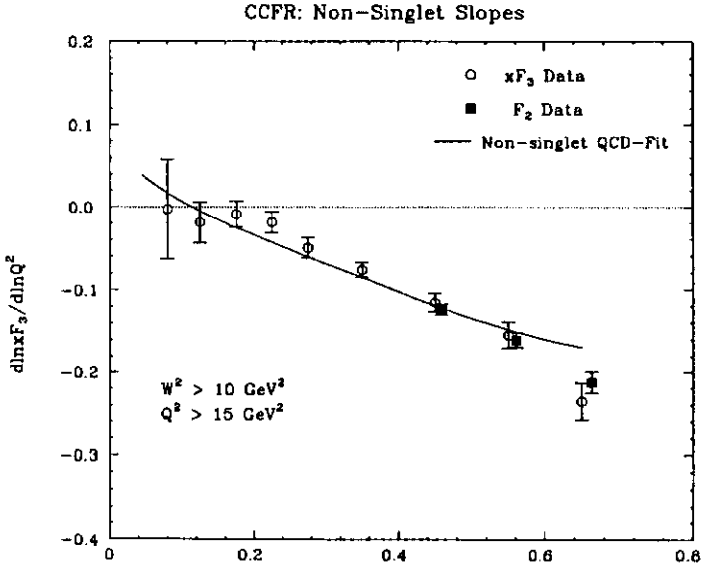

FIGURE 5.10: Logarithmic Derivative of $xF3$ vs. Q^2, showing QCD evolution.

5.3.4 Rare Processes

With a factor of ten greater statistics than ever before and a significantly upgraded detector, limits on and searches for rare processes will be greatly improved. In particular, searches for neutral heavy leptons and wrong-sign muons will be improved by an order-of-magnitude and we may set significantly improved limits for $\nu_\mu \rightarrow \nu_\tau$ oscillations at large Δm^2. We describe some others below:

- *Inverse Muon Decay* The purely leptonic reaction, $\nu_\mu + e^- \rightarrow \mu^- + \nu_e$, offers an elegant test of the Standard Model. We could examine the structure of the

Lorentz current of the weak interaction and search for the scalar coupling of leptons, as well as the energy dependence of its cross section. It offers an absolute normalization of the ν-flux, since the Standard Model prediction is accurately known.

- *Measurement of V_{cd}* Opposite sign dimuons are the most direct means of measuring the Cabibbo-Kobayashi-Maskawa matrix element. The present measurements could be vastly improved.

- *Neutrino Tridents* Measurement of the destructive interference between the neutral current and charged current channels of neutrino scattering off the Coulomb field of the nucleus (the so called ν-induced trident events) directly tests the gauge structure of the Standard Model. Recently the CCFR collaboration has reported the first demonstration of the predicted destructive interference between the W and Z channels in neutrino tridents.[18] The new experiment, which would observe more than 600 tridents, would permit a precise test ($\geq 6\ \sigma$) of this important Standard Model prediction.

- *Neutral Heavy Leptons* Neutrino experiments are sensitive to iso-singlet type neutral heavy leptons (as opposed to sequential fourth generation neutrinos). These leptons are not excluded by the LEP data, and would continue to be of interest even with 10^7 Z events from LEP. The current best limits in the appropriate mass regions come from the CCFR searches.[19] For low mass neutral heavy leptons (< 5 GeV), the sensitivity in the new experiment will be far superior to the e^+e^- experiments. By instrumenting the apparatus suitably, we could extend the search domain with masses down to 10 MeV and with coupling suppressions down to 10^{-9}.

- *Search for Right Handed Currents* The y-distributions of neutrino and antineutrino CC events constrain the right handed currents in the most model independent way. The current limit on the mixing of the right handed currents from the CCFR(QTB) experiments is the most stringent. The corresponding limit from the muon-decay are sensitive to the theoretical assumptions such as the mass of the right handed neutrino. In the new experiment the derived limit on the mass of the right handed boson should be the most stringent.

- *Trimuons* Neutrino-induced trimuons predominantly arise from hadronic sources (vector meson resonances). The new sample should have over 1300 of these events, offering an opportunity to do a quantitative test of various hypotheses.

5.3.5 Summary

We have seen that the Main Injector neutrino program is both a comprehensive and deep program, simultaneously offering the potential for major discovery and important improvements of existing measurements.

The primary goal of the 120 GeV physics program is the search for neutrino oscillations. The discovery of neutrino oscillations would be the first demonstration of the violation of lepton number and hence would be our first glimpse of physics at the Grand Unification scale. The long-baseline experiments, especially working in tandem with the short-baseline effort, can explore territory accessible in no other way and are elegant and beautiful experiments in their own right. The combination could potentially (1) find the source of 90% of the mass of the Universe, (2) establish the violation of lepton number, and (3) discover the ν_τ. The discovery potential of such a program is enormous. In addition, the experiments can perform valuable measurements of physics at low Q^2, a topic of both theoretical and practical interest.

The Tevatron experiments offer solid, precise measurements of structure functions which both incisively test QCD and provide much-needed data for Fermilab and the SSC. The measurements of electroweak parameters are essential for probing physics at the TeV mass scale and will both complement and extend the measurements which can be made at colliders. In the case of the ρ parameter neutrino-nucleon scattering provides unique information on a wide variety of new physics. Limits on rare processes also provide constraints on new physics, and with an order-of-magnitude more data, offer the possibility of a solid discovery of new phenomena.

These experiments will create a new generation of neutrino physics in the 1990's, testing the Standard Model and searching for new physics across an enormous arena of energy and distance scales. They will provide accurate and decisive measurements on topics ranging from precise tests of QCD to the nature of the Higgs sector to the most profound questions of cosmology.

In the next century, Fermilab will be ideally prepared to explore new physics and capitalize on the existing detectors. Upgraded experiments could be systematically mapping out the oscillation parameters, telling us precise values for $\sin^2 2\theta$ and Δm^2. Dedicated Tevatron beams could be studying discrepancies among electroweak parameters reflecting physics beyond the SSC scale; measurements of structure functions will be studying the nature of the glue and of the coupling constant of QCD. This range and depth, providing at the same time both increased precision and increased reach, are unique to the Main Injector and testify to its vast potential.

5.4 REFERENCES

1. R. Bernstein, *et al.*, Conceptual Design Report: Main Injector Neutrino Program (1991). Also see the specific proposals for P–803, P–805, P–822, and P–824. The first is the $\nu_\mu \rightarrow \nu_\tau$ search, and the last three are long-baseline proposals from IMB, Soudan 2, and DUMAND respectively.

2. M. J. Murtagh, *et al.*, Fermilab Proposal P–860.

3. K. Abe, F. Taylor, and D.H. White, Snowmass 1986.

4. K.S. Hirata, *et al.*, *Phys. Lett.* **B205** (1989) 518. D. Casper, *et al.*, *Phys. Rev. Lett.* **66**, 2561 (1991).

5. N. Ushida, *et al.*, *Phys. Rev. Lett.* **57**, 2897 (1986).

6. A. Sirlin, *Phys. Rev.* D29 (1984) 89; W. Marciano and A. Sirlin, *Phys. Rev. Lett.* **46**, (1981) 163.; M. Peskin, SLAC-Pub-5210 (Published in Proceedings of the Seventeenth SLAC Summer Institute, Physics at the 100 GeV Mass Scale).

7. J. Rosner, *Phys. Rev.* D42, 3107 (1990) and references therein.

8. M. Peskin and T. Takeuchi, *Phys. Rev. Lett.* **65**, 964 (1990).

9. Lectures presented at the IV Lake Louise Winter Institute; also UCLA/90/TEP/39.

10. M. Veltman, *Nucl. Phys.* **B123**, 89 (1977).

11. R. Brock, DPF '90, Houston, Tx.

12. C.H. Llewellyn Smith, *Nucl. Phys.* **B228**, 205 (1983).

13. P–815 proposal and references therein.

14. E.A. Paschos, L. Wolfenstein, *Phys. Rev.* D7, 91 (1973).

15. C. Foudas, *et al.*, *Phys. Rev. Lett.*, (1990); For recent experimental results from CCFR, see M. Shaevitz in Proc. of Neutrino '90.

16. B. Vallage, PhD thesis, Saclay CEA-IV-2513, Jan('87); to be published.; E. Oltman, PhD thesis, Columbia University, Nevis-270, Apr('89); to be published.

17. S.R. Mishra and F.J. Sciulli, *Phys. Lett.* **B244**, 341 (1990).

18. S.R. Mishra, *et al.*, "Neutrino Tridents and W-Z Interference", Nevis Preprint #1430, Dec. 1990; submitted to *Phys. Rev. Lett.*

19. S. R. Mishra, *et al.*, *Phys. Rev. Lett.*, 59,(1987) 1397. Also P. De Barbaro, A Search for Neutral Heavy Leptons in ν_μN Interactions, in New and Exotic Phenomena '90, Rencontres de Moriond, Jan. 1990, Editions Frontières.

20. P. Z. Quintas, *et al.*, to be submitted to *Phys. Rev. Lett.*

6 KAON PHYSICS

6 KAON PHYSICS

6.1 INTRODUCTION

For *high precision* and *high sensitivity* studies of the physics of kaon decays, the important characteristics of the new Main Injector are its *high energy* (relative to other "factories") and its *high intensity*. Experiments of this kind are becoming increasingly important in the study of CP violation and for searches for new interactions. An extracted beam of 120 GeV will produce a source of high energy kaons (10-50 GeV) that will not be surpassed in intensity by any facility now under consideration world-wide[1].

The search for the *origin* of CP violation has been a major effort at Fermilab in the kaon physics over the last decade. The most recent efforts[2] have been concentrated on a search for "direct" CP violation in $K_{L,S} \rightarrow 2\pi$ decay (ε'/ε), a test of CPT conservation ($\Delta\phi$), on a search for the mode $K_S \rightarrow \pi^+\pi^-\pi^0$ (η_{+-0}), and on a search for $K_L \rightarrow \pi^0 e^+ e^-$ which, in the Standard Model model, has a large "direct" CP violating component. These efforts provide means of distinguishing the Superweak hypothesis from the Standard Model. The latest result on ε'/ε from the full analysis[3] of Fermilab experiment E731 ($+0.0006 \pm 0.0007$) does not confirm the CERN NA31 experiment claim[4] of significant evidence for "direct" CP violation ($+0.0023 \pm 0.0007$). The question of Standard Model *versus* Superweak remains open. Experimental efforts aimed at addressing this question will be pursued well into the 90's, first at the Tevatron[5] (KTeV) and then at the Main Injector[1] (KAMI) as described below.

At present, the Fermilab experiments at the Tevatron have superb sensitivity for these modes even in comparison to the dedicated rare kaon decay program at BNL where the proton intensity is significantly higher. The advantage for these and other modes arises primarily from the *higher energy* of the decay products. However, to make substantial progress, much more flux than is available at the Tevatron is required.

6.2 PRIOR TO THE MAIN INJECTOR

Let's consider the likely evolution of this field in the years prior to the Main Injector. If we look broadly at the field of "rare" and "CP-violating" kaon decay physics, we note that the best searches for the lepton number violating decays $K_L \rightarrow \mu e$ and $K^+ \rightarrow \pi^+\mu^+e^-$ come from BNL experiments[6] and the sensitivities for these are nearing the 10^{-11} level. These results might be improved[7] by another order of magnitude there. The interesting

mode $K^+ \rightarrow \pi^+ +$ "nothing" seems to be best done with a stopped charged kaon beam and there BNL-E787 has the best experiment with a limit of 5×10^{-9} on the branching ratio of $K^+ \rightarrow \pi^+ \nu\bar{\nu}$. This effort could probably be upgraded[8] to better than 10^{-10} sensitivity at the level of Standard Model prediction; both these upgrades make use of the BNL Booster.

We now consider the CP violating modes. There are continued movement toward higher sensitivities along with the development of needed techniques and byproduct physics at the Fermilab Tevatron. The $K_L \rightarrow \pi^0 e^+ e^-$ sensitivity is now in the 10^{-9} range as a result of a combination of BNL-E845[9] and FNAL-E731[10] and it will be pushed to nearly the 10^{-11} level, approaching the level expected from Standard Model, in a KTeV experiment E799II. There is also a dedicated experiment[11] at KEK pursuing the $K_L \rightarrow \pi^0 e^+ e^-$ mode to the sensitivity at 10^{-10} level. The sensitivity to ε'/ε is now at the level of 7×10^{-4}, with all of the E731 data, and is similar for NA31 at CERN; it is proposed to improve the sensitivity to about 1.0×10^{-4} in a KTeV experiment E832. The E773, an experiment to test CPT conservation, which has taken data in 1991, will measure both $\Delta\phi$ and ϕ_{+-} to 0.5°.

For the proper execution of both KTeV experiments E799 and E832 at the Tevatron, the detector and the kaon beam need substantial upgrades. A new large, high-resolution electromagnetic calorimeter (an array of bars of pure CsI crystals) is proposed for the two KTeV experiments. Results[5] on a CsI test array have shown that good energy resolution (<1%) and good position resolution (~1 mm) can be achieved. The pure CsI crystals can be made transparent enough to reduce the non-linearity by more than factor of 10 compared to lead-glass. The longer block (27 radiation lengths) and the reduced non-linearity will also greatly improve the constant term in the resolution. Thus the line-shape becomes more and more Gaussian, greatly facilitating the understanding of the calorimeter response. The radiation hardness test in the hadron beam has also shown that the CsI crystal can be made hard enough to resist high radiation dosage up to 15 kRad without degradation on the light output and uniformity. The studies are still in progress, but it appears that a systematic uncertainty of better than 10^{-4} in the K_S/K_L ratio for the ε'/ε measurement can be obtained; and a π^0 mass resolution better than 1 MeV for the rare decay search can be achieved. The required upgrades will be important for the subsequent utilization of the much higher intensity kaon beam using the Main Injector. The same CsI calorimeter can be used in the Main Injector kaon experiment.

6.3 KAONS AT THE MAIN INJECTOR

When the Main Injector first delivers a high intensity kaon beam in five to six years, what issues should be confronted? The answer will, of course, depend very much of the results in the intervening years. In all likelihood, a new generation of ε'/ε experiment will be needed. Of course, if the results of the previous generation experiment still leave in doubt the issue of a non-zero signal, the case for motivating a new effort is quite clear. Even a first signal in the B system is unlikely by this time so we would still have only the one (laboratory) manifestation of this important phenomenon. However, even if there is an established non-zero result, it will be important to pin down the result with higher precision. Some recent calculations of ε'/ε tend toward lower amounts of direct CP violation, $\varepsilon'/\varepsilon < 0.001$. In the Standard Model, as the value of the top quark mass increases, the expected value[12] of ε'/ε decreases. When the value of the top mass is known, the range of possible values for ε'/ε will decrease motivating a more definitive test. Such an experiment in the 2π system will likely require over 10^8 $K_L \rightarrow 2\pi^0$ decays with very little background; this would permit a measurement of ε'/ε with a precision of a few 10^{-5}, at a level where it would be extremely hard for the Standard Model to accommodate a null result.

Closely coupled with the issue of a non-zero ε'/ε is the branching ratio for the $K_L \rightarrow \pi^0 e^+ e^-$ mode which is expected to be of the order of 10^{-11}. A substantial fraction of this decay should be direct CP violation, arising from contributions with virtual top quarks as shown in the diagrams in Fig. 6.1. The direct branching ratio has been calculated[13] to be

$$BR\left(K_2 \rightarrow \pi^0 e^+ e^-\right) = 1.0 \times 10^{-5} \left(s_2 s_3 s_\delta\right)^2 G(M_t),$$

where G is a function of the top quark mass of order unity and the original CKM matrix element notation is used. It is easy to show that one can use the constraint on the CKM mixing angles provided by the observed size of the mixing in the neutral B system to express this branching ratio in terms of β, one of the angles of the so-called unitarity triangle, B_B, the bag factor for the B_u meson system, and f_B, the B meson decay constant as well as another function of M_t of order unity:

$$BR\left(K_2 \rightarrow \pi^0 e^+ e^-\right) = \frac{5 \times 10^{-13} \sin^2 \beta}{\left(B_B f_B^2 F(M_t)\right)}.$$

Given what we know about the unknowns in the above expression, the value for the "direct" CP violating branching ratio could range from about 10^{-12} to 4×10^{-11} with a central value of about 6×10^{-12}.

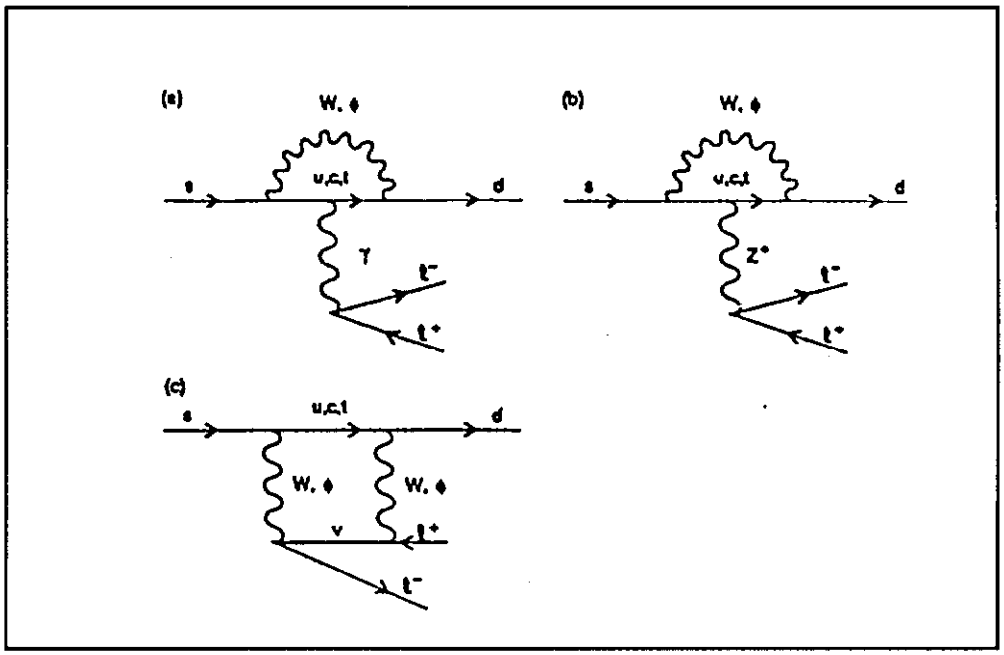

FIGURE 6.1: Three diagrams giving a short distance contribution to the process $K_L \rightarrow \pi l^+ l^-$: (a) the "electromagnetic penguin", (b) the "Z penguin", (c) the "W box". (From C.O.Dib, I. Dunietz, and F. Gilman)

With an extracted beam from the Main Injector, the flux necessary to permit sensitivities to this and other modes in the range of 10^{-10} per hour of running are obtainable. Further, we point out that this will be the best place to perform such experiments of any presently existing or planned facility. The acceptance of the detector to be described for the $\pi^0 e^+ e^-$ mode is about 20% with the requirement that both photons exceed 1 GeV. The decay rate for kaons greater than 10 GeV is about 33×10^6 per spill. However simply accumulating events unfortunately is not enough since there are, in addition to the "direct" CP violating term, three other contributions which need to be untangled. These are an indirect term, coming from the $K_1 \rightarrow \pi^0 e^+ e^-$ transition; a CP conserving term, coming from the $K_2 \rightarrow \pi^0 \gamma\gamma$ intermediate state; and a background coming from the $K_L \rightarrow e^+ e^- \gamma\gamma$ radiative decay. These have been discussed extensively in the literature.

There is a prediction[14] for the size of the indirect term. Using Chiral Perturbation Theory (and the assumption of octet dominance), the prediction for the branching ratio can

be reduced to a two-fold ambiguity: the value should be either 1.5×10^{-12} or 2.4×10^{-11}. This should be directly determined. For the time being, the ambiguity can be broken by a study of the similar $K^+ \rightarrow \pi^+ e^+ e^-$ rate. Experiment E777 at Brookhaven has about 500 of these events with relatively high *ee* invariant mass. Their spectrum favors[15] a rather stiff distribution for the e^+e^- which suggests the lower value for the corresponding K_1 transition. However, because of the assumptions involved, it will be necessary to determine the K_S rate directly. This could be done at the Tevatron, where the Lorentz factor is favorable, if the rate is high enough. Otherwise, one will need the very high rates at the Main Injector where the K_S amplitude would be determined in an interference experiment as discussed below.

For the CP conserving transition, there are competing theories[14] which give values between 10^{-14} and 10^{-11} for the two-photon (CP conserving) K_2 transition to $\pi^0 ee$. There are now two observations[16] of the decay $K_L \rightarrow \pi^0 \gamma\gamma$ with high values for the $\gamma\gamma$ invariant mass strongly favored in both. This again favors the Chiral Perturbation Theory prediction of the lower branching ratio, although, since the observed rate is in excess of that predicted in lowest order, the conclusion is not yet definite. Further experimental data on $K_L \rightarrow \pi^0 \gamma\gamma$ will be provided by Fermilab E799.

An important related decay[17] is $K_L \rightarrow \pi^0 \nu\bar{\nu}$. In the Standard Model this decay is essentially *pure* "direct" CP violating: in principle, the clean observation of just a single unambiguous event would establish the long-sought for effect! Also, the expected branching ratio[18] is about six times greater than for the $\pi^0 e^+ e^-$ case: a factor of 2 comes because one has both vector and axial vector couplings and a factor of 3 is for three types of neutrinos. Thus the central value is expected to be about 4×10^{-11}. While the background and instrumental problems are challenging, it is worth pointing out that the flux to do the measurement is clearly there at the Main Injector and the relatively higher photon energies are much easier to detect, and to veto.

Another way to see direct CP violation in $\pi^0 e^+ e^-$ decays is to observe the interference between K_S and K_L near the target. The CP conserving term does not contribute to the interference, and because the K_S branching ratio is about a factor of 300 larger than that of the K_L, the $e^+e^-\gamma\gamma$ background (discussed later) is less of a problem. Thus the result would be much easier to interpret. One way to quote the sensitivity of such an interference experiment is to say that if the branching ratio for the direct CP violating term in the K_L decay were 10^{-12}, we would measure it to 30% precision. The same detector would be used for the interference measurement but with a modified K_S beam.

The ability to study decays close to the production target will also allow measurements of the CP violating parameters η_{+-0} and η_{000}. These, especially the latter, are poorly determined and although the LEAR facility at CERN[19] will make improvements, it is unlikely that they will see a positive signal let alone be able to be sensitive to departures from the Standard Model predictions. At the Main Injector, one should be able to determine these parameters with much more precision than is presently known, based upon scaling from the experience of E621 and E731. In a similar vein, very precise tests of CPT conservation can be made.

We finally mention the search for lepton flavor violation. Although there are no compelling arguments for the level where such violations should become observable, many classes of theories[20] for extensions of the Standard Model include such new interactions. The higher the sensitivity, the greater the mass reach; while there is dependence upon coupling constants, an experiment with a sensitivity of 10^{-13} will probe mass scales up to about 350 TeV! We should mention that while it is important to also look for the corresponding decays in the B meson system, the sensitivity to a broad class of new phenomena there is significantly less.

We are thus considering essentially *four* classes of experiments for the kaon facility at the Main Injector. Each would run separately and would utilize and emphasize different elements of the detector; in addition, the configuration of the beam would be optimized for each effort.

The four different classes we denote by "High Precision" (ε'/ε); "High Sensitivity" ($K_L \to \mu e$, $\pi^0 \mu e$, $\pi^0 ee$, $\pi^0 \mu\mu$, etc); "K-short" (K_S decays, including η_{+-0} and η_{000}); and "Hermetic" ($K_L \to \pi^0 \nu\bar{\nu}$). A clean and bright beam of neutral kaons and a high rate, high (4-body) acceptance spectrometer are needed. These must combine to yield statistical sensitivities of 10^{-10} per hour, along with corresponding controls of systematic effects. The Main Injector with 120 GeV protons will provide a unique and copious source of neutral kaons of sufficient energy to make the necessary detection (and vetoing) of photons for theses measurements possible. Figure 6.2 shows the plan view of the KAMI Facility as it will be configured for many K_L experiments. Other experiments will require rearangement of the detector elements (e.g. $K_L \to \pi^0 \nu\bar{\nu}$), or rearangement of the secondary beam production elements (e.g. $K_S \to \pi^0 ee$).

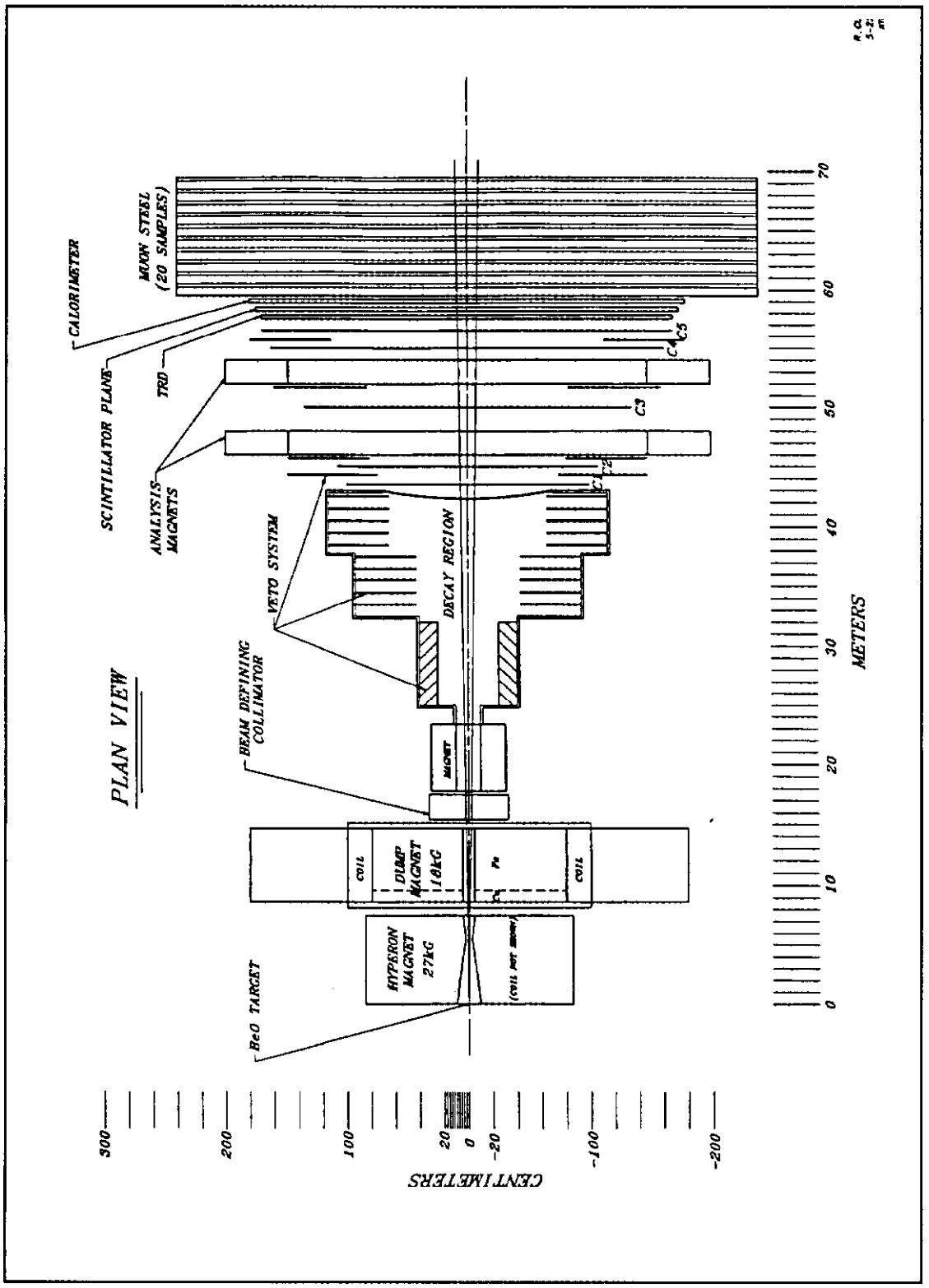

FIGURE 6.2: Plan view of KAMI Facility from design report showing secondary beam formation, decay space and apparatus. This figure illustrates the "standard" K_L configuration.

The kaon production spectrum[21] at a targeting angle of 20 mr is shown in Fig 6.3 to compare with the spectrum of the proposed higher flux, lower energy TRIUMF "Kaon Factory". This targeting angle is sufficient to reduce the intense neutron flux by a factor of about 50. The spectra shown assumes no (lead) gamma filter and Beryllium moderator for the purpose of comparison; the loss in kaon flux due to filter and modulator could be recovered for some experiments. The advantage of Main Injector over TRIUMF Kaon Factory is clearly seen, where more kaon flux of higher kaon energy (above 10 GeV) is available for the experiment at Main Injector.

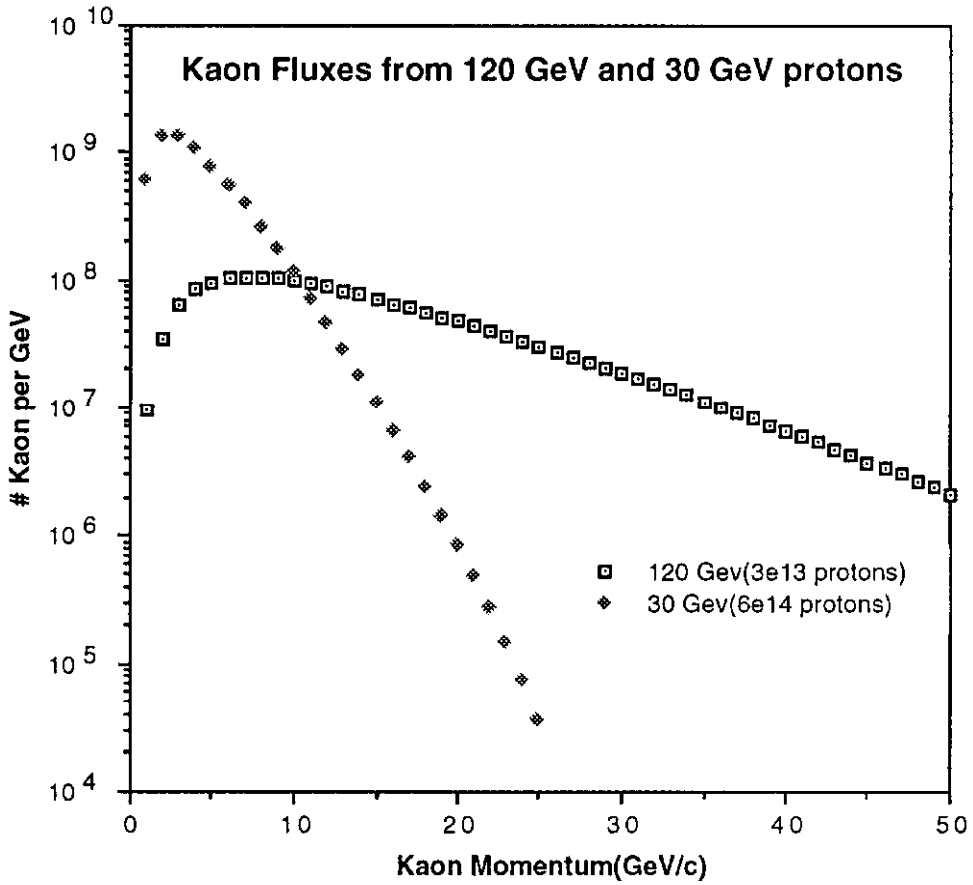

FIGURE 6.3: Kaon fluxes per GeV for comparison between 120 GeV Main Injector beam and 30 GeV TRIUMF Kaon Factory beam.

We will list some of the advantages of a higher energy machine for such experiments. These have primarily to do with those factors in the experiments which do not scale with energy.

1) With careful attention to reducing the constant term, the resolution of electromagnetic calorimeters will be dominated by the $1/\sqrt{E}$ term so that the

higher the energy the better the resolution and resolution is at a premium in such experiments.

2) Background of minimum ionizing particles does not scale with energy: a muon will simulate about 600 MeV energy deposit in an electromagnetic calorimeter so that it is difficult to maintain the same relative threshold level as one decreases the energy. This point is illustrated by the fact that the minimum detectable photon cluster energy was about 1 GeV for both BNL and FNAL Tevatron experiments on ε'/ε and $\pi^0 e^+ e^-$ although the mean kaon energy was more than 10 times greater at FNAL. As a result, the acceptance for the FNAL experiments was significantly greater.

3) Since the growth of hadronic showers is governed by ln(E) rather than E, one needs a fractionally shorter beam dump region at a higher energy facility. As an important consequence, one can be situated relatively closer to the target and thus be more sensitive to K_S decays.

4) The ability to reject events with soft photons outside of the aperture of one's electromagnetic detector is important in reducing background. Again, the dominant problem with a low threshold will be the (non-scaling) minimum ionizing background. This is important for ε'/ε, for $\pi^0 e^+ e^-$ and *especially* for $\pi^0 \nu\bar{\nu}$ where the primary background comes from the $\pi^0\pi^0$ mode.

The successful execution of each of the classes makes demands on the facility and on the detector. The beam on target should be "de-bunched" with only a minimal residual structure (~10%) permitted This is because of the very high rates of kaon decays: at a decay rate of 100 MHz; at the usual 53 MHz of RF structure this would imply near certainty of an overlap of more than one event and, for the high sensitivity experiments where pile-up in the detector is especially troublesome. Debunching of RF structure provides a significant increase in effective duty cycle, enabling essentially uniform spill structure over the 1 second flat top. The incident proton beam should be as free of muon halo as possible and the configuration of the beam definition and beam dump are most important to avoid unacceptable halo (both muon and hadron) around the neutral beam. The kaon decay region contains an anti-coincidence system throughout and must have excellent vacuum. Large aperture high field analysis magnets of suitable uniformity are required for enough precision of the momentum of the kaon decay products and for adequate acceptance. Large aperture tracking detector must also sustain the high singles rate environment due to kaon decays.

We now consider the physics reach of each of the classes of experiments in a one year running period. At this stage, many (but obviously not all) backgrounds[22] have been dealt with and the attainment of the listed sensitivities looks promising.

The "year" that we consider assumes the following. The machine runs with a 1 sec slow spill and a repetition rate of 2.9 sec. The running efficiency is taken to be 35% which translates into 4×10^6 pulses in a year period. Note that this is very close to the definition of a "Snowmass year", namely 10^7 seconds of operation. Of course one can run for this "year" every year. The beam energy is assumed to be 120 GeV.

We list in Table 6.1 the rates and sensitivities for each of the measurements and then follow with a discussion of the major features of each. The detector for which the rates and acceptance figures are given were discussed in detail in the KAMI Conceptual Design Report[1].

6.3.1 ε'/ε (High Precision)

For the accurate determination of ε'/ε, one must obtain very high statistics as well as reduced systematic uncertainty. At the Main Injector, the flux is great enough that one can still accumulate the required level of statistics while employing a small target and very small solid angle beams to reduce the level of systematic uncertainty. Very likely a variation of the double beam method of E731 will be employed. To aid in understanding the relative beam acceptances, the proton beam needs to be as stable as possible and we should be able to monitor its position on the target at the 10 μm level. The singles rate in the detectors is modest and is dominated by the interaction rate in the regenerator which is placed in one of the beams. For this to be so, it is necessary that the muon flux at the detector be $\leq 10^{-7}$ per incident proton.

The decay rate shown in Table 6.1 is only for K_L decays within the fiducial decay volume of about 18 m. The acceptance shown is for the four body $\pi^0\pi^0$ mode and it is large for the higher momentum range indicated; this range is also favorable since the gamma energy resolution improves with energy and, to accurately compare bin-by-bin the decay rates into $2\pi^0$ and $\pi^+\pi^-$, the best possible energy resolution is needed. In the analysis, only 2π decays in a 2 m region downstream of the regenerator for both beams are used; in this fashion systematic uncertainty from any acceptance difference between the two beams becomes small.

Mode	Class	Sensitivity		Beam flux	Target length [cm]	Solid Angle [μstr]	P range [GeV]	Decay rate [MHz]	accep. [%]	singles rate [MHz]	single event sensitivity (per year)
		Today	in 5 yrs.								
ε'/ε	High precision	10^{-3}	10^{-4}	3×10^{13}	8	1	10-50	0.6	35	7.5	$2. \times 10^{-5}$
$K_L \to \pi^0 e^+ e^-$	High rate	10^{-9}	10^{-11}	3×10^{13}	50	12	10-50	33	20	100	3.8×10^{-14}
$K_L \to \mu e$	High rate	10^{-11}	10^{-12}	3×10^{13}	50	12	1-15	33	34	100	2.2×10^{-14}
$K_L \to \pi^0 \mu e$	High rate	–	10^{-10}	3×10^{13}	50	12	10-50	33	20	100	3.8×10^{-14}
$K_L \to \pi^0 \nu \bar{\nu}$	Hermetic	10^{-3}	10^{-8}	3×10^{13}	20	4	2-50	10	20	10	3.0×10^{-12}
$K_S \to \pi^0 e^+ e^-$	K-short	10^{-5}	10^{-8}	1×10^{12}	50	36	10-50	15	30	75	1.0×10^{-12}

TABLE 6.1: Rates and sensitivities for several K_L decay modes in KAMI.

The final source of systematic error will be the uncertainty in the residual background. There are effects arising from scattering in the regenerator where a K_S decay can wind up in the vacuum beam (in the neutral mode). With the small beams used and with a fully active regenerator[23] in vacuum (*i.e.* one made entirely of scintillator), this effect is less than 1% and more importantly is identical for charged and neutral decays so that it largely cancels and in any case, it can be very well determined. The background from $3\pi^0$ decays which fake $2\pi^0$ decays is at the 0.4% level in E731; this background is not as easy to simulate and thus it should be lowered significantly. This will be accomplished with a fine grained, high precision electromagnetic calorimeter and in addition an extensive anti-counter system surrounding the decay region to catch missing gammas from this mode. Thus is appears that a determination with nearly 10^{-5} precision could be performed.

6.3.2 $K_L \rightarrow \pi^0 e^+ e^-$ (High Rate)

To reach the level of direct CP violation in this mode, it is necessary to run the detector in a much higher rate environment. Many backgrounds are understood[24] for this mode, including a whole variety of accidental effects. The most severe background[25] appears to arise from the $K_L \rightarrow e^+e^-\gamma\gamma$ decay; its branching ratio has recently been determined to be at the level of 5×10^{-7} (depending upon cutoff). These decays tend to have one very low energy gamma and a very low mass *ee* pair. However, after reasonable cuts on these quantities, still a sizable background remains and one has only the π^0 mass as a final constraint. With a high precision CsI calorimeter, this background is about 10^{-11} and one will probably have to live with it at this level. For the indicated configuration and a high sensitivity and high flux experiment at 2×10^{-14} for two years running, a 3 standard deviation measurement of a signal over background can be reached at 3.8×10^{-12} in branching ratio. This corresponds to 80 signal events (presumably direct CP violation) on top of 600 background $e^+e^-\gamma\gamma$ events with a $\pm$ 2 MeV π^0 mass cut, where, according to the Standard Model, a signal should be seen. Figure 6.4 shows the Main Injector discovering sensitivity in branching ratio at the 40% optimum signal efficiency cut with the presence $e^+e^-\gamma\gamma$ background for a two years running. For this and the other high-rate running conditions, the singles rates are about 100 MHz in the largest chamber but the maximum rate on a single wire (3 mm pitch) is about 600 kHz.

$K_L \rightarrow \pi^0\mu^+\mu^-$ can be sought simultaneously with the $\pi^0 e^+e^-$ mode. Although the expect direct branching ratio is smaller than the $\pi^0 e^+e^-$ mode, it provides another avenue to search for the direct CP violation.

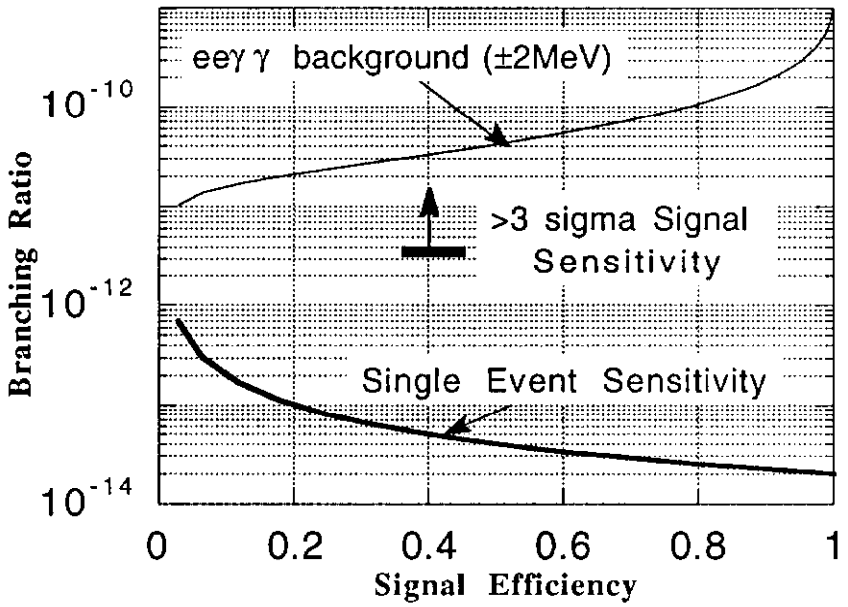

FIGURE.6.4: Main Injector $K_L \to \pi^0 e^+ e^-$ discovering sensitivity with the presence $e^+e^-\gamma\gamma$ background for a two year run at the single event sensitivity of 2×10^{-14}. The optimal signal efficiency over the entire Dalitz plot is about 40%.

6.3.3 $K_L \to \mu e$ (High Rate)

The backgrounds to this mode arise from $K_L \to \pi e \nu$ where either the π is mis-identified as a muon, or as an electron with the e mis-identified as a muon. For these backgrounds, it is important to have an extra kinematic handle and this comes from a measurement of the muon range. Hence, the experiment is optimally run in the lower momentum range indicated in Table 6.1 although the same spectrometer as for the four body decays can be employed. Hence the rates are the same as those discussed above for $K_L \to \pi^0 e^+ e^-$. Two analyzing magnets (or one with a high enough transverse momentum kick with a chamber in its center) permitting redundant momentum determinations are required for background suppression. At this time, the backgrounds for this mode are only really understood to be less than about 10^{-13} but it is clear that a highly sensitive experiment can be performed.

Currently BNL-E791 has the upper limit $BR(K_L \to \mu e) < 8.4 \times 10^{-11}$ corresponds to 70 TeV mass reach. The new proposal from BNL-E791 collaboration is pursuing to

push the limit to 2×10^{-12} (180 TeV mass reach) with the upgrade of Brookhaven AGS booster.

6.3.4 $K_L \rightarrow \pi^0 \mu e$ (High Rate)

This mode could also be sought simultaneously with the $K_L \rightarrow \pi^0 e^+ e^-$ and $K_L \rightarrow \mu e$ searches. The backgrounds are probably less than for the $K_L \rightarrow \mu e$ case because the corresponding background process, $K_L \rightarrow \pi^0 \pi^{\pm} e \nu$, has a much smaller branching ratio. Both should be sought in that one does not know *a priori* whether the flavor violating interaction is vector or axial vector, or both. The Main Injector would offer the single event sensitivity to 3.8×10^{-14} for a year running.

6.3.5 $K_L \rightarrow \pi^0 \nu \bar{\nu}$ (Hermetic)

For this search, only the instrumented decay volume and the electromagnetic calorimeter are needed. The signature is not terribly stringent: only two electromagnetic clusters in the event, consistent with coming from a single π^0. The dominant, and perhaps only, background comes from the $\pi^0 \pi^0$ decay at a branching ratio of 10^{-3}. It is possible to effectively exclude this background by making a P_T cut above the end-point for the $\pi^0 \pi^0$ decay. However, because of the finite beam size and the lack of precise information on the transverse vertex position, a Dalitz decay is required to make this cut cleanly. In the end, one would loose about a factor of 10^3 in sensitivity which is probably too great a price to pay. Hence the emphasis is on effectively vetoing the extra gammas. Since the large photon veto system and the calorimeter must form a totally hermetic detector, the calorimeter is re-stacked at the end of the decay space for this experiment.

The decay volume needs a system of anti-counters within the vacuum and the vacuum itself needs to be 10^{-6} Torr in order to eliminate the background from the hadron beam interacting in the residual gas. The problem is difficult because there are many mechanisms by which a photon can be missed and these largely nuclear effects are not well enough known to be certain of the residual inefficiency. This problem has been faced already by the BNL-E787 collaboration at Brookhaven, but in a lower and more difficult energy region and we have benefitted from their experience[26]. Nevertheless, a detailed simulation[27] shows that the single event background level with a hermetic veto system would be better than 10^{-11}. Of course, to be certain, dedicated tests will be in order.

For the exposure indicated in the Table 6.1, one would have about 80 of these background events and, with the plausible assumption that we would be able to determine

this background level independently, after subtraction we would have a three standard deviation sensitivity at about 3×10^{-12}. The rates are modest and the beam is well defined to help exclude background. By using the large P_T Dalitz decays, however, the sensitivity would be about 10^{-10} and could probably be improved by running at higher rates. Considering that at present, the deduced branching ratio is little less than 10^{-3} and that at the Tevatron, one will improve this to perhaps 10^{-8} level, this represents a major advance. We also should point out that with such a hermetic detector there is the potential for the discovery of other unexpected decay modes.

6.4 CONCLUSION

With the advent of the Main Injector, there is the possibility of doing a whole new generation of experiments in neutral kaon physics. Although the energy of the Main Injector is not as high as the Tevatron, the average number of protons deliverable per hour is about two orders of magnitude greater! With these beams, it is possible to probe with ever greater precision and sensitivity the fundamental questions of CP violation and rare decays. The greater levels of precision in probing CP violation (ε'/ε, $K_L \rightarrow \pi^0 e^+ e^-$, $K_L \rightarrow \pi^0 \nu\bar{\nu}$, $K_S \rightarrow \pi^0 e^+ e^-$) and of sensitivity in testing lepton flavour conservation ($K_L \rightarrow \mu e$, $K_L \rightarrow \pi^0 \mu e$) achievable in these experiments will provide stringent tests of the Standard Model and important windows on potential new physics.

6.5 REFERENCES

1. K. Arisaka, *et al.*, *Conceptual Design Report: Kaons at the Main Injector*, Fermilab Report FN-568 (June, 1991) and the references therein; a letter of intent to pursue high precision, high sensitivity kaon physics at the Main Injector was submitted by a collaboration from Chicago, Elmhurst, Fermilab, Irvine, Illinois, Rutgers and Saclay (P804).

2. These experiments include E731 a collaboration between Chicago, Elmhurst, Fermilab, Illinois and Saclay; E773, a collaboration between Chicago, Elmhurst, Fermilab, Illinois, and Rutgers; E799 and E832, a collaboration between Chicago, Elmhurst, Fermilab, Illinois, Rutgers and UCLA; and E621, a collaboration between Michigan, Rutgers and Minnesota.

3. E.C. Swallow (E731 Collaboration), to appear in the *Proceedings of the APS DPF Meeting*, Vancouver, Canada, August 1991. See Also the summary talk by B. Winstein, Enrico Fermi Institute preprint EFI-91-52, to appear in the *Proceedings of the APS DPF Meeting*, Vancouver, Canada, August 1991.

4. G. Barr (NA31 Collaboration), to appear in *Proceedings of the Lepton Photon Conference*, Geneva, Switzerland, August 1991. See also A.C. Schaffer, to appear in *Proceedings of the APS DPF Meeting*, Vancouver, Canada, August 1991.

5. K. Arisaka, *et al.*, *KTeV Design Report*, Fermilab Report FN-580 (Jan. 1992) for experiment E799 phase II and E832.

6. BNL-E791 collaboration; BNL-E777 collaboration.

7. Upgrade proposals presented to BNL.

8. Upgrade proposal to BNL E787.

9. K.E. Ohl, *et al.*, *Phys. Rev. Lett.* **64**, 2755 (1990).

10. *New Limit on* $K_L \rightarrow \pi^0 e^+ e^-$, A. Barker, *et al.*, *Phys. Rev.* **D41**, 3546 (1990).

11. KEK-E162 collaboration.

12. G. Buchalla, A.J. Buras, M. Harlander, MPI-PAE-Pth-30/90, July 1990.

13. C.O. Dib, I. Dunietz, F.J. Gilman, *Phys. Rev.* **D39**, 2639 (1989).

14. G. Ecker, A. Pich and E. de Raphael, *Nuc. Phys.* **B291,** 692 (1987).

15. C. Alliegro, *et al.*, *Phys. Rev. Lett.* **68**, 278 (1992).

16. G. Barr, *et al.*, *Phys. Lett.* **242B**, 523 (1990); V. Papadimitriou, *et al.*, Phys. Rev. **D44**, 573 (1991).

17. L. Littenberg, *Phys. Rev.* **D39**, 3322 (1989).

18. C.O. Dib, I. Dunietz, F.J. Gilman, *Phys. Lett.* **218B,** 487 (1989).

19. CPLEAR experiment.

20. R.N. Cahn and H. Harrari, *Nucl. Phys.* **B176**, 135 (1980).

21. This spectrum uses the phenomenological fit to a variety of data by A. Malensek; it works very well at the Tevatron and is expected to be a good estimate at the Main Injector.

22. See T. Yamanaka, KAMI-60, internal note, and the proceedings of the Breckenridge workshop and of Snowmass 1990, for a discussion of simulations of many of the backgrounds.

23. Such a regenerator, made of plastic scintillator, has been built for E773 and the preliminary results already show a substantial suppression of inelastic regeneration.

24. See Fermilab E799 proposal and addenda, also T. Yamanaka, KAMI-60, internal note.

25. H. Greenlee, *Phys. Rev.* **D42**, 3724 (1990).

26. D. Marlow, BNL E787 TN #31.

27. S. Somalwar, KAMI internal notes.

7 OTHER FIXED TARGET PHYSICS

7 OTHER FIXED TARGET PHYSICS

7.1 INTRODUCTION

The Fermilab Fixed-Target program of experiments has produced discoveries, made precision measurements, and developed a vast amount of knowledge of how to do experiments. The diversity of this program in attacking the issues of particle physics is one of its strongest assets as evidenced by experiments measuring charm production and decays with hadron and photon beams, hyperon magnetic moments and decays, deep-inelastic scattering using muons and neutrinos, direct photon production, high p_t, Drell-Yan, polarization phenomena and *CP* violation parameters and rare decays in the Kaon system.

The next Fixed target run, scheduled for 1994, will mark the end of the first decade of Tevatron operation. A 900 GeV fixed target run is possible following Collider Run 2. The upgraded Linac will increase the available proton intensity for this run to 3×10^{13} protons per spill. The Kaon and Neutrino experiments have a natural evolution into the Main Injector era and will use a significant fraction of this intensity (see sections 5 and 6 of this document). This section presents some of the current thinking on other aspects of the fixed-target program. These include charm and beauty physics, muon-scattering, dedicated spin physics and experiments using the antiproton source. A rich field of charmonium physics is already being explored by experiment E760 using a hydrogen gas-jet in the Accumulator ring and the increased flux of antiprotons expected with the Main Injector has led to a letter of intent for an experiment investigating CP violation.

It should be stated that designs for the charm and beauty experiments are not yet fully developed. While the physics interest in these areas remains compelling, it is recognized that significant improvements in areas such as data acquisition and detector capability need to be made to improve the reach of these experiments. Given the history of the charm experiments, however, we can expect them to meet these challenges. Specific experiments on hyperon decays, muon scattering, or dedicated spin physics experiments are presently in the conceptual phase.

7.2 PROSPECTS FOR CHARM PHYSICS IN THE MAIN INJECTOR ERA

Progress in charm physics has been characterized by the number of fully reconstructed charm decays obtained per experiment. Beginning in 1985, when E-691 obtained a sample of 10,000 fully reconstructed decays, Fermilab experiments have developed the technology, particularly in data-acquisition and silicon microstrip detectors, to become the leading source of data. The latest round of completed experiments using unrestrictive triggers, E687 and E791, expect to have samples of over 100,000 fully reconstructed charm particles. Experiments with more restrictive triggers and/or acceptance, such as E653 and E789, are making sensitive measurements on a select set of specific topics. When data from these experiments are fully analyzed, Fermilab will solidify its pre-eminence in several areas: the measurement of charm particle lifetimes, the observation of rare decay modes, the measurement of semi-leptonic form factors, and the establishment of limits for rare processes such as mixing. An approved experiment, E781, that uses incident hyperons should enhance data on charmed baryons.

There are many motivations for pushing to 1,000,000 and eventually 10,000,000 fully reconstructed charm particles. First, of the heavy quarks, charm is the only one that offers high enough yields of fully reconstructed decays to permit a thorough study of the delicate interplay of the weak and strong interaction which determines the exact patterns of the decays. This investigation begins with several possible quark level diagrams for the weak decay and studies effects like final state interactions, color suppression, helicity suppression, and Fermi and Bose-Einstein correlations. Second, much of the basic spectroscopy of charm particles is poorly studied or unknown. Very little information on charmed baryons exists, especially those containing strange quarks or more than one charm quark. The spectroscopy of charm and charmonium states with orbital angular momentum 1 is still not thoroughly studied. Third, these experiments will have significant numbers of reconstructed charm pairs. These will help reveal more about production dynamics and open up other possibilities, such as the determination of absolute branching fractions. Fourth, several very interesting rare decays will become accessible. For example, the purely leptonic decay, $D \rightarrow \mu \nu$ should be observable. This provides a measure of f_D, the weak decay constant. Fifth, one can expect either the observation of or new stringent limits on rare processes such as mixing. Some models predict that mixing will occur at levels observable in these experiments. Sixth, one can begin to look for truly rare phenomena such as *CP* violation (either Standard Model *CP* violation or *CP* violation produced by new

physics outside the Standard Model) and for physics completely outside the standard model such as lepton flavor violating decays.

In the future, one expects to be able to increase the number of fully reconstructed charm particles by a factor of 10 in each of the next two running periods. In hadroproduction, very high rates are possible but will require progress in detector technology, triggering and data acquisition and analysis to cope with the large amount of data. Given the rapid advance of electronics, one can already see the solutions to these problems beginning to emerge. Photoproduction, which has been a very successful source of information on charm, can advance by one order of magnitude to 1,000,000 reconstructed charm. At that point, the program will become flux-limited and some of the new ideas under consideration for enhancing the flux will need to be developed.

7.3 SPIN STRUCTURE FUNCTIONS USING THE FERMILAB MUON BEAM

The EMC measurement of the spin-structure function $g^1_p(x,Q^2)$ was originally interpreted to imply that very little of the proton's spin was carried by the constituent quarks. Though this interpretation has been vigorously challenged, there is not one universally agreed upon explanation of the data Several authors have discussed the possibilities offered by combining the traditional DIS measurement of $g^1_p(x,Q^2)$ with additional information from the produced hadrons. In particular, Carlitz, Collins and Mueller and also Manohar have pointed out that measuring the two-jet production in polarized DIS is a way of determining the gluonic contribution to the proton spin.

On the experimental front, SMC took its first data late last year, running with deuterated ammonia (ND_3) in the old EMC target and plans on taking more data in the early part of 1992. While beam polarization has been measured at HERA, the polarization was less than desired. A new experiment at SLAC (E142) has been approved and plans to take data at the end of this year using a 25 GeV electron beam. Each of these experiments is designed to measure both the proton and neutron spin-structure functions, with the goal of evaluating the Bjorken sum rule with little emphasis being placed on the hadrons produced.

At Fermilab, the muon scattering experiment E665 has completed data-taking (on unpolarized targets). The experiment has demonstrated the advantages of the high energy muon beam by presenting data down to x_{bj} of 10^{-5} and W (the hadronic center-of-momentum energy) up to 30 GeV. Of particular interest is the first measurement of the

multiple forward jet rates in a lepton deep-inelastic scattering experiment. E665 has shown that the unambiguous identification of these two forward jet events is only possible for $W > 20$ GeV. At present, the only places where these energies can be reached are Fermilab and Hera. If Hera does not upgrade to include a polarized proton option, Fermilab is the only place where the study of di-jet production using a polarized beam and polarized target can be performed.

The existing Tevatron muon beam, an experimental apparatus similar to E665 (if not identical) and a polarized target would allow one to make a qualitatively new measurement - the contribution by the gluons to the proton spin. The standard measurements of $g^1_p(x,Q^2)$ and $g^1_n(x,Q^2)$ would complement (compete with) the previously mentioned experiments, greatly extending the available kinematic regime. The particle ID available in the E665 apparatus would open other avenues of investigation. In particular, the study of high energy kaons produced in the deep-inelastic interaction probes the polarization of the sea quarks.

7.4 PROSPECTS FOR FIXED-TARGET BEAUTY PHYSICS IN THE MAIN-INJECTOR ERA

Although present fixed-target *B* experiments are not limited by available beam intensity, technological developments, which may be anticipated during the remainder of the decade, could result in a thriving experimental program to exploit fully the Tevatron luminosity available during the Main-Injector era. The ultimate goal of such a program is the observation of *CP* violation in beauty decays, or the demonstration at a significant level of sensitivity that *CP* is conserved. Of course, this is an audacious and futuristic goal. At present, one fixed-target experiment, E-653, has observed beauty decays and two more, E-789 and E-771 expect to have some dozens of events in their present data. In practice, a successful Beauty program would have to evolve by exploiting new technology rather like the charm program.

The most promising path to the study of *CP* violation in beauty decays is the study of rare decays, for example $B^0 \rightarrow \pi^+\pi^-$ and $B^0 \rightarrow \psi K_S$, which have large predicted *CP* asymmetries; study of both of these modes is desirable, since in the standard model they give complementary information about the "unitarity triangle". We choose as a sensitivity benchmark $\sim 10^3$ tagged and reconstructed events in either of these two modes. In the spirit of an exercise for the future, we shall describe below the steps needed to achieve this goal.The potential of fixed-target experiments to achieve this goal depends on crucial

parameters such as the $b\bar{b}$ production cross section and the $B^0 \rightarrow \pi^+\pi^-$ and $B^0 \rightarrow \psi K_S$, branching ratios, at present unknown. Plausible estimates, however, suggest that *CP*-level sensitivity could come within reach as experimental techniques are advanced.

At present, limitations from data-acquisition bandwidth, radiation damage to silicon-strip detectors, and rates in tracking detectors lead to maximum interaction rates of 10^7/s for an open-geometry experiment and 5×10^8/s for a restrictive-geometry experiment (E789). We assume that beauty experiments in the Main-Injector era will have data-acquisition and triggering capabilities improved by at least an order of magnitude. Limitations due to radiation damage and track multiplicity may both be substantially alleviated by the advent of radiation-hard silicon pixel detectors. We envision an open-geometry experiment composed largely of silicon pixel detectors surrounding a short, high-field, superconducting magnet with a filament target transverse to the beam to separate the production and decay vertices. The charged-particle tracking is followed by a beam dump/muon filter with a muon spectrometer capable of generating prompt ψ and high-p_t muon triggers. Given the pace of pixel-plane development, pixel devices to cover the necessary area may be available by the end of the decade. Table 1 lists various parameters of the apparatus. Due to their differing resolution requirements, the tracking detectors are divided into two classes, "vertex" and "spectrometer" detectors, even though they may be the same type of device. The $B^0 \rightarrow \psi K_S$, data are triggered on the $\psi \rightarrow \mu^+\mu^-$ decay detected in the muon spectrometer, while the $B^0 \rightarrow \pi^+\pi^-$ data are triggered on a single high-p_t muon from the "tagging" B. A Level-2 trigger reconstructs track impact parameters in the vertex detector to reduce the single-muon trigger rate sufficiently for recording the data. Tables 2 and 3 show sensitivity estimates for the two benchmark modes in terms of tagged, reconstructed events per year of running time. The resulting sensitivities suggest the feasibility of *CP*-violation measurements in these modes. Of course, this approach could also yield interesting levels of sensitivity to other important issues in B physics; for example, the fixed-target boost can enhance the study of B_s mixing (using $B_s \rightarrow \psi\phi$) given the rapid oscillations of the decay rate vs. time. Finally, we note that 10^9 interactions/s is by no means a hard-and-fast upper limit.

1) Pixel Vertex Detector	
	- 5 stations, from 50 to 150 cm from target
	- From 10 to 30 cm radius with 5 mm hole (200 mrad acceptance)
	- Operates at > 90% efficiency to 50 MRad
	- 30 μm elements
	- 5 μs readout time
2) DAQ System	
	- 200 MB/s to tape capability
	- 10 GB buffer
	- Readout time < 20μs
3) Spectrometer	
	- Fine-grained, 100 μm pixels in center to 1 mm at 200 mrad
	- Momentum resolution dp/p < 1% for p < 100 GeV/c
	- As short as possible (< 4 m to beam dump)
4) ψ Trigger	
	- Can handle rates up to 2×10^5 muons/cm^2/s
	- First-level muon trigger in < 19 ns
	- Reconstruct in < 1 μs
	- ψ trigger rate 1×10^4/s
5) Single-Muon Trigger	
	- First-level muon trigger in < 19 ns
	- Single muon with p_t > 0.8 GeV/c
	- Rate $\approx 2 \times 10^{-4}$/interaction or 2×10^5/s
6) Level-2 Trigger	
	- Reconstruct track impact parameters at target
	- Pipeline at 5 μs/trigger
	- $\times$ 20 rejection at 50% efficiency

TABLE 7.1: Apparatus assumptions

Assume:	1×10^{16} interactions/year
I. *B* Detection	
$\sigma_{b\bar{b}}/\sigma_{tot}$	1×10^{-6}
B^0 or $\bar{B}^0$ produced	5×10^{-1}
BR ($B^0 \rightarrow \psi K_S$	1×10^{-3}
BR $\psi \rightarrow \mu^+\mu^-$)	7×10^{-2}
BR ($K_S \rightarrow \pi^+\pi^-$)	7×10^{-1}
K_S decay in 2.5 m	6×10^{-1}
Acceptance x efficiency	3×10^{-1}
Total	4×10^{-12}
	$\rightarrow 4 \times 10^4$ reconstructed/year
II. Tagging fraction	
BR ($B \rightarrow \mu X$)	1×10^{-1}
Efficiency	3×10^{-1}
Total	3×10^{-2}
Grand Total	1.2×10^{-13}
	$\rightarrow$ 1200 tagged events/year

TABLE 7.2: $B^0 \rightarrow \psi K_S$

Assume:	1×10^{16} interactions/year
B Detection and Tagging	
$\sigma_{b\bar{b}}/\sigma_{tot}$	1×10^{-6}
B^0 or $\bar{B}^0$ produced	5×10^{-1}
BR ($B^0 \rightarrow \pi^+\pi^-$)	2×10^{-5}
Acceptance x efficiency	3×10^{-1}
Tagging fraction	3×10^{-2}
Total	9×10^{-14}
	$\rightarrow$ 900 tagged events/year

TABLE 7.3: $B^0 \rightarrow \pi^+\pi^-$

7.5 PROSPECTS FOR SPIN PHYSICS IN THE MAIN-INJECTOR ERA

In contrast to the triumphs of the Standard Model in explaining the spin dependence of experimental results in the electro-weak sector, it has had little success where strong interactions are involved. With little guidance from theory, however, experiments have revealed a rich structure of large spin effects in hadronic interactions, the physics of quarks and gluons. (See, for example, Proceedings of the 1990 High Energy Spin Physics Conference, K.-H. Althoff, W. Meyer (ed), Springer-Verlag (1991)). Perturbation expansions of QCD require "massless" constituents and thus strict helicity conservation. One might expect as one approached the region of perturbative QCD, high energies and high transverse momenta, that spin phenomena would become less important. Thus far, this has not proved to be the case. Fermilab experiments have found hyperons are produced with large polarizations at the highest energies (800 GeV fixed target) and the highest transverse momentum, 4 GeV/c, measured. The Fermilab polarized beam experiment has found large spin asymmetries in pion production. Experiments at the highest energy accelerator of a polarized protons, the AGS, show large spin dependence in proton-proton elastic scattering which increase with transverse momentum.

It may be short-sighted to simply ignore these phenomena as not being "fundamental" without at least a qualitative understanding of how they approach the spin independent domain of PQCD. This implies extending the kinematic reach of the spin experiments to the higher transverse momenta within the range of the Main Injector program. Without a positive result of this type of test, it is possible that incorrect elements of PQCD or even QCD itself would remain undiscovered. If the large spin effects of hadronic physics do go away as predicted by PQCD, it will be an indication of the validity of QCD. Even if this is the case and the strong force is "known", spin effects still probe the majority of all quark production and structure. "Soft" hadronic physics, it may be argued is at least as important to our understanding of nature as nuclear physics, atomic physics, and condensed matter physics where the fundamental theory is "known" but much needs to be understood. No effective theory of the static spin structure of baryons has survived the Fermilab program of hyperon magnetic moment measurements. We must remember that the discovery at Fermilab of strange baryon polarization was unexpected and completely unmotivated by the then fashionable Regge theory. The recent discovery, again at Fermilab, of these polarization effects in anti-hyperons was just as surprising and again not expected based on current phenomenological models. The question of what happens when the strange-quark

is replaced by a heavier charm-quark is one for which the present generation of theories have no prediction.

With polarized beam from the Main Injector added to the Tevatron, Fermilab will be in a unique position to carry out a program of investigating hadronic physics. The high intensities and dedicated running of the Main Injector will allow the inclusive spin measurements to reach higher transverse momenta and systematically determine the kinematic behavior of strong interaction spin dependence. Even though a polarized Main Injector will have an intensity somewhere between 1% (current technology) and 10%(projected improvements of current technology in the next 10 years) of the unpolarized Main Injector, it will still be the world's most intense source of high energy polarized protons.

The use of a polarized proton beam in the fixed target mode is particularly meaningful and informative in combination with a polarized target, since such a setting provides a variety of spin combinations and cleaner experimental data than when the target is unpolarized. The major class of processes sensitive to the correlation of the quark and gluon helicity with that of the proton is that associated with the electromagnetic interactions in which a real or a virtual photon carries the information about the helicity of the proton constituents. These processes are direct photon production by the polarized beam and the production of $\mu^+\mu^-$ pairs (the Drell-Yan process). Direct photon production is associated with the Compton scattering of gluon on quark into photon and quark: $g+q \rightarrow \gamma+q$, while the Drell-Yan process is due to quark-antiquark electromagnetic annihilation. Therefore, the former process measures a combination of the quark and the gluon helicity structure functions while the latter one gives information about a similar combination of the quark and the antiquark helicity distributions. Studying both these processes with a polarized beam would require no new experimental techniques since both processes are routinely observed and studied in a non-polarized setting.

A systematic study of the kinematic behavior of hyperon (and anti-hyperon) polarization for all of the hyperons is easily within the reach of the Main Injector and the Main Injector fed Tevatron using unpolarized protons. The understanding gained by these experimental results could then be tested and extended by spin transfer measurements producing hyperons using the polarized proton beam. Exploring the systematics of polarization phenomena with charm baryons to compare to strange baryons should provide important new information to model-builders. Of course, experiments to measure the polarization of charm baryon states from unpolarized proton collisions have not yet been

attempted. Whatever the results of such experiments, the ability to use a polarized proton beam to test the spin transfer properties of charmed quark systems may prove useful. The ability to polarize charmed baryons would open the possibility of measuring their magnetic moments. The measurement of the magnetic moment of the charm baryons is not easy but is probably less ambitious that the first hyperon magnetic moment measurements made at Berkeley, Brookhaven, and CERN in the pre-Fermilab era. Since the spin precession angle, which determines the magnetic moment measurement error, of the charmed baryon is determined by its flight path, high laboratory energy and high field, short length magnets would be essential. If the quark is indeed a fundamental particle, its magnetic moment is inversely proportional to its mass so that charmed quark moments would be significantly less than those of strange quarks. We believe that a facility with a polarized proton beam of high energy would provide a unique opportunity to investigate new areas of particle physics and clarify the uncertainties in the dynamics of strong interactions raised by current spin experiments. In particular, a vigorous Main Injector and Tevatron program, beginning with hyperon and charmed particle polarization studies using unpolarized beam, leads naturally to one using polarized beam in both the fixed target mode, with and without a polarized target. If past experience in high energy spin physics is any guide, our main expectation would be to expect spin effects which defy all expectations.

7.6 *CP* VIOLATION IN HYPERON DECAY

The observation of *CP* violation in decays of the $\bar{\Lambda}\Lambda$ system formed in the reaction: $\bar{p} + p \rightarrow \bar{\Lambda} + \Lambda \rightarrow \bar{p}\,\pi^+ + p\,\pi^-$ is an experiment that requires a large number of antiprotons; it becomes a very attractive option during the Main Injector era. A letter of intent for such an experiment has been submitted to the Laboratory (proposal P-859). A stored antiproton beam of 1.641 GeV/c interacting with a hydrogen gas-jet is used to produce $\bar{\Lambda}\Lambda$ pairs exclusively. The advantage of such an arrangement comes from the fact that the initial state is *CP* invariant. Since final states must have identical *CP* symmetry if *CP* is conserved, the observation of a *CP* odd quantity is a signal of *CP* violation.

CP odd quantities are measured by comparing the Λ decay with the $\bar{\Lambda}$ decay, in particular, by comparing the angular distributions in the center of mass frames of the Λ and the $\bar{\Lambda}$. The angular distribution of the final proton is $1 + \alpha P \cos\theta$ where P is the polarization of Λ. In the strong production process, the $\bar{\Lambda}\Lambda$ will be produced with equal polarization normal to the production plane. The quantity measured is $\tilde{A} = (N_p^{up} - N_p^{down} + N_{\bar{p}}^{up} - N_{\bar{p}}^{down})/N = \frac{1}{2}P(\alpha + \bar{\alpha})$ for $\bar{\Lambda}\Lambda$ decays where up(down) refers to particles above or

below the production plane defined by $\vec{p}_i \times \vec{\Lambda}$. A non-zero value for $\tilde{A}$ implies *CP* violation. Theoretical predictions lie in the range of $(1.5 - 0.15) \times 10^{-4}$.

Approximately 10^{10} $\bar{\Lambda}\Lambda$ pairs are required for this measurement. In order to achieve a high luminosity, a smaller antiproton storage ring ($\sim \frac{1}{4}$ of the circumference of the present Accumulator) will have to be built. The physics payoff, however, is significant; the observation of *direct CP* violation in the hyperon system will test if *a single* set of KM matrix elements will explain all of the *CP* violation effects. Finally, the existence of such a low energy ring may serve as the stepping stone towards a program of physics with stopped antiprotons at a future time.

7.7 CONCLUSION

The commissioning of the Main Injector will bring a new era of opportunity for fixed target experiments which will rise to meet the technical challenge. The availability of extracted beam during collider operation also offers a year round opportunity to meet the demand for test beams needed for detector R&D for Fermilab and the SSC.

8 1993-1997 AND BEYOND

8 FERMILAB 1993 - 1997 AND BEYOND

Fermilab III—a series of improvements including the Linac upgrade, the Main Injector and detector upgrades—will give the U.S. a vital high-energy physics program in the decade to come and keep Fermilab a forefront research institution after the SSC takes up its mission at the high-energy frontier. It will provide a natural transition for experimenters who plan to use the SSC; and it will provide exceptional opportunities for those who search for new phenomena at mass scales accessible at Fermilab.

The Fermilab program will explore some of the most compelling questions in high-energy physics: What are the precise values of the properties of the electroweak bosons and their couplings to fermions? Does the top quark exist? If it does exist, what is its mass? Do its decays suggest something other than the minimal model? Do neutrinos have masses? Can a neutrino of one generation change into a neutrino of another generation? What gives rise to CP violation?

We have just begun to ask the more deeply significant questions about the weak decays of charmed particles. The study of spectroscopy and weak decays of bottom particles is just beginning, but it has a promising future at Fermilab.

Today, 1,300 scientists and 450 graduate students work on experiments at Fermilab. In the years to come, new men and women will arrive, drawn by the richness of Fermilab's program—richness not only in diversity but in the opportunity to answer questions of compelling scientific interest.

Where lies the future of Fermilab's programs? How will they evolve in the context of several budget scenarios.

8.1 THE FERMILAB BUDGET

As requested in Chairman Witherell's letter of January 13, 1992, we present the Fermilab budget request in four parts: a) costs of maintaining the laboratory in a condition ready to run, including ES&H costs, but without accelerator operations ("hot standby"); b) incremental costs to operate the accelerator complex; c) additional costs to operate the experimental program; and d) costs of other program elements.

"Hot standby" costs in FY92 would be $131M. Table 8.1 shows the expected evolution of this budget. While it shows an increase compatible with inflation, funds

available to the research program will decline because of new DOE requirements placed on the Laboratory. Among the many escalating costs: costs of compliance with DOE orders pertaining to ES&H, and the costs of reporting compliance with such orders; the cost of greater emphasis on building and road maintenance, and the costs of reporting such programs; the cost of greater emphasis on formal quality assurance programs, and the cost of documenting our response. These costs could shrink the funds available to the experimental program by as much as $5M per year. The "hot standby" costs in Table 8.1 present the declining programmatic operating costs and the rising "new requirement" costs in such a way that the sum rises only with inflation. Clearly, given a constant-effort budget, such a scenario requires reducing the number of experimental efforts that can be supported.

Table 8.2 shows the incremental costs to operate the accelerator complex. Electrical energy at Fermilab costs roughly $17 million per year. Note that the Collider program uses less electrical energy than the Fixed Target program. Table 8.3 shows the additional power costs for the experimental program. Secondary beam lines and large analysis magnets use extra energy—another reason why the number of fixed target experiments will have to decrease.

Table 8.3 gives the incremental costs for the experimental program.

Table 8.4 gives the costs of other program elements. They include Theoretical Physics, Theoretical Astrophysics, Advanced Computing R&D, SDC, and the Accelerator R&D not directly related to implementing the experimental program.

TABLE 8.1

TABLE 8.1

COST OF "HOT STANDBY"

(Constant FY1993 $: $000)

ITEM a.	FY92	FY93	FY94	FY95	FY96	FY97
PERSONNEL COSTS	92,685	92,754	92,754	92,754	92,754	92,754
M&S OPERATING FOR G&A SECTIONS	22,672	20,752	20,347	20,484	21,610	21,250
GENERAL PLANT PROJECTS (GPP)	4,301	4,350	4,400	4,400	4,400	4,400
EQUIPMENT IN SUPPORT OF G&A SECTIONS	799	1,000	750	750	750	750
STANDBY POWER	10,000	10,000	10,000	10,000	10,000	10,000
TOTAL ITEM a.	130,457	128,856	128,251	128,388	129,514	129,154

TABLE 8.2

INCREMENTAL COST FOR ACCELERATOR OPERATIONS

(Constant FY1993 $: $000)

ITEM b.	FY92	FY93	FY94	FY95	FY96	FY97
PERSONNEL COSTS	1,292	1,350	1,350	1,350	1,350	1,350
Incremental Personnel Costs: Overtime for Accelerator Division Sections and related groups						
M&S FOR ACCELERATOR OPERATIONS	15,850	14,142	13,949	14,336	14,515	14,712
EQUIPMENT IN SUPPORT OF ACCELERATOR DIVISION AND TECHNICAL SUPPORT SECTION	1,556	1,100	900	1,000	1,100	1,200
INCREMENTAL POWER FOR ACCELERATOR OPERATIONS	2,589	2,500	2,500	2,500	2,500	3,450
TOTAL INCREMENTAL FOR ITEM b.	21,286	19,092	18,699	19,186	19,465	20,712

TABLE 8.2

TABLE 8.3a

INCREMENTAL COST FOR EXPERIMENTAL PROGRAM

Constant FY1993 $: $000

ITEM c.	FY92	FY93	FY94	FY95	FY96	FY97
PERSONNEL COSTS	9,922	10,002	10,002	10,002	10,002	10,002
M&S FOR EXPERIMENTAL PROGRAM OPERATIONS	11,377	10,999	11,094	11,149	11,703	11,282
EQUIPMENT IN SUPPORT OF EXPERIMENTAL PROGRAM	1,567	1,237	1,237	1,237	1,237	1,237
AIP IN SUPPORT OF COLLIDER AND FIXED TARGET PROGRAMS	7,377	7,605	7,600	7,600	7,600	7,600
ACCELERATOR, RESEARCH AND COMPUTING R&D IN SUPPORT OF THE APPROVED EXPERIMENTAL PROGRAM	2,700	2,850	2,850	2,850	2,850	2,850
EQUIPMENT FOR EXPERIMENTS *	18,163	18,860	19,210	19,210	19,210	19,210
POWER	4,618	4,500	5,250	4,250	2,000	6,000
TOTAL INCREMENTAL FOR ITEM c.	55,724	56,053	57,243	56,298	54,602	58,181

* reference Table 8.3b

TABLE 8.3b

TABLE 8.3b

EQUIPMENT FOR EXPERIMENTS

(Constant FY1993 $: $000)

EXPERIMENTAL PROGRAM	FY92	FY93	FY94	FY95	FY96	FY97
CDF	2,340	3,100	5,200	2,600	0	0
DØ	3,610	1,800	1,800	0	0	0
B Detector	0	0	0	3,000	6,000	8,250
Collider Contingency @	500	700	1,400	3,150	750	0
KTeV	4,200	5,000	4,800	1,000	0	0
E781	1,040	1,770	1,320	0	0	0
P815	270	1,480	330	0	0	0
Other FT	2,090 ◊	1,000	500	3,000	6,000	6,500
Offline Computing †	3,700	2,900	2,400	5,000	5,000	3,000
Other *	413	1,110	1,460	1,460	1,460	1,460
Total Equipment for Experiments	18,163	18,860	19,210	19,210	19,210	19,210

@ Available for not yet approved CDF, DØ upgrades including Run II tracking
* Sloan Digital Sky Survey, . . .
† for Collider and Fixed Target
◊ Includes $1,166k costed for 1991 run

TABLE 8.4

OTHER PROGRAMS †

(Constant FY1993 $: $000)

Item d.	FY92	FY93	FY94	FY95	FY96	FY97
Advanced Accelerator R&D (Tesla)	259	500	500	500	500	500
Solenoid Detector Collaboration	1,512	2,012	2,012	2,012	2,012	2,012
Advanced Magnet R&D	504	0	0	0	0	0
Experimental Astrophysics	336	336	336	336	336	336
Main Injector R&D and Pre-Op	2,900	4,000	3,854	4,175	4,465	0
HEPNET *	0	0	0	0	0	0
ACPMAPS	1,070	0	0	0	0	0
Theoretical Physics	2,226	2,226	2,226	2,226	2,226	2,226
Equipment in support of Central Computing ◊	2,629	2,629	2,629	2,629	2,629	2,629
Subtotal Program Costs	11,436	11,703	11,557	11,878	12,169	7,703
Billed G&A	-1,650	-1,650	-1,650	-1,650	-1,650	-1,650
SSC Magnet Program G&A	-5,168	0	0	0	0	0
TOTAL INCREMENTAL FOR ITEM d.	4,618	10,053	9,907	10,228	10,519	6,053

† Other Programs contain Personnel Costs and M&S unless otherwise noted

◊ Equipment only, no personnel costs included

* HEPNET is a separately funded activity

Table 8.5 summarizes the budget requests for "Line Item Construction" projects. Since these projects benefit the Collider and Fixed Target programs, no attempt to split these costs between Collider and Fixed Target was made. The Linac Upgrade Project, a three year project totaling $22.8M in construction funds, will be completed in FY92. The total estimated cost (TEC) for the Main Injector project based on the current cost estimate is $185M in then-year dollars. Table 8.6 summarizes the Fermilab budget projection over all categories through the fiscal year 1997 in constant FY93 dollars.

These budget figures require some assumptions about the life expectancy of individual subprograms. The proposal for evolution of the program assumes an annual budget equal to the FY93 President's Budget Request in constant dollars over the period 1993 to 1997. Keeping the plan within that constraint meant leaving some excellent things out. The plan reduces the total number of fixed target experiments to five or six. Funding for a Tevatron Collider detector dedicated to B physics can only begin in FY95. Similarly, funding for a neutrino oscillation experiment cannot begin until the middle of the decade. Ultimately, advice from the Fermilab Physics Advisory Committee will guide the relative allocation among the various programs.

TABLE 8.5

TABLE 8.5

LINE ITEM CONSTRUCTION PROJECTS

($000)

	FY92	FY93	FY94	FY95	FY96	FY97
THEN-YEAR $						
LINAC UPGRADE	6,166	--	--	--	--	--
MAIN INJECTOR	15,000	30,000	50,000	55,000	35,000	--
120 GeV NEUTRINO BEAM	--	--	--	--	--	15,000
TOTAL	21,166	30,000	50,000	55,000	35,000	15,000
CONSTANT FY1993 $						
LINAC UPGRADE	6,384	--	--	--	--	--
MAIN INJECTOR	15,531	30,000	48,170	51,027	31,259	--
120 GeV NEUTRINO BEAM	--	--	--	--	--	12,455
TOTAL	21,915	30,000	48,170	51,027	31,259	12,455

TABLE 8.6

SUMMARY TABLE

(Constant FY1993 $: $000)

		FY92	FY93	FY94	FY95	FY96	FY97
ITEM a.	COST OF "HOT STANDBY"	130,457	128,856	128,251	128,388	129,514	129,154
ITEM b.	INCREMENTAL COST FOR ACCELERATOR OPERATIONS	21,286	19,092	18,699	19,186	19,465	20,712
ITEM c.	INCREMENTAL COST FOR EXPERIMENTAL PROGRAM	55,724	56,053	57,243	56,298	54,602	58,181
ITEM d.	OTHER PROGRAMS	4,618	10,053	9,907	10,228	10,519	6,053
Subtotal Items a. - d.		212,085	214,055	214,100	214,100	214,100	214,100
LINE ITEM CONSTRUCTION		21,915	30,000	48,170	51,027	31,259	12,455
TOTAL - ALL ITEMS		234,000	244,055	262,270	265,127	245,359	226,555
TOTAL POWER (INCLUDED IN ABOVE TOTALS)		*17,207*	*17,000*	*17,750*	*16,750*	*14,500*	*19,450*

TABLE 8.6

8.2 THE EVOLUTION OF THE FERMILAB PROGRAM

The Fermilab program does not fall neatly into Fixed Target and Collider programs, except in the case of the procrustean budget categories. To make things easier to understand, the charm and beauty experiments were not included in either category but were given their own. The 800 GeV Fixed Target program, excluding charm and beauty experiments, comprises four types of experiments: CP Violation and Weak Decays, Parton Distributions and Hard Collisions, Static Properties of Hadrons, and Neutrino Experiments.

8.2.1 CP Violation and Weak Decays

Table 8.7 gives the current list of approved experiments in this category. E-773 will provide the most accurate measurement of the phase difference of the two charged pion amplitude and the two neutral pion amplitude. E-799 will search for rare neutral K decays and will seek to find $K_L^0 \rightarrow \pi^0 e^+ e^-$. E-773 finished data acquisition in 1991 and E-799 completed Phase I data acquisition in 1992. The value for the magnitude of $Re(\varepsilon'/\varepsilon) = (6.0 +\!\!- 6.9) \times 10^{-4}$ measured by Fermilab E-731 is consistent with zero. The latest result from CERN NA-31 is $(23+\!\!-7) \times 10^{-4}$ which is three standard deviations from zero. E-832, a continuation of the search for direct CP violation in the 2π decays of the K^0 by the same collaboration that has done E-731, E-773 and E-799 Phase I, was given Stage I approval in February for an improved experiment capable of 10^{-4} accuracy. The collaboration will build the KTeV detector to do both E-832 and E799 Phase II.

Approved CP Violation and Rare Decays Experiments	
E-773 (Gollin)*	Phase Difference Between η_{00} and η_{+-} (5/29)
E-799 (Wah/Yamanaka)**	Studies of CP Violation Using Rare K_L Decays (6/39)
E-832 (Hsiung/Winstein)	Search for Direct CP Violation in the 2π Decays of K^0 (6/41)
* Data taking completed January 1992 ** Letter of Intent	(institutions/physicists)

TABLE 8.7

8.2.2 Parton Distributions and Hard Collisions

This category includes a few experiments that do not fit neatly in any single category. Table 8.8 gives a list of these experiments. E683, E706 and E665 finished data acquisition in the recent very successful fixed target run completed January 1992. E-706 measured inclusive cross sections for direct γ's up to a p_t of 10 GeV/c. This process is directly sensitive to the gluon structure of the colliding hadrons. P834 is a letter of intent to continue these studies in 1994. E-683 used a photon in the initial state and detected jets in the final state. The μ scattering experiment, E-665, designed to measure F_2 and quark fragmentation, was completed in 1991. All three experiments study hard collisions in a kinematic regime differenct from that of the Collider.

Parton Distribution and Hard Collisions Experiments recently completed and Proposals/Letters of Intent	
E-683 (Corcoran)*	Photoproduction of Jets (10/35)
E-706 (Slattery)*	Direct Photon Production (9/58)
E-665 (Schellman)*	Muon Scattering with Hadron Detection (17/92)
P-834 (Slattery)**	Direct Photon Production - Continuation of E-706 (9/53)
P-857 (Sarycheva)**	SPIN-TENSOR (1/9)
P-858 (Krisch)	Spin Effects in High-P_t^2 P-P Scattering (8/77)
* Data taking completed January 1992 ** Letter of Intent	(institutions/physicists)

TABLE 8.8

The data taking for ν scattering experiments E-744/E-770 was completed in 1988. This experiment was designed to measure $\sin^2\theta_W$ and structure functions. Over three years of taking data, it obtained more than 10^6 ν and $\bar{\nu}$ events, the largest sample of such events ever recorded. The experiment used a beam that contained a mixture of neutrinos and anti-neutrinos to provide precise measurements of F_2 and xF_3. These measurements yielded a value of Λ_{QCD}. The analysis of the data has encouraged some of the proponents to plan a similar experiment with higher statistics for neutral current events using separate beams of neutrinos and anti-neutrinos. The Laboratory is considering a proposal for such an

experiment, P815, (Table 8.9) for 1994-96. It will improve the measurements of $\sin^2\theta_W$ and ρ by factors of 2 to 3 and 4 respectively.

Nearly all the experiments in the category of Parton Distributions and Hard Collision Experiments use large sophisticated spectrometers built incrementally over the last decade. E-665 used the Chicago Cyclotron magnet —the same iron yoke Enrico Fermi used more than forty years ago. Any additional experiments that receive approval for running in 1994 will use existing detectors with modest improvements. Because of the funding level, only two or three additional experiments will receive approval to run in 1994.

Neutrino Experiments	
P-815 (Shaevitz)	Precision Measurements of Neutral Current Interactions (7/16)
Note: Numbers in parentheses denote total number of institutions and physicists, respectively.	

TABLE 8.9

8.2.3 Static Properties of Elementary Particles

This category contains two completed experiments, E-760 and E-800 and one proposal, P-835, see Table 8.10. Experiment E-760 used a circulating antiproton beam and a gas jet in the Accumulator ring to make very precise measurements of the widths and masses of charmonium. This experiment demonstrates the unique capabilities of the Accumulator for low-energy antiproton experiments. E-800 is a precision measurement of hyperon magnetic moments. This experiment, also completed in January 1992, is the most recent in a series of superb experiments that began in 1972 with E-8.

Static Properties of Hadrons Experiments recently completed and Proposals/Letters of Intent	
E-760 (Cester)*	Charmonium States (7/65)
E-800 (Johns/Rameika)*	Magnetic Moment of Ω^- Hyperon (4/15)
P-835 (Cester)	Continuation of E-760 (7/64)
* Data taking completed January 1992	(institutions/physicists)

TABLE 8.10

8.2.4 Test Beam Activities

Fermilab can fulfill the SSCL request for two beams for detector development and testing for SDC and GEM in 1994. The Main Injector will make it easier to accommodate test beam requests. Leaving aside requests from the SSCL for test beams, Fermilab will be forced to decommission beams, but decommissioning will achieve only small operating savings. Unfortunately, the increase described earlier in the cost of doing business will more than counterbalance these savings. Demands on Fermilab for test beams exceeded all expectations during the last fixed target run. Twenty (20) completed tests included 13 related to the SSC.

8.2.5 Charm and Beauty Experiments

Experimenters at Fermilab carry out more experiments devoted to charm and beauty than to any other single topic. Table 8.11 gives the list of these experiments. Two of the charm experiments (E687 and E791) accumulated samples which should yield greater than 10^5 fully reconstructed charm decays. Until now the best previous experiment of this type, E691, a photoproduction experiment, amassed a sample of 10^4 fully reconstructed decays. Experiments E690, E771, and E789 expect to detect some B decays. All of the Fixed Target charm and beauty experiments completed data taking during the recent fixed target run. Several have submitted letters of intent for 1994 and are among the candidates for the remaining two or three possible fixed target slots.

Work reported in papers from the Breckenridge Workshop and in Chapter 7 shows that some of these experiments could reach > 10^6 fully reconstructed charm decays in the 1994-96 time frame. If so, the best could continue, with improvements, to acquire these larger samples of charm and modest samples of B's. Potential mergers of teams with a common interest could lead to even stronger experiments.

The continuing CDF collaboration, E-775, will have its first experience with a silicon microstrip detector during Collider Run Ia,b, beginning in May 1992. This collaboration has received an infusion of talent that wishes to work with the large 60 microbarn cross section available at the Tevatron Collider. Such an infusion will help speed the development of the technology needed to make B detection practical at a hadron collider. The Laboratory has received a proposal to add a silicon microstrip detector to the D0 detector, and to add new collaborators; the June 1992 PAC meeting should produce a recommendation.

At this time, no one can say for sure whether any of the presently approved efforts in their current form will reach the goal of CP violation. However, these experiments are developing the technology that will lead to the next step, and that step will develop the technology for the next step. When these steps are successful, we can expect most of the participants to coalesce in a collaboration whose goal is to build a collider detector dedicated to B physics. Fermilab will solicit proposals for such a detector in 1993, for commissioning near the end of the decade. Such a detector would either be a substantial upgrade of CDF or D0 or an entirely new detector. Major funding for the construction of such a detector could not start until 1995.

Charm and Beauty Experiments Recently Completed and Proposals/Letters of Intent

E-672 (Zieminski)*	High Mass Dimuon and High P_t Jets (6/29)
E-687 (Butler)*	Photoproduction of Charm and Beauty (12/92)
E-690 (Knapp)*	Hadronic Production of Charm and Beauty (5/28)
E-771 (Cox)*	Beauty Production by Protons (21/112)
E-775 (Shochet/Tollestrup)	CDF-Silicon Microvertex Detector
E-781 (Russ)	Large-X Baryon Spectrometer (13/48)
E-789 (Kaplan/Peng)*	Production and Decay of b-Quark Mesons and Baryons (8/35)
E-791 (Appel/Purohit)*	Hadronic Production of Beauty and Charm Particles (13/77)
P-829 (Appel/Purohit)	Continuation of E-791 (10/45)
P-831 (Cumalat)**	Continuation of E-687 (15/32)

* Data taking completed January 1992 ** Letter of Intent (institutions/physicists)

TABLE 8.11

8.2.6 Two TeV Collider Physics

CDF and D0 are the flagships of Fermilab III's voyage to the region beyond the electroweak scale. They will define the horizon. To see as far as the Tevatron and its higher luminosity will permit, CDF and D0 will continue to make significant improvements through 1996. The budget tables include allocations for these upgrades. Improvements to the Tevatron will continue until it reaches a luminosity of greater than $5 \times 10^{31} cm^{-2} sec^{-1}$ and a center of mass energy of 2.2 TeV. The schedule of the Main Injector project will determine whether Fermilab achieves this goal in 1997 or 1998.

CDF and D0 will continue data taking through 1999. During the intervening years ever larger numbers of the senior members of these collaborations will shift their attention to the SSC. The remaining senior physicists, the postdoctoral fellows and students will continue working with many of the Fermilab staff to discover the top, measure its mass, measure M_W/M_Z very accurately, and much more.

8.2.7 120 GeV Fixed-Target Physics

The Main Injector, a very impressive machine, will make physics research with the 120 GeV Main Injector beam a truly impressive program. One of the best kept secrets is that the 400 MeV Linac and 8 GeV, 15 Hz, Booster are also very impressive machines.

Around 1998, the program of neutral K experiments that has done so well at 800 GeV will move to the more intense neutral K beams that the Main Injector can provide. Funding will dictate the timing. Fermilab has received a letter of intent to carry out such a program of experiments, and the Laboratory has approved a Tevatron experiment for which much of the apparatus is the same.

The Laboratory has received three proposals and one letter of intent for ν experiments that intend to use the very intense neutrino beam that can be created by the Main Injector. These experiments all pursue neutrino oscillations. Chapter 5 discusses these possibilities extensively. A fifth neutrino experiment, P-860, which uses the Debuncher as a muon storage ring, becomes feasible with the Main Injector. The idea of using the neutrinos from the decays of a circulating muon beam was first proposed more than thirty years ago. The technique may allow a very sensitive test of ν_e oscillations into ν_μ or ν_τ.

Proponents presented conceptual designs of these experiments at the long-baseline neutrino oscillation workshop held in November 1991. The Fermilab PAC has not yet fully

considered these proposals to determine whether the experiments are feasible or affordable. They certainly address extremely interesting and fundamental topics and will receive careful review in the coming year. Table 8.12 lists the present proposals for experiments at the Main Injector.

Letters of Intent for 120 GeV Fixed-Target Experiment	
P-803 (Reay)	$\nu_\mu - \nu_\tau$ Oscillation
P-804 (Winstein)	Kaon Physics at Main Injector
P-805 (Gajewski)	Long Baseline ν Oscillation (IMB)
P-823 (Goodman)	Long Baseline ν Oscillation (SOUDAN II)
P-824 (Webster)**	Long Baseline ν Oscillation (DUMAND)
P-860 (Lee)	Neutrino Oscillations Using Fermilab Debuncher
** Letter of Intent	

TABLE 8.12

8.2.8 Fermilab User Demographics

If dollars are one important resource, then people are surely another. The great diversity of Fermilab's program comes from the large numbers of physicists with diverse ideas. Table 8.13 provides information on the population statistics for Fermilab experiments.

This table reveals a number of startling facts. First, the number of students, 450, working at Fermilab is very large—a big part of the entire U. S. high energy physics graduate student population. In five or six years, many of these students will become the senior postdoctoral fellows and junior faculty who will make the SSC experiments successful. Students choose to work on exciting, forefront experiments—provided that the experiments have a realistic prospect of taking data in a timely way. Fermilab experiments, properly funded, provide the kinds of excellent scientific opportunities that will attract students to our field and allow them to complete their dissertations in a reasonable length of time. Today, Fermilab is a magnet for graduate students. If the next five years can be funded at the level of the Presidents FY93 budget request, then the SSCL will be assured

an experienced and enthusiastic team of scientists. If 1993 is the first of many lean years, it portends grim prospects for forming a group of young U. S. physicists to use the SSCL in the 21st century.

PARTICIPANTS IN FERMILAB EXPERIMENTS

Category			Ph. D.s	Students	Total
Tevatron Fixed-Target	1990-91 Run	Experiments	537	187	724
		Detector R&D	99	8	107
		SSC R&D	149	9	158
	Users of Fermilab Computer for data taken before 1990		281	127	408
	Experiments and Proposals/LOI for Future Runs		288	76	364
Collider	CDF & D0		449	104	553
	All other completed collider experiments		52	22	74
	Proposals		71	3	74
Antiproton Source		E760	48	17	65
		Proposals	51	17	68
Main Injector Proposals			194	3	197

TABLE 8.13

The number of physicists who use Fermilab is also large. Over twenty five percent come from abroad, with the largest contingents from Italy and Japan and a significant number from Latin America. These colleagues contribute significantly to the health of high energy physics research.

8.3 NEW DIRECTIONS FOR FERMILAB

Fermilab, and its community of users, have created a vision of the Laboratory's scientific future. Fermilab, like the U.S. high energy physics community, must succeed in the 1990s if it is to succeed in the following decade. While the year 2000 is still far away, we have begun to determine new directions that Fermilab will explore to remain vital in the 21st century. At present, an important effort is Fermilab's participation in the Solenoidal Detector Collaboration. Forty Fermilab physicists spend 20 percent or more of their time working on this effort. The Laboratory supports this effort now and will give it even greater support in the future.

Besides the forefront particle physics program that will exploit the capabilities of the upgraded Tevatron, we are also exploring other, new directions. We have joined the Sloan Digital Sky Survey Project and the TESLA collaboration. Clearly, Fermilab can do extremely interesting physics and accelerator development in these areas. We have developed strong capabilities—for example in high performance computing and cryogenics—that will allow us to contribute where we have not previously contributed. We will also continue to do forefront physics at the highest energies available anywhere in the world for the remainder of the decade. Fermilab's unique capabilities and strengths will make it a vital center for high-energy physics research in the 21st century.